ARTICLE

Received 00th January 20xx,

Accepted 00th January 20xx

DOI: 10.1039/x0xx00000x

Iron Catalysts with N-Ligands for Carbene Transfer of Diazo Reagents

Caterina Damiano,[a] Paolo Sonzini[a] and Emma Gallo[a]*

Transition-metal-catalyzed carbene transfer reactions, involving diazo compounds and their precursors, are powerful tools for creating new C-C bonds. Depending on the involved catalytic system, the carbene insertion can efficiently be driven towards a specific functional group for the synthesis of a wide portfolio of fine chemicals. The present report is focused on the catalytic activity of iron catalysts in promoting alkene cyclopropanations, C-H and X-H (X = N, O, S, Se, Si, Sn, Ge) functionalizations. Porphyrin, porphyrinoid and non-heme iron complexes are discussed by analyzing experimental studies and theoretical calculations performed for proposing reaction mechanisms. The catalytic activity of artificial iron biocatalysts is also briefly reported in order to underline the similarities and differences between reaction mechanisms mediated by modified biocatalysts and synthetic catalysts. This review summarizes the achievements made in this field since 2006.

1. Introduction

The metal-catalyzed carbene transfer reaction from a diazo compound (R_2CN_2) to an organic molecule is a sustainable synthetic strategy. A vast number of substrates are reactive towards diazo reagents and new C-C bonds are formed by inserting a 'CR_2' moiety into the organic skeleton. Depending on the electronic and steric nature[1,2] of R_2CN_2 (Fig. 1) as well as the engaged catalytic system, compounds containing C=C, C≡C, C=O, C-H and X-H (X = Si, Se, Ge, Sn, heteroatom) bonds can be chosen as target reaction substrates (Fig. 2).[3-6] The mass conservation of the synthetic procedure is very high due to the formation of N_2 as the sole by-product. Even if the great chemical versatility of diazo compounds is recognized,[7] the employment of these carbene sources in a large scale has been limited due to their hazardous nature. However, it is worth noting that diazo compounds **A**-**C** types have been more used than **D** and **E** types due to their better stability (Fig. 1).

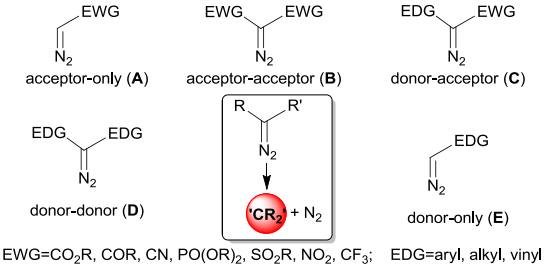

Fig. 1. Diazo derivatives employed for carbene transfer reactions

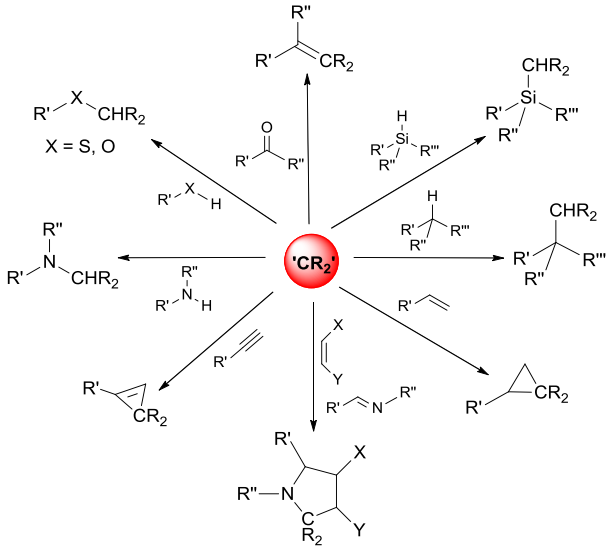

Fig. 2. Some important carbene transfer reactions

This drawback has more recently been overcome by applying continuous-flow technologies for handling such very reactive reagents and allowing the safe applicability of carbene-based procedures, also on a large scale.[8] In addition, in order to further increase the sustainability of diazo-based processes, alternative reagents, producing the desired diazo molecule *in situ*,[9] have been employed with a consequent improvement of the safety of the experimental methodology.

The key-point to carry out these reactions, by respecting the societal demand for sustainable chemistry, is the selection of catalytic systems showing a convenient activity/bio-tolerability combination. Currently, the use of iron complexes for promoting these organic transformations is receiving an

[a] *Department of Chemistry, University of Milan, Via Golgi 19, 20133 Milan, Italy. E-mail: emma.gallo@unimi.it*

increased interest from the scientific community, due to the importance of applying non-noble and low-toxic metal catalysts for the fine-chemical production.[10-13]

The present review furnishes a comprehensive picture of the most relevant catalytic applications of iron catalysts to carbene transfer reactions of diazo reagents under homogeneous conditions. Considering that the review is focused on the activity of iron catalysts, carbene transfer reactions by metal-free activation of diazo species[14] and diazo precursors[15] will not be addressed here. It should be noted that the activity of artificial iron biocatalysts, obtained by conjugation of iron porphyrinoid units with biological scaffolds, will also be reported briefly in order to underline similarities and differences between reaction mechanisms mediated by modified biocatalysts and synthetic catalysts.

Literature data published from 2006 will be discussed, except when the discussion of older references is essential for clarifying important points. We sincerely apologize in advance if some important contributions have been unintentionally omitted.

2. Cyclopropanation

The introduction of a cyclopropane unit into an organic skeleton confers specific chemo-physical features to the target molecule and, in many cases, peculiar pharmaceutical activities.[16-20] The high chemical reactivity of cyclopropane-containing species is due to the high bond-strain of the three-membered ring; many other valuable compounds can be easily synthesized by inducing ring-opening reactions of the cyclopropyl fragment.[21-26] Frequently, the cleavage of the cyclopropyl carbon-carbon bond is also a way, in which active drug molecules produce their pharmacological effects.[16]

The cyclopropanation reaction, which takes place by transferring the carbene unit from the diazo compound to the double bond,[27] can occur with a specific diastereoselectivity and, if conducted in the presence of a chiral promoter, a pair of enantiomers are obtained for each diastereomer (Scheme 1). The reaction selectivity can be modulated by using the opportune metal catalyst and, also in the case of iron-promoted reactions, the choice of the ligand that coordinates the metal center is crucial for enhancing both the chemo- and stereoselectivity (diastereo- and enantioselectivity) of the process.[28] In order to maximize the reaction chemoselectivity, it is crucial to avoid the dimerization of carbene fragments (:CR) deriving from the diazo decomposition.

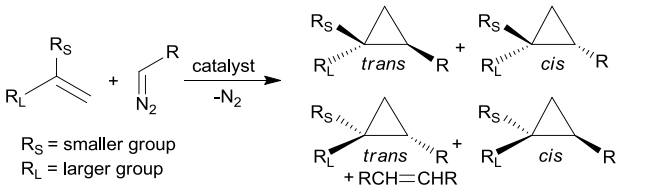

Scheme 1. General reaction between a *mono*-substituted diazo reagent and a terminal alkene yielding cyclopropanes and RCH=CHR as the side-product

This side-reaction, producing RCH=CHR, is responsible for a drastic decrease of products yields and it is usually limited by slowly adding the diazo species during the cyclopropanation. Low concentrations of carbene units are thus achieved and, as a consequence, coupling reactions are depressed.

2.1 Iron porphyrin and other porphyrinoid catalysts

The alkene cyclopropanation by diazo derivatives is efficiently catalyzed by metal porphyrinoid compounds and several reviews have been published on this topic over the past decades.[28-31] Among all the active metal porphyrin cyclopropanation catalysts, iron derivatives have emerged as a very active class of promoters, ever since T. Kodadek, L. K. Woo and co-authors published the first report on the catalytic activity of iron(II) porphyrins in 1995.[32] The increasing interest in developing iron porphyrin-based catalytic cyclopropanations is also due to the activity of heme-containing enzymes in cyclopropane biosynthesis (not involving direct carbene transfer reactions),[33,34] which makes synthetic iron porphyrins an interesting class of bio-inspired catalysts. It is important to point out that, while the direct alkene cyclopropanation is not promoted by natural enzymes, the reaction is now efficiently mediated by engineered enzymes, whose employment allows us to take advantage of the benefits of using natural systems for non-natural organic transformations (see below).

2.1.1 Achiral porphyrin catalysts. When the cyclopropanation reaction is promoted by an achiral iron porphyrin catalyst, the diastereomeric ratio is determined by the three-dimensional arrangement of the porphyrin structure, which usually favors the formation of the more thermodynamic stable *trans*-isomer. The reaction diastereoselectivity can be efficiently modulated thanks to the numerous structural modifications, which can be executed by functionalizing both β-pyrrolic and *meso* positions of the porphyrin skeleton, as well as inserting opportune axial ligands (L) onto the iron metal center (Fig. 3).

It is generally assumed that the first step of cyclopropanations mediated by an iron porphyrin is its reaction with the diazo reagent yielding an iron-carbene intermediate, which is able to transfer the carbene moiety to the incoming alkene. The usually observed *trans*-diastereoselectivity is due to the favorable formation of transition state **A**, in which the steric interaction between the large R_L group on the alkene and the R substituent on the carbene unit is minimized (Scheme 2).[30]

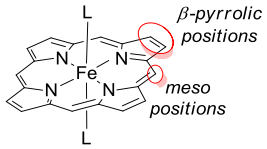

Fig. 3. General structure of iron porphyrin complexes

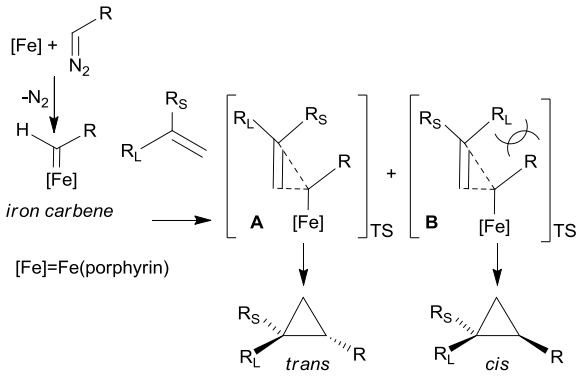

Scheme 2. Generally proposed mechanism of the alkene cyclopropanation by a diazo reagent

Considering that the formation of a terminal and electrophilic carbene is generally assumed, the best catalytic performances are usually obtained by reacting electron-rich alkenes, which show a reduced steric hindrance around the double bond. Thus, the cyclopropanation of sterically encumbered (such as internal alkenes) and electron-deficient alkenes is still considered a challenging reaction both for electronic reasons and for the alkene difficulty of approaching the iron-carbene functionality.

The first studies on the activity of iron porphyrin catalysts reported the employment of iron(II) derivatives and then, in view of the better chemical stability of iron(III) equivalent compounds, the latter class of porphyrin complexes have emerged as more useful and easier to handle cyclopropanation promoters.[32] It is supposed that, independently of the oxidation state of the iron precursor, an iron(II) complex is formed *in situ*, thanks to the mild reducing capability of the diazo reagent, which plays the double role of carbene source and reductant.[29,32,35,36] This proposal was supported by the good catalytic activity that was achieved by using iron(III) derivatives in combination with reducing agents such as cobaltocene ($CoCp_2$).[32,37]

In some cases the addition of $CoCp_2$ was essential to achieve the alkene cyclopropanation, as when the biologically active *N*- and *O*- protected 6-diazo-5-oxo-L-norleucine (DON) was used as the diazo derivative (Scheme 3).[38] It was presumed that the employed diazo reagent was not effective in reducing the ferric state of Fe(TPP)Cl (**1**) (TPP = dianion of tetraphenyl porphyrin) into the ferrous state and consequently, the cyclopropanation did not occur in the absence of $CoCp_2$.

The porphyrin skeleton of iron(III) derivatives have been largely modified in order to tune the chemo-physical characteristics of the catalyst.[29]

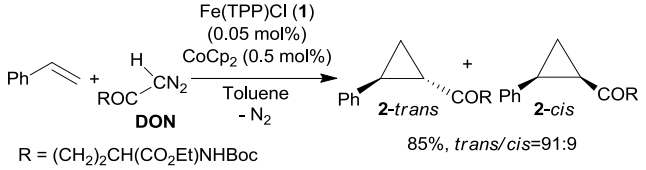

Scheme 3. Reaction between styrene and *N*- and *O*- protected DON catalyzed by Fe(TPP)Cl (**1**)/$CoCp_2$ combination

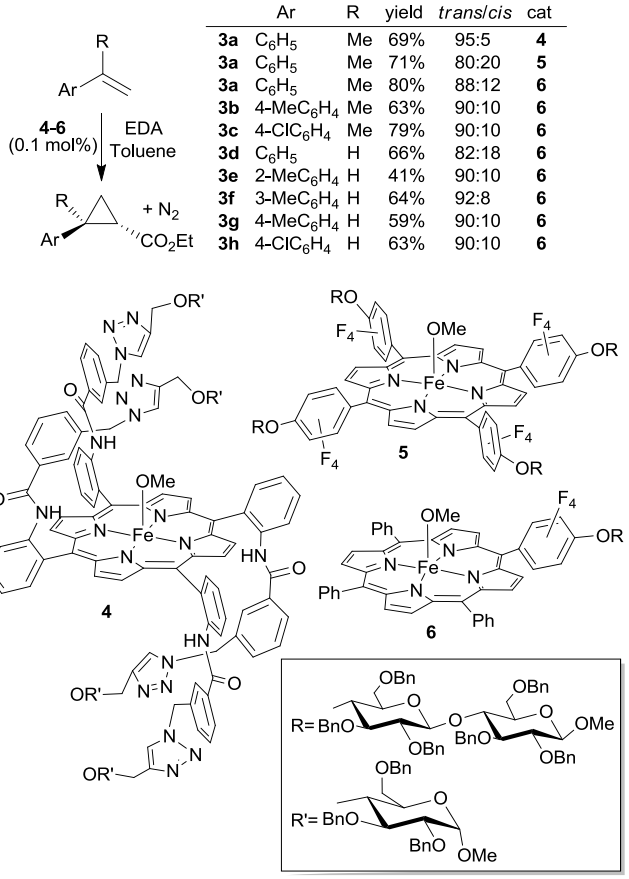

	Ar	R	yield	*trans*/*cis*	cat
3a	C_6H_5	Me	69%	95:5	**4**
3a	C_6H_5	Me	71%	80:20	**5**
3a	C_6H_5	Me	80%	88:12	**6**
3b	4-MeC_6H_4	Me	63%	90:10	**6**
3c	4-ClC_6H_4	Me	79%	90:10	**6**
3d	C_6H_5	H	66%	82:18	**6**
3e	2-MeC_6H_4	H	41%	90:10	**6**
3f	3-MeC_6H_4	H	64%	92:8	**6**
3g	4-MeC_6H_4	H	59%	90:10	**6**
3h	4-ClC_6H_4	H	63%	90:10	**6**

Scheme 4. Iron(III) glicoporphyrins **4**-**6** used as cyclopropanation catalysts

For example, the functionalization of the porphyrin core with carbohydrate units enhanced the reaction *trans*-diasteroselectivity, with respect to the unsubstituted porphyrin ligand, and the catalyst solubility in organic solvents.[39] Even if chiral carbohydrate units were present, the reaction was not enantioselective, due to the distance of the catalytically active metal center from the chiral portion of the molecule. The authors envisaged a potential use of glycoporphyrins, to promote cyclopropanation reactions in biphasic media by taking advantage of their amphiphilic nature.[39]

As depicted in Scheme 4, the tridimensional arrangement of iron porphyrin **4** was the most effective for inducing very good *trans*-diastero discriminations. Even if catalyst **6** was less efficient in terms of diastereoselectivity, it was chosen to study the scope of the reaction between ethyl diazoacetate (EDA) and eight differently substituted styrenes, in view of the facility of synthesizing it with respect to catalyst **4**. The catalytic **6**/EDA/alkene molar ratio of 1:1100:5000 was employed.[39]

As already stated, a reduced catalytic performance is usually observed when electron-deficient alkenes are the chosen reagents. To overcome this limitation, an umpolung approach was developed in which the electron density of alkenes was increased by inserting a phosphorus ylide moiety in the α-position with respect to the double bond.[40] Initial attempts

in reacting allylic phosphorus ylide compounds with methyl diazoacetate, $(CO_2Me)CHN_2$ (MDA), in the presence of Fe(TCP)Cl (**7**) (TCP = dianion of tetra(4-chlorophenyl) porphyrin) did not afford corresponding cyclopropane. However, when 4-chloro benzaldehyde (PCBA) was added to the reaction mixture to trap the final organic product, the insertion of the carbene moiety in the alkene C-H bond was observed.[41,42] Mechanistic studies revealed that the iron porphyrin catalyst **7** forms an active iron-carbene catalyst whose reaction with ylide **8** yields a very reactive cyclopropylmethyl ylide intermediate, which is involved in a ring-opening reaction as soon as it is formed. The proposed mechanism was further supported by the isolation of vinyl cyclopropane **9** in a low amount (6% yield) alongside the product **10** deriving from the ring-opening reaction of the cyclopropyl ring (Scheme 5).

On the basis of the above reported results and a mechanistic investigation by DFT (density functional theory) calculations, Y. Tang and co-authors proposed the mechanism of Scheme 6 for the formation of compound **10**.[40,42]

Thus, in order to synthesize vinyl cyclopropanes, it was imperative to suppress the ring-opening reaction of cyclopropylmethyl ylide intermediate **11** by maintaining a very low concentration of **11** in the reaction medium. To reach this goal, the synthesis was performed by using a phosphonium salt which, in the presence of the iron carbene and a base, was transformed into the cyclopropylmethyl ylide derivative. The *in situ* formed ylide was immediately trapped by the aldehyde PCBA before being involved in the ring-opening reaction described in Scheme 6.

This synthetic strategy was applied for the synthesis of vinylcyclopropanes **13a-13n** starting from crotonate-derived phosphonium salt **12**, *tert*-butyl diazoacetate (^{t}BDA) and differently substituted aldehydes, in the presence of the catalyst Fe(TCP)Cl (**7**) and K_2CO_3 as the base (Scheme 7).[40]

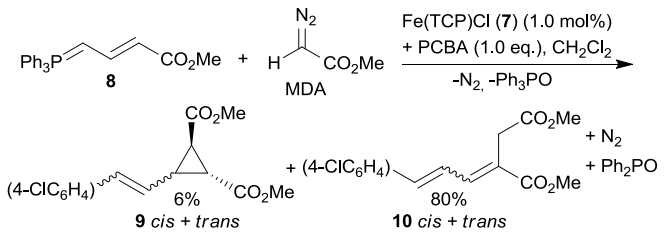

Scheme 5. Formation of **9** and **10** by the reaction of phosphorus ylide **8** and methyl diazoacetate promoted by Fe(TCP)Cl (**7**)

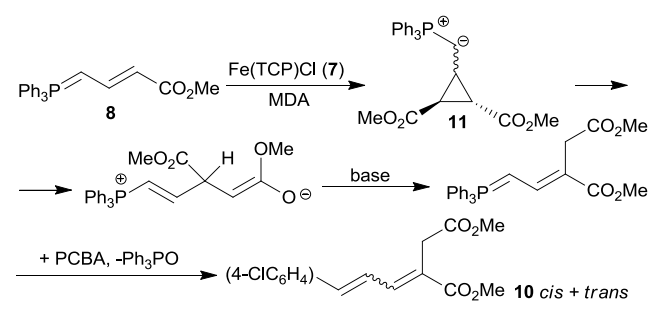

Scheme 6. Proposed mechanism for the formation of compound **10**

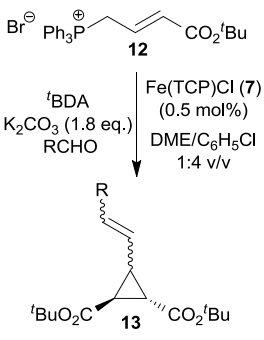

	R	yield	*Z*/*E*
13a	4-ClC_6H_4	88%	82:18
13b	3-ClC_6H_4	87%	82:18
13c	2-ClC_6H_4	76%	66:34
13d	4-$NO_2C_6H_4$	79%	75:25
13e	3-$NO_2C_6H_4$	87%	79:21
13f	2-$NO_2C_6H_4$	73%	55:45
13g	4-CNC_6H_4	94%	79:21
13h	4-BrC_6H_4	90%	81:19
13i	4-$CF_3C_6H_4$	93%	79:21
13j	2,4-$Cl_2C_6H_3$	88%	46:54
13k	C_6H_5	57%	86:14
13l	4-MeC_6H_4	57%	88:12
13m	(*E*)-PhCH=CH	63%	77:23
13n	CO_2Et	81%	48:52

Scheme 7. Synthesis of vinylcyclopropanes **13a**-**13n**

The formation of iron-carbene porphyrins, as active intermediates in the cyclopropanation of alkenes by diazo derivatives, is well recognized when halodiazo compounds, aryldiazomethane or alkyl diazo esters are employed as the carbene sources.[43] On the other hand, the formation of iron-dialkylcarbene intermediate has only been proposed due to the high chemical instability of donor-donor dialkyldiazomethanes, which prevents experimental mechanistic studies. As discussed in the successive section, instable diazo compounds are usually formed *in situ* starting from more stable diazo-precursors. Recently, iron-dialkylcarbene compounds were synthesized by C. M. Che and co-authors by following a different procedure. Complexes Fe(TPFPP)Ad (**14**) (TPFPP = dianion of tetra(pentafluorophenyl porphyrin, Ad = 2-adamantylidene) and Fe(TTP)(Ad) (**15**) (TTP = dianion of tetratolyl porphyrin) were synthesized by treating iron(II) porphyrins with aziadamantane under UV irradiation (365 nm) at room temperature (Scheme 8).[44] It should be noted that although carbene complexes **14** and **15** can be also obtained from commercially available iron(III) porphyrin chloride, isolated yields were lower than those attained by using iron(II) derivatives as starting materials. It was suggested that the free Ad was able to reduce the iron(III) into an iron(II) center, which is the active species reacting with the diazo reagent. It is worth noting that the formation of low-valent Fe(II)-carbene complexes with a neutral coordinated carbene ligand was proposed on the basis of the study of the electronic structures of **14** and **15** complexes. Iron complexes **14** and **15** displayed a significant thermal and chemical stability and complex **14** resulted in being an efficient catalyst for the cylopropanation of styrenes with donor-acceptor and donor-donor diazo reagents, such as $(Ph)(CF_3)CN_2$, Ar_2CN_2 and $(Ph)(Me)CN_2$ (Scheme 8); the latter diazo compound was generated *in situ* from acetophenone hydrazone, $(Ph)(Me)CNNH_2$, in the presence of Ag_2O.

Even if the cyclopropanation of alkenes by diazo compounds can be carried out in water by using water-soluble porphyrins (see the section on the use of chiral porphyrin catalysts), the usual low solubility of organic reaction components in water prevents its extensive use as a cyclopropanation solvent.

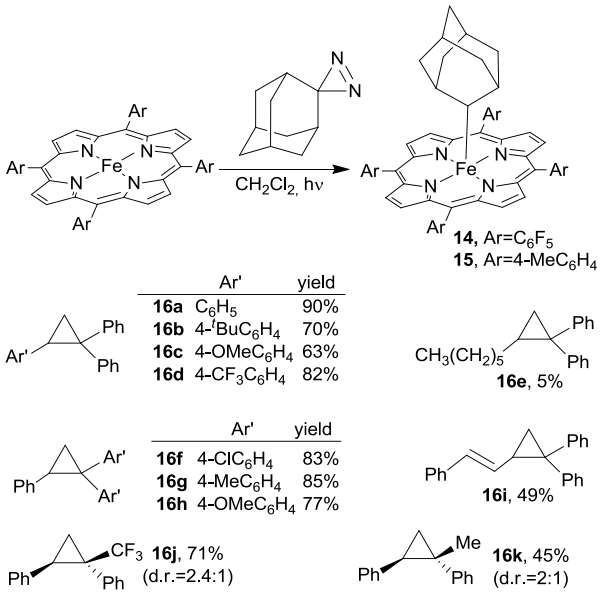

Scheme 8. Synthesis of iron carbene catalysts **14** and **15** and their use for promoting the synthesis of cyclopropanes **16a**-**16k**

In order to overcome this drawback, the cationic iron(III) *meso*-tetra(*N*-methyl-4-pyridyl)porphyrin pentachloride complex **17** was associated with the anionic surfactant sodium dodecyl sulphate (SDS) in amounts above the critical micelle concentration (CMC). The so-formed micelles were hydrophilic on the exterior and showed an apolar interior space where organic compounds can be concentrated to react in an acceptable rate.[45] The resulting water-soluble micellar catalyst, constituted by 1.0 mol% **17** and 20 mM SDS, was employed for the cyclopropanation of differently substituted alkenes with EDA; yields from moderate to very good were achieved (Scheme 9). Note that, in order to avoid the formation of side-products deriving from the carbene dimerization, the diazo compound was added in small consecutive portions to the reaction mixture.

Alongside the water medium, biphasic systems (H_2O/organic solvent) were also applied for cyclopropanations by using chemically stable diazo-precursors, which are safely transformed into the desired diazo species *in situ*.

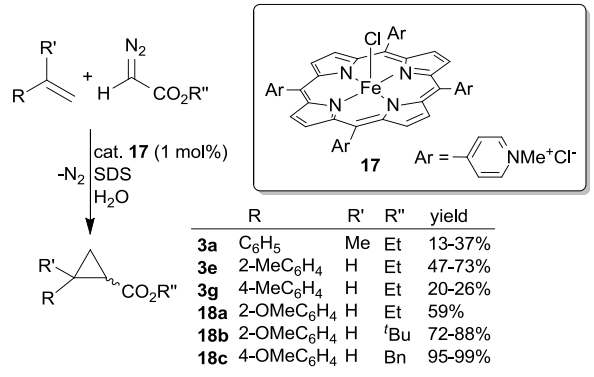

Scheme 9. Synthesis of cyclopropanes in water promoted by the micellar catalyst **17**/SDS

This experimental approach is of particular interest when the high reactivity of the required diazo reagents (such as mono-substituted, low-molecular weight alkyl-, aryl diazo compounds, diazoacetonitrile) prevents their safe handling in a laboratory.[46]

Many papers have been published on the use of stable diazo-precursors[14,27] since V. K. Aggarwal and co-authors[47] first described the transformation of *N*-tosylhydrazones salts (RCH=NNTsNa) into diazo compounds ($RCHN_2$) by the Bamford–Stevens reaction[48] and their iron-porphyrin-catalyzed reaction with alkenes to form cyclopropanes. Besides all the diazo-precursors employed, Diazald is one of the most interesting reagents because it is able to generate the simplest diazo compound: diazomethane (CH_2N_2). The very low carbon content of CH_2N_2 renders this species extremely reactive and very difficult to handle. Some years ago, B. Morandi and E. M. Carreira reported on the transformation of a water soluble derivative of Diazald into diazomethane when treated in strong basic aqueous conditions (6.0 mol/L KOH).[49] The reaction was conducted in a biphasic system to permit the migration of the so-formed CH_2N_2 from the aqueous to the organic phase, where the iron-catalyzed cyclopropanation of alkenes took place. This protocol was very efficient for the cyclopropanation of styrenes, enynes, and dienes by using low catalytic loadings (up to 0.1 mol % of catalyst **1**).[49,50]

The reaction efficiency strongly depended on the immiscibility of the two phases, which is crucial for an efficient separation of the water-soluble Diazald derivative from the organic solution, where the very water-sensitive 'Fe(TPP)(CH_2)' intermediate can be safely formed. The observed high TON values (up to 600) (TON = turnover number) pointed out the high chemical robustness of the iron catalyst under the employed experimental conditions. This methodology was applicable to a wide range of substrates, and good yields were obtained by employing styrene derivatives bearing both EWG and EDG substituents (Scheme 10).[49]

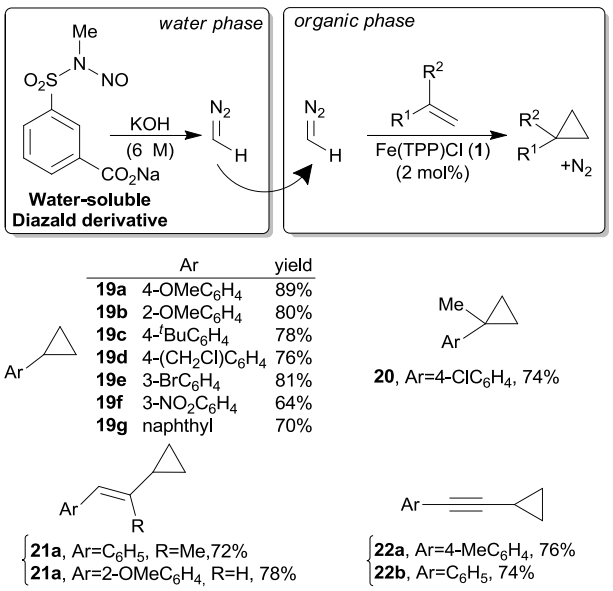

Scheme 10. Synthesis of cyclopropanes in a biphasic medium catalyzed by Fe(TPP)Cl (**1**) using a water-soluble derivative of Diazald as CH_2N_2 source

The above described procedure to generate diazomethane *in situ* was tested in cyclopropanations mediated by catalytic dendrimers. These macromolecular catalysts were synthesized by applying a convergent approach[51] and show the porphyrin molecule anchored to dendrons by ethereal bonds.[52] The analysis of the catalytic activity of Fe(TPP)Cl-based dendrimers species of different generations, disclosed that the cyclopropanation of 4-chloro-α-methylstyrene by CH_2N_2 occurred to a similar extent to that promoted by the corresponding 'free' iron porphyrin catalyst. Achieved data could open the door to a more general use of dendrimer-containing catalysts with the beneficial outputs of their easy recovery by precipitation, nano-, or ultrafiltration.

Diazomethane can be also generated from the decomposition of temozolomide (TMZ), an imidazotetrazine derivative which is normally used as an anti-tumour agent in therapy.

TMZ is a commercially available and safe compound that was very recently employed by P. Hergenrother and R. L. Svec to methylate different classes of molecules, including cyclopropanes (Scheme 11).[53]

The reaction was effective with different alkenes under mild conditions and using an aqueous KOH solution as the reaction medium. Besides diazomethane, the TMZ hydrolysis produced 4-amino-5-imidazolecarboxamide, which was separated from the desired cyclopropane by a simple extraction.

Trifluoromethyl diazomethane ($(CF_3)CHN_2$) is another diazo species of great synthetic interest because it can be used as the starting material of trifluoromethylated compounds that often present interesting medicinal features.[54] Trifluoroethylamine hydrochloride, $(CF_3)CH_2NH_2{\cdot}HCl$, was very efficient in forming the hazardous and very toxic $(CF_3)CHN_2$ reagent *in situ* by a simple procedure. The latter diazo species, once formed, reacted with styrenes,[55] dienes,[56] and enynes[56] yielding the corresponding cyclopropanes with outstanding yields (up to 95%) and *trans*-diastereoselectivities (up to 99%). Whilst dienes and enynes reacted in the presence of the sole $NaNO_2$, the cyclopropanation of styrenes also required the presence of H_2SO_4/NaOAc buffer and 4-(dimethylamino)pyridine (DMAP) to progress. All the reactions were efficiently catalyzed by Fe(TPP)Cl (**1**) porphyrin complex (Scheme 12).

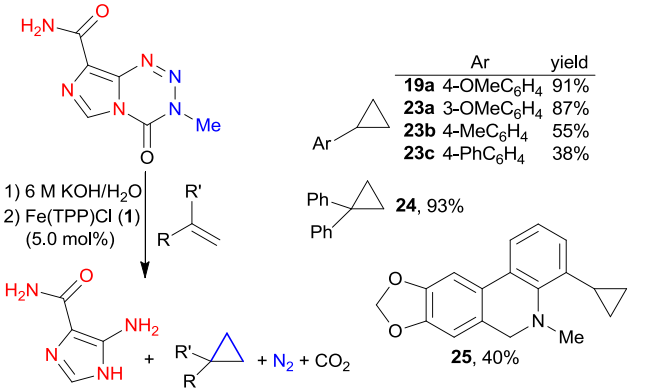

	Ar	yield
19a	4-OMeC$_6$H$_4$	91%
23a	3-OMeC$_6$H$_4$	87%
23b	4-MeC$_6$H$_4$	55%
23c	4-PhC$_6$H$_4$	38%

Scheme 11. Synthesis of cyclopropanes in a biphasic medium catalyzed by Fe(TPP)Cl (**1**) using temozolomide (TMZ) as CH_2N_2 source

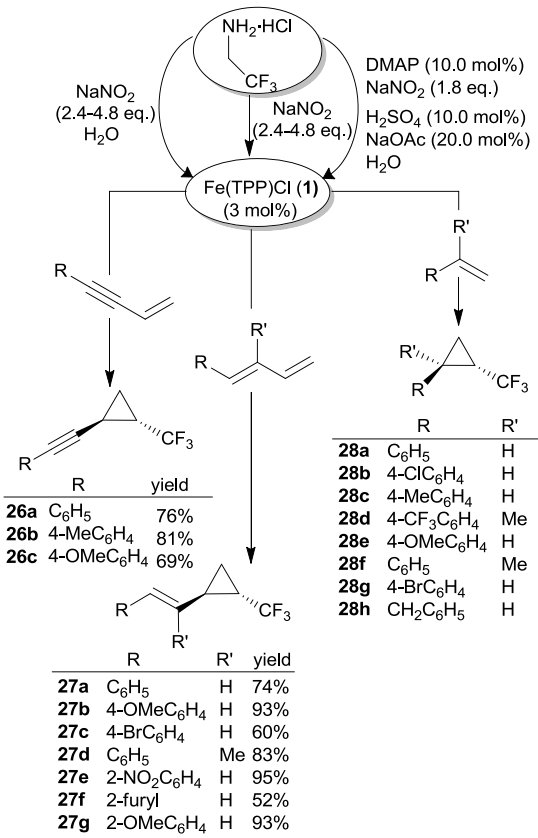

	R	yield
26a	C_6H_5	76%
26b	4-MeC$_6$H$_4$	81%
26c	4-OMeC$_6$H$_4$	69%

	R	R'	yield
27a	C_6H_5	H	74%
27b	4-OMeC$_6$H$_4$	H	93%
27c	4-BrC$_6$H$_4$	H	60%
27d	C_6H_5	Me	83%
27e	2-NO$_2$C$_6$H$_4$	H	95%
27f	2-furyl	H	52%
27g	2-OMeC$_6$H$_4$	H	93%

	R	R'	yield
28a	C_6H_5	H	86%
28b	4-ClC$_6$H$_4$	H	85%
28c	4-MeC$_6$H$_4$	H	99%
28d	4-CF$_3$C$_6$H$_4$	Me	77%
28e	4-OMeC$_6$H$_4$	H	89%
28f	C_6H_5	Me	86%
28g	4-BrC$_6$H$_4$	H	95%
28h	$CH_2C_6H_5$	H	10%

Scheme 12. *In situ* formation of $(CF_3)CHN_2$ and its Fe(TPP)Cl (**1**)-catalyzed reaction with unsaturated substrates

The commercially available Fe(TPP)Cl (**1**) complex was also active in promoting the synthesis of nitrile-substituted cyclopropanes by using aminoacetonitrile hydrochloride, $(NC)CH_2NH_2{\cdot}HCl$, as the source of diazo acetonitrile, $(CN)CHN_2$. The experimental protocol, reported by E. Carreira and B. Morandi (see above), was employed by R. Koenigs and co-authors[57] to generate, in a H_2O/CH_2Cl_2 (1:1) reaction mixture, the very reactive and difficult to handle $(CN)CHN_2$ reagent. The safety of the procedure was assured by the continuous release of the diazo reagent *in situ* during the diazotization step, which reacted with alkene before reaching high and dangerous concentration values. The tandem methodology (diazotization/cyclopropanation) permitted the safe cyclopropanation of several aromatic alkenes in very good yields and good *trans*-diastereoselectivities (Scheme 13).

In view of the importance of using water as the reaction medium for synthetic transformations, including cyclopropanations, the employment of diazo precursors, instead of water-sensitive diazo compounds, assumes a practical importance. With this goal in mind, EDA, which is quite stable in organic solvents but cannot be handled in water, was formed *in situ* from glycine ethyl ester hydrochloride, $(CO_2Et)CH_2NH_2{\cdot}HCl$. This EDA-precursor was reacted in water with electronically different alkenes in the presence of Fe(TPP)Cl (**1**) catalysts. The procedure was effective to form corresponding cyclopropanes in good yields and *trans*-diastereoselectivities (Scheme 14).[58]

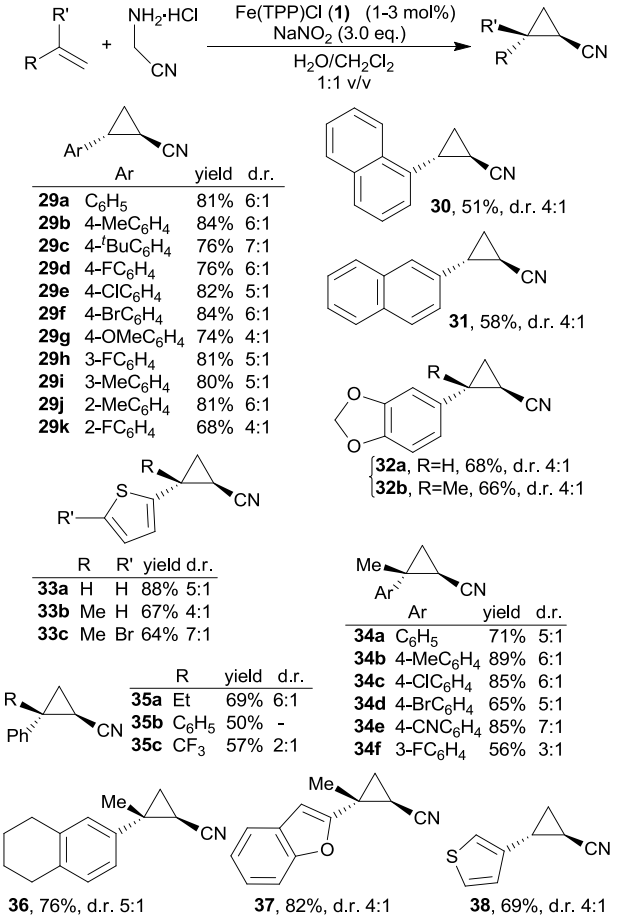

	Ar	yield	d.r.
29a	C_6H_5	81%	6:1
29b	4-MeC_6H_4	84%	6:1
29c	4-^{t}BuC_6H_4	76%	7:1
29d	4-FC_6H_4	76%	6:1
29e	4-ClC_6H_4	82%	5:1
29f	4-BrC_6H_4	84%	6:1
29g	4-$OMeC_6H_4$	74%	4:1
29h	3-FC_6H_4	81%	5:1
29i	3-MeC_6H_4	80%	5:1
29j	2-MeC_6H_4	81%	6:1
29k	2-FC_6H_4	68%	4:1

	R	R'	yield	d.r.
33a	H	H	88%	5:1
33b	Me	H	67%	4:1
33c	Me	Br	64%	7:1

	R	yield	d.r.
35a	Et	69%	6:1
35b	C_6H_5	50%	-
35c	CF_3	57%	2:1

	Ar	yield	d.r.
34a	C_6H_5	71%	5:1
34b	4-MeC_6H_4	89%	6:1
34c	4-ClC_6H_4	85%	6:1
34d	4-BrC_6H_4	65%	5:1
34e	4-CNC_6H_4	85%	7:1
34f	3-FC_6H_4	56%	3:1

Scheme 13. Fe(TPP)Cl (**1**)-catalyzed synthesis of nitrile-substituted cyclopropanes

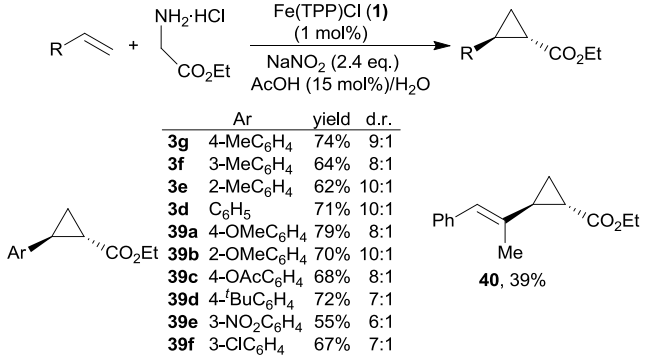

	Ar	yield	d.r.
3g	4-MeC_6H_4	74%	9:1
3f	3-MeC_6H_4	64%	8:1
3e	2-MeC_6H_4	62%	10:1
3d	C_6H_5	71%	10:1
39a	4-$OMeC_6H_4$	79%	8:1
39b	2-$OMeC_6H_4$	70%	10:1
39c	4-$OAcC_6H_4$	68%	8:1
39d	4-^{t}BuC_6H_4	72%	7:1
39e	3-$NO_2C_6H_4$	55%	6:1
39f	3-ClC_6H_4	67%	7:1

Scheme 14. Fe(TPP)Cl (**1**)-catalyzed synthesis of cyclopropanes using $(CO_2Et)CH_2NH_2$·HCl as the EDA source

The tandem diazotization/cyclopropanation protocol was also applied by G. Haufe and co-authors[59] to synthesize ethyl 2-aryl-2-fluoro-cyclopropane carboxylates by reacting differently substituted α-fluorostyrenes with $(CO_2Et)CH_2NH_2$·HCl in the presence of Fe(TPP)Cl (**1**) catalyst. As depicted in Scheme 15, except in one case (compare yield of **39e**, Scheme 14 with that of **41f**, Scheme 15), the reaction efficiency was lower, in terms of both yield and diastereoselectivity, than that previously observed in the cyclopropanation of non-fluorinated parent compounds.[58]

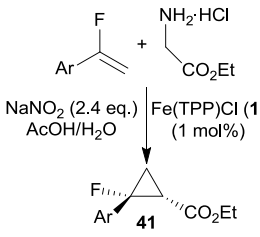

	Ar	yield	d.r.
41a	4-$OMeC_6H_4$	70%	3:1
41b	3-$OMeC_6H_4$	55%	3:1
41c	4-$OAcC_6H_4$	47%	3:1
41d	4-MeC_6H_4	24%	4:1
41e	C_6H_5	53%	3:1
41f	3-$NO_2C_6H_4$	86%	2:1
41g	4-ClC_6H_4	21%	3:1

Scheme 15. Fe(TPP)Cl (**1**)-catalyzed synthesis of ethyl 2-aryl-2-fluoro-cyclopropane from $(CO_2Et)CH_2NH_2$·HCl and α-fluorostyrenes

As stated before, under basic conditions *N*-tosylhydrazones generated diazo species *in situ*, which once formed, were involved in the carbene transfer reaction before decomposing.[47]

One of the main drawbacks for a larger employment of this tandem procedure has been the lack of a mild experimental procedure (compatible with the cyclopropanation step) to convert a large portfolio of hydrazones into corresponding cyclopropanes.[60] In order to enlarge the scope of the reaction, A. B. Charette and co-authors recently reported the Fe(TPP)Cl (**1**)-catalyzed synthesis of *trans*-1,2-disubstituted cyclopropanes by using *N*-nosyl hydrazones as the source of differently substituted diazo compounds.[61] Achieved data indicated a better reactivity of hydrazones bearing an electron-poor aromatic moiety (R in the general reaction of Scheme 16) and showing a reduced steric hindrance. Alkenes, showing different electronic and steric features, were cyclopropanated with very good yields and diastereoselectivities by simply adjusting experimental conditions (temperature and time).

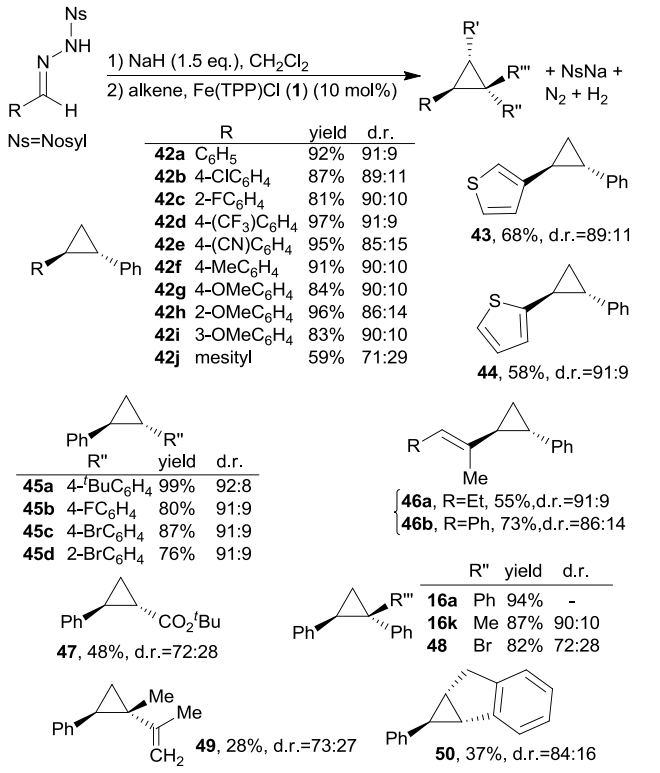

	R	yield	d.r.
42a	C_6H_5	92%	91:9
42b	4-ClC_6H_4	87%	89:11
42c	2-FC_6H_4	81%	90:10
42d	4-$(CF_3)C_6H_4$	97%	91:9
42e	4-$(CN)C_6H_4$	95%	85:15
42f	4-MeC_6H_4	91%	90:10
42g	4-$OMeC_6H_4$	84%	90:10
42h	2-$OMeC_6H_4$	96%	86:14
42i	3-$OMeC_6H_4$	83%	90:10
42j	mesityl	59%	71:29

	R"	yield	d.r.
45a	4-^{t}BuC_6H_4	99%	92:8
45b	4-FC_6H_4	80%	91:9
45c	4-BrC_6H_4	87%	91:9
45d	2-BrC_6H_4	76%	91:9

	R"	yield	d.r.
16a	Ph	94%	-
16k	Me	87%	90:10
48	Br	82%	72:28

Scheme 16. Fe(TPP)Cl (**1**)-catalyzed synthesis of differently substituted cyclopropanes using *N*-nosyl hydrazones as the source of diazo compounds

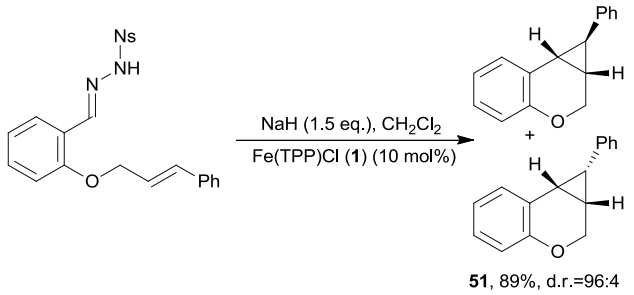

Scheme 17. Fe(TPP)Cl (**1**)-catalyzed intramolecular cyclopropanation by *N*-nosyl hydrazone compounds

Considering that the catalytic performance was optimized by applying different temperatures and times, only the best achieved results are reported in Scheme 16. The reaction also worked well for an intramolecular cyclopropanation, as shown in Scheme 17.[61]

Alongside *N*-tosyl hydrazones,[60,62] other derivatives emerged as useful classes of diazo precursors for performing cyclopropanations. X. Bi and co-authors developed a procedure in which the very reactive $(CF_3)CHN_2$ diazo compound was generated from the decomposition of trifluoroacetaldehyde *N*-tfsylhydrazone ($(CF_3)CH{=}NNHTfs$) under basic conditions. The so-formed $(CF_3)C$: carbene moiety was successfully transferred to a variety of alkenes to form compounds illustrated in Scheme 18.[63] Cyclopropanes were formed in yields comparable to those achieved by using $(CF_3)CH_2NH_2{\cdot}HCl$[55,56] and with a stereoselectivity > 20:1.[63]

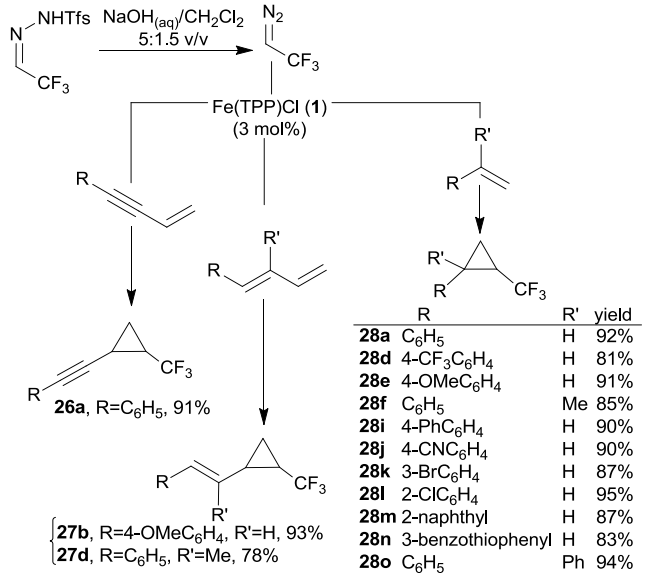

	R	R'	yield
28a	C_6H_5	H	92%
28d	4-$CF_3C_6H_4$	H	81%
28e	4-$OMeC_6H_4$	H	91%
28f	C_6H_5	Me	85%
28i	4-PhC_6H_4	H	90%
28j	4-CNC_6H_4	H	90%
28k	3-BrC_6H_4	H	87%
28l	2-ClC_6H_4	H	95%
28m	2-naphthyl	H	87%
28n	3-benzothiophenyl	H	83%
28o	C_6H_5	Ph	94%

Scheme 18. Fe(TPP)Cl (**1**)-catalyzed intramolecular cyclopropanation by trifluoroacetaldehyde *N*-tfsylhydrazone

2.1.2 Other achiral porphyrinoid catalysts. Besides porphyrins, phthalocyanines and porphyrazines, in which methine bridges of porphyrin ligands are replaced by azamethine units, have been used for the synthesis of cyclopropanation iron catalysts. However, these complexes have been less engaged in catalytic reactions than iron porphyrins due to the occurrence of molecular π-π stacking interactions, which cause low solubility in organic solvents and a high tendency of these porphyrinoids to form aggregates. On the other hand, these chemo-physical characteristics can be modulated by introducing lipophilic substituents onto the ligand scaffold and coordinating axial ligands to the active metal, and thus exploited for facilitating the recovery and recycling of these chemically stable catalytic species. (Fig. 4).

The use of Fe(II)(Pc) (**52**), (Pc= unsubstituted phthalocyanine with R=H in Fig. 4) ligand, as a cyclopropanation catalyst was reported for the first time by B. Sains and co-authors. The cyclopropanation of 4-methylstyrene by EDA, yielding **3g**, occurred in the moderate yield of 55% indicating a modest catalytic activity of complex **52**.[64] The catalytic efficiency dropped by replacing the acceptor-only EDA diazo species with the donor–acceptor methyl phenyl diazoacetate, $(CO_2Me)(Ph)CN_2$, as the carbene source. In this latter case, the reaction between methyl phenyl diazoacetate and styrene, in the presence of catalyst **52**, yielded the corresponding cyclopropane in very low yield of 8% and with a low diastereoselectivity.[65]

Better results were obtained in the Fe(II)(Pc) (**52**)-catalyzed reaction of 4-methylstyrene with trimethylsilyldiazomethane ($(Me_3Si)CHN_2$). In this case, the *trans*-*C*-silyl cyclopropane **53** was obtained in the acceptable yield of 65% (Scheme 19).[66]

It should be noted that the reaction was conducted under heterogeneous conditions (complex **52** is completely insoluble in 1,2-dichloroethane), which permitted to easily recover the catalyst by a simple filtration. The catalytic efficiency of the recovered complex was maintained to allow its recycle for several catalytic cycles.[66]

In order to enhance the catalytic activity of iron phthalocyanine complexes, different ligands were used to synthesize a small class of catalysts. The so-obtained **54** and **55** iron(II) complexes as well as **56**-**58** iron(III) derivatives were employed to promote the synthesis of cyclopropane **3d** through the reaction of styrene with EDA (Scheme 20).[67]

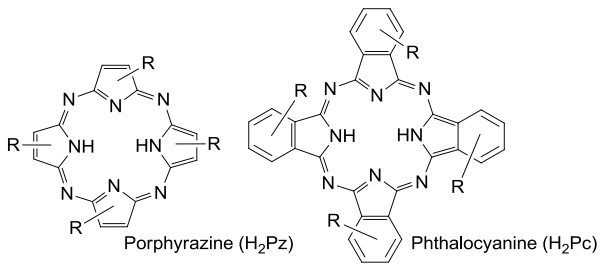

Fig. 4. General structures of phthalocyanines and porphyrazines

Although the iron(III) catalyst **57**, showing EWGs on the phthalocyanine skeleton, quantitatively promoted the formation of **3d,** the achieved *trans*-diastereoselectivity was low (*trans*/*cis* = 2). Similar results were obtained by using either iron(II) or iron(III) phthalocyanine catalysts indicating that both classes of complexes are probably transformed in the same catalytically active intermediate *in situ*.

The synthesis of cyclopropane **3d** was also carried out in the presence of the bridged diiron octapropylporphyrazine complexes Fe(III)(L)−O−Fe(III)(L) (**59**), Fe(III)(L)−N−Fe(IV)(L) (**60**) and Fe(IV)(L)−C−Fe(IV)(L) (**61**) (L = dianion of octapropylporphyrazine), whose structural parameters and iron oxidation states were analyzed in detail.[68] The Mössbauer spectroscopy disclosed the existence of low-spin systems for all the tested iron complexes and the DFT study revealed that, while complexes **59** and **61** exist in a singlet state, the μ-nitrido complex **60** is more stable in the doublet state.

Catalytic data pointed out that **59** and **61** complexes performed better than **60** in the model cyclopropanation reaction but unfortunately, none of the employed catalysts achieved very good reaction diastereoselectivities (Scheme 21). The reaction scope of the cyclopropanation mediated by the iron phthalocyanine complex **59** was studied by testing the reactivity of styrene towards diazo compounds with different electronic and steric characteristics, such as benzyl diazoacetate (BDA), *tert*-butyl diazoacetate (^{t}BDA) and $(Me_3Si)CHN_2$, as well as by reacting EDA with several alkenes. Obtained results are listed in Fig. 5. It is worth noting that all the catalysts maintained their dimeric structure during the cyclopropanation, as proven by the recovery of unmodified complexes at the end of the catalytic reaction. DFT studies suggested the occurrence of a carbene active intermediate, which bears the carbene unit at one of the two iron metal centers.

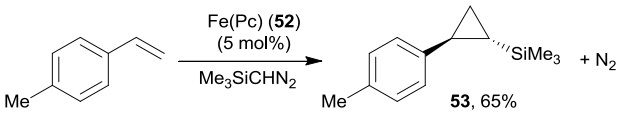

Scheme 19. Synthesis of cyclopropane **53**.

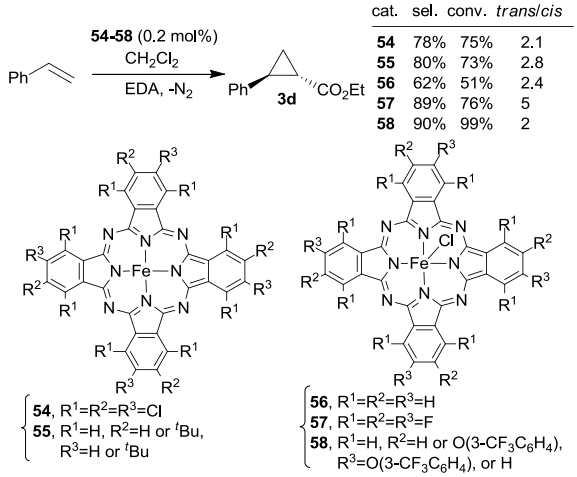

Scheme 20. Synthesis of cyclopropane **3d** catalyzed by complexes **54**-**58**

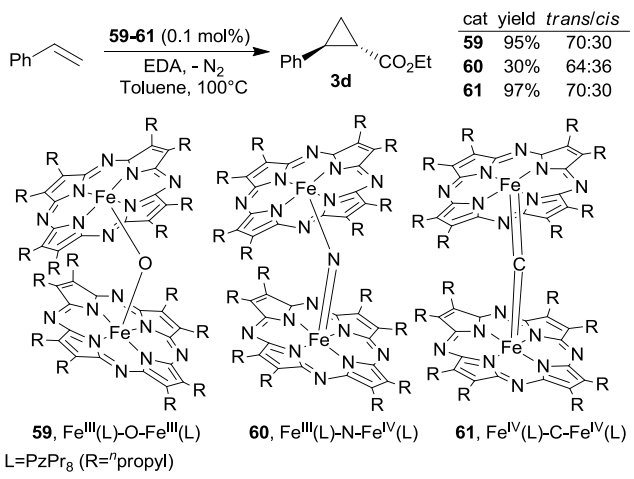

Scheme 21. Synthesis of cyclopropane **3d** catalyzed by complexes **59**-**61**

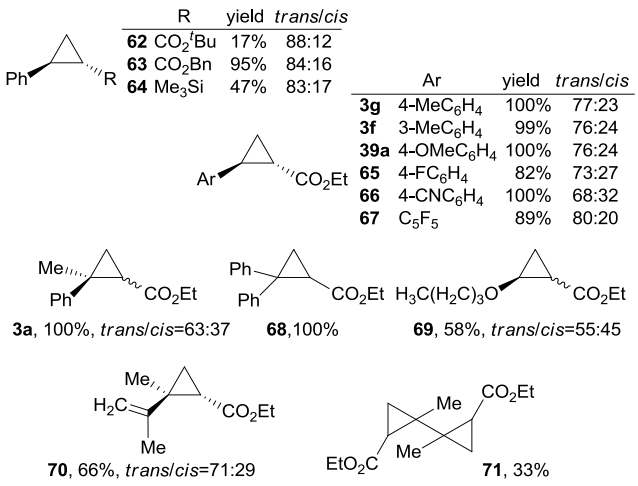

Fig. 5. Cyclopropanes synthesized in the presence of the dimeric iron porphyrazine complex **59**

2.1.3 Chiral porphyrin catalysts. Among all chiral iron porphyrins active in carbene transfer reactions, those showing a D_4, D_2 and C_2 symmetry[28] (Fig. 6) have been applied to mediate enantioselective cyclopropanations.

The Halterman porphyrin (Halt*)[69] and structurally related ligands were largely employed for synthesizing chiral cyclopropanation catalysts. After its first use as ruthenium(II) Ru(Halt*)(CO)[70] and Ru(Halt*)(CO)(EtOH)[71] complexes, this D_4 symmetric porphyrin was employed by C. M. Che and co-authors, to synthesize Fe(Halt*)Cl catalyst **72**. This latter chiral complex mediated the reaction of EDA with differently substituted alkenes and, as shown in Scheme 22, very good diastereo- and enantioselectivities were achieved.[36]

The catalytic efficiency decreased when the reactions were run in open air suggesting the formation of a sensitive iron carbene intermediate. It was proposed that the first step of the reaction was the reduction of the electron-deficient **72** by EDA forming the corresponding iron(II) species, which represents the active catalyst of the cyclopropanation. The putative iron carbene intermediate was suggested on the basis

of some experimental evidence collected in the presence of different electron-donor axial ligands, such as pyridine (py) or 1-methylimidazole (MeIm). The addition of an axial ligand could be responsible for the formation of a more stable octahedral carbene complex, where L and the carbene moiety occupy the two axial positions. The formation of Fe(Halt*)($CHCO_2Et$)(L) (L = py or MeIm) complex, upon the addition of EDA and L to **72**, was detected by electrospray mass spectrometry (ESMS). The proposed catalytic cycle is illustrated in Scheme 23. The suggested formation of a six-coordinated carbene intermediate is in accordance to an end-on approach of the alkene to the active carbene functionality, which justifies the increased *trans*-diastereoselectivity observed upon the addition of the L axial ligand.

The catalytic competence of Fe(Halt*)Cl catalyst **72** was tested by using more challenging diazo compounds, such as diazoacetophenone, $(PhCO)CHN_2$[72] and trifluoromethyl diazomethane ($(CF_3)CHN_2$).[73]

Catalyst **72** mediated the cyclopropanation of several styrenes with $(PhCO)CHN_2$ and collected data (Fig. 7) revealed the reaction *trans*-diastereoselectivity and enantiomeric excesses of cyclopropanes up to 80%. It is worth noting that, as previously mentioned, the reaction occurred only in the presence of pyridine highlighting the fundamental role of the axial ligand.[36].

Concerning the activity of complex **72** in the cyclopropanation of styrenes by $(CF_3)CHN_2$,[73] the reaction was less productive when the instable diazo compound was formed *in situ*[55] (compare data of Scheme 24 with those of Scheme 12). It should be pointed out that the lower catalytic productivity can be also due to the different catalyst employed (Fe(TPPP)Cl, **1** in scheme 12 *versus* Fe(Halt*)Cl, **72** in scheme 24). However, in the presence of the chiral complex **72**, three styrenes were cyclopropanated with a complete *trans*-diasteroselectivity and moderate enantioselectivities.

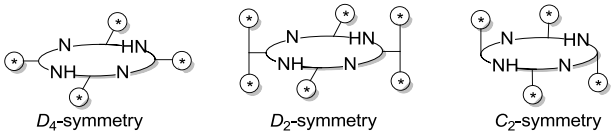

Fig. 6. General structures of D_4, D_2 and C_2 symmetrical porphyrin ligands used in cyclopropanations

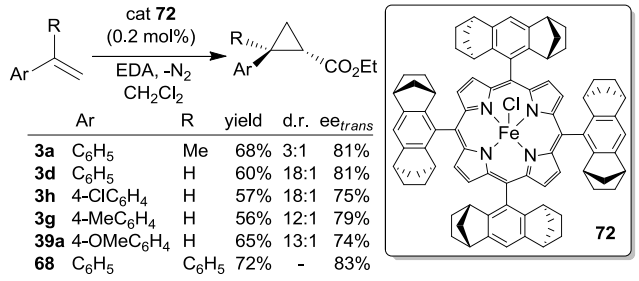

	Ar	R	yield	d.r.	ee_{trans}
3a	C_6H_5	Me	68%	3:1	81%
3d	C_6H_5	H	60%	18:1	81%
3h	4-ClC_6H_4	H	57%	18:1	75%
3g	4-MeC_6H_4	H	56%	12:1	79%
39a	4-$OMeC_6H_4$	H	65%	13:1	74%
68	C_6H_5	C_6H_5	72%	-	83%

Scheme 22. Enantioselective cyclopropanation of styrenes by EDA catalyzed by chiral complexes **72**

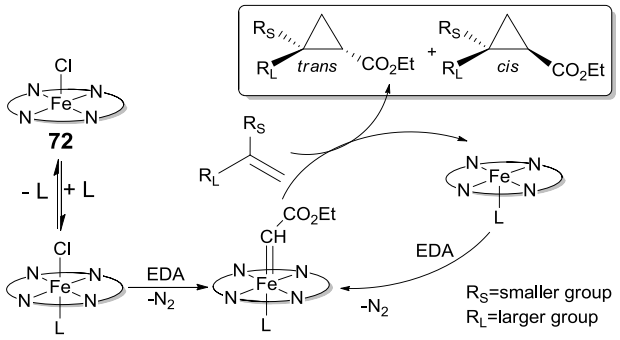

Scheme 23. Proposed mechanism of the cyclopropane formation catalyzed by **72**

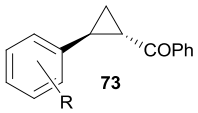

	R	yield	*trans*/*cis*	ee_{trans}
73a	H	67%	93:7	76%
73b	4-Me	53%	96:4	76%
73c	4-OMe	58%	93:7	76%
73d	4-CF_3	54%	93:7	62%
73e	4-Cl	58%	94:6	76%
73f	4-Br	58%	92:8	69%
73g	3-Me	64%	92:8	68%
73h	2-Me	58%	92:8	80%
73i	3-CF_3	25%	90:10	74%
73j	2-CF_3	24%	90:10	78%

Fig. 7. Enantioselective cyclopropanation of styrenes by $(PhCO)CHN_2$ catalyzed by complex **72**

When catalyst **72** was anchored onto a polymeric support and used in a heterogeneous medium, cyclopropanes were formed in similar yields and diastereoselectivities than those observed under homogeneous conditions. A decrease of the enantioselectivity was always observed.[73] The chiral catalyst **72** was also competent in mediating the reaction of styrene with *N*- and *O*- protected 6-diazo-5-oxo-L-norleucine (DON).[38] Cyclopropane **2** was formed in 95% yield, d.r.=95:5 and 80% ee_{trans}. The addition of the reducing agent $CoCp_2$ was necessary for completing the reaction.

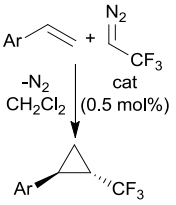

	Ar	yield	*trans*/*cis*	ee_{trans}	cat.
28a	C_6H_5	50%	99:1	61%	**72**
28a	C_6H_5	52%	97:3	56%	**72-polymer**
28e	4-$OMeC_6H_4$	42%	99:1	69%	**72**
28e	4-$OMeC_6H_4$	51%	96:4	17%	**72-polymer**
28f	4-BrC_6H_4	43%	99:1	67%	**72**
28f	4-BrC_6H_4	42%	97:3	37%	**72-polymer**

Scheme 24. Enantioselective cyclopropanation of styrenes by $(CF_3)CHN_2$ catalyzed by **72** and **72-polymer**

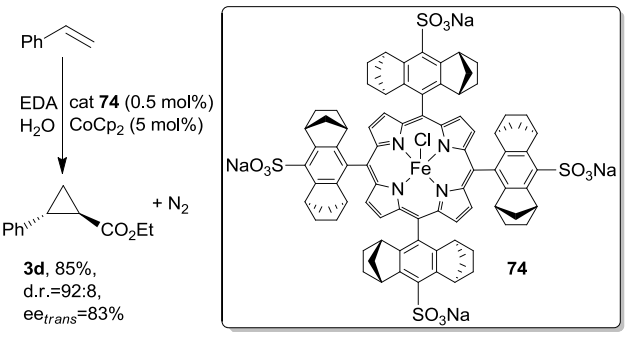

Scheme 25. Synthesis of cyclopropane **3d** in water medium catalyzed by **74**

The introduction of SO_3Na groups onto the Halterman porphyrin backbone permitted executing the reaction in an aqueous medium. The water-soluble catalyst **74** mediated the reaction between styrene and EDA forming **3d** in 85% yield, d.r.=92:8 and 83% ee_{trans} (Scheme 25). Also in this case the presence of $CoCp_2$ was required.[74]

X. P. Zhang and co-authors reported the synthesis and the catalytic application of a large class of D_2-symmetrical porphyrins, which have been mainly used as cobalt(II) derivatives in both carbene and nitrene transfer reactions.[75] The catalytic activity of iron complexes was also tested and they resulted less active than their cobalt equivalents. Several styrene derivatives were reacted with EDA in the presence of chiral iron(III) porphyrin **75** and corresponding *trans*-cyclopropanes were formed with a very good diastereoselectivity but unfortunately, with a modest enantiocontrol (Scheme 26).[76]

C_2-symmetrical porphyrins have emerged as a very useful class of ligands inducing good stereocontrol in cyclopropanation reactions. These chiral ligands were first used as cobalt(II) derivatives[77,78] and more recently as iron(III) complexes by E. Gallo, B. Boitrel and co-authors.[79,80] The parent compound of this class of ligands is αααβ-tetra-(2-aminophenyl)porphyrin (αααβ–$TAPPH_2$) (**78**) (Scheme 27) whose functionalization of the four amino groups permitted the building of different C_2-symmetrical frames onto the N_4 porphyrin core. The '*bis*-strapped' porphyrin, which shows the chiral environment surrounding both faces of the tetrapyrrolic core, was used to synthesize Fe(III)(**79**)OMe, which promoted the reaction of several alkenes with acceptor-only diazo derivatives.

Because carbene dimerization side-reactions were not efficiently promoted by Fe(III)(**79**)OMe, the use of an alkene stoichiometric excess was not required, with the consequent benefit of reducing costs. As described in Scheme 27, the reaction worked well when terminal alkenes and low sterically hindered diazo compounds were employed. This suggested that the active iron metal center was embedded into a crowded tridimensional porphyrin framework, which selects the size of approaching reagents.

	Ar	R	yield	*trans*/*cis*	ee_{trans}
3d	C_6H_5	Et	77%	92:8	4%
3g	4-MeC_6H_4	Et	72%	93:7	11%
39a	4-$OMeC_6H_4$	Et	75%	91:9	15%
62	C_6H_5	^{t}Bu	63%	94:6	24%
65	4-FC_6H_4	Et	64%	93:7	28%
76	4-BrC_6H_4	Et	60%	93:7	20%
77	4-$CF_3C_6H_4$	Et	35%	92:8	11%

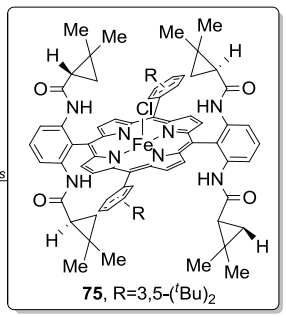

Scheme 26. Cyclopropanation of styrenes catalyzed by **75**

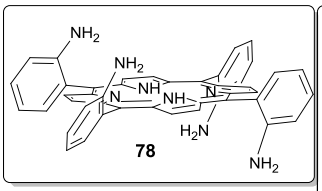

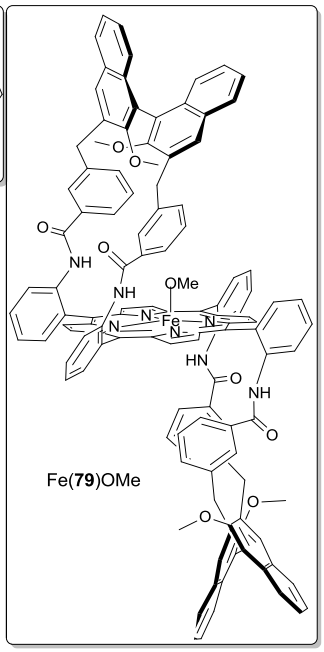

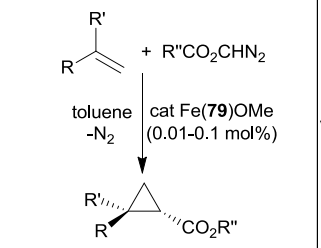

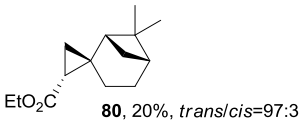

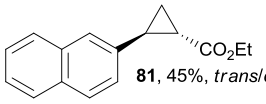

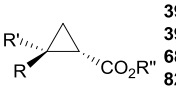

	R	R'	R"	yield	*trans*/*cis*	ee_{trans}
3a	C_6H_5	Me	Et	98%	98:2	87%
3c	4-ClC_6H_4	Me	Et	80%	99:1	80%
3h	4-ClC_6H_4	H	Et	60%	98:2	60%
3g	4-MeC_6H_4	H	Et	72%	99:1	68%
39a	4-$OMeC_6H_4$	H	Et	72%	99:1	60%
39d	4-^{t}BuC_6H_4	H	Et	85%	98:2	63%
68	C_6H_5	C_6H_5	Et	25%	-	48%
82	C_6H_5	Me	^{i}Pr	60%	98:2	67%
83	C_6H_5	Me	^{n}Pr	73%	98:2	40%
84	C_6H_5	Me	^{t}Bu	42%	63:37	7%
85	4-FC_6H_4	Me	Et	46%	95:5	65%
86	4-(CH_2Cl)C_6H_4	H	Et	60%	98:2	-

Scheme 27. Cyclopropanations catalyzed by the iron(III) methoxy complex Fe(**79**)OMe

Considering that many reactions were performed to optimize experimental conditions, only the best results, in terms of *trans*-diastereoselectivity and enantioselectivity, are listed in Scheme 27. Many reactions were promoted by the low catalytic loading of 0.01 mol% and occurred in a very short reaction time, achieving significant TON and TOF values (TON up to 10,000 and TOF (turnover frequency) up to 120,000 h^{-1}).[80] The same catalytic reactions were repeated in the presence of the iron(III) methoxy complex of the porphyrin **87**, which is the achiral precursor of **79**. The reactions occurred with similar diastereoselectivities indicating that, independently from the nature of the chiral portion of the molecule, the reaction diastereocontrol is mainly due to the tridimensional arrangement of the porphyrin backbone.

In view of the achieved results, the final chiral binaphthyl units of **79** were replaced by other chiral 'hats', by reacting **87** with (L)-alanine *tert*-butyl ester, (S)-α-methylbenzylamine, and (L) phenylalanine methyl ester obtaining the corresponding strap-porphyrins **88**-**90** (Scheme 28).[81]

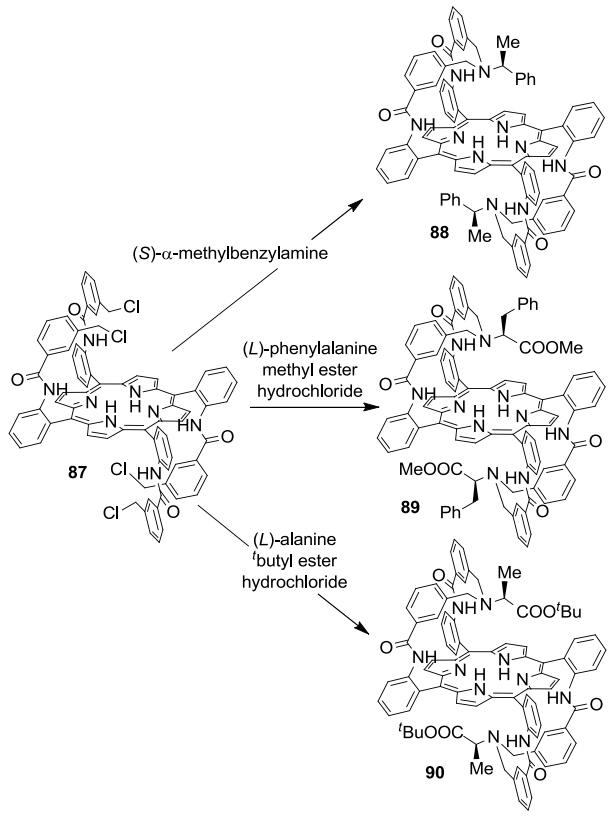

Scheme 28. Synthesis of chiral porphyrins **88**-**90**

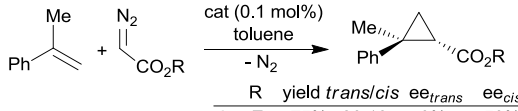

	R	yield	*trans*/*cis*	ee_{trans}	ee_{cis}	cat.
3a	Et	75%	90:10	8%	50%	Fe(**88**)OMe)
3a	Et	78%	95:5	9%	54%	Fe(**89**)OMe)
3a	Et	52%	88:12	4%	53%	Fe(**90**)OMe)
91	Bn	45%	90:10	4%	72%	Fe(**90**)OMe)

Scheme 29. Cyclopropanations catalyzed by chiral porphyrins **88**-**90**

Porphyrins **88**-**90** were employed to synthesize corresponding iron complexes Fe(**88**)(OMe), Fe(**89**)(OMe) and Fe(**90**)(OMe), which were tested as cyclopropanation catalysts, as shown in Scheme 29. Obtained results evidenced a poor enantiocontrol of the procedure and the *cis*-diasteromer, which was formed to a lesser extent, was obtained in the best enantiomeric excess.

The unsatisfactory reaction outcome was justified by a DFT study which revealed that the chiral pickets of tested iron complexes were too flexible for creating a definite chiral environment and in turn, for inducing an efficient enantiodiscrimination.

2.1.4 Artificial iron porphyrinoid biocatalysts. Homogenous catalysis and biocatalysis have been traditionally considered as two different approaches to achieve the same purpose: the efficient and sustainable production of fine chemicals.[82] Nowadays, the development of synthetic strategies based on the use of artificial biocatalysts has permitted the bridging of these two catalytic strategies. Consequently, more attention has been focused on the synthesis of artificial metalloenzymes (ArMs) and the study of their catalytic activity.

The most popular method for obtaining ArMs involves the engineering of natural metalloenzymes. The replacement of aminoacidic residues[82-85] or metal cofactors[86-90] confers unusual and 'non-natural functions' to the bio-hybrid molecule (Scheme 30, *path a* and *path b*). Nevertheless, ArMs can also be obtained either by the supramolecular self-assembly or covalent anchorage of functionalized catalytic systems onto host bio-scaffolds, such as proteins or DNA (Scheme 30, pathways c and d).[91,92] It is worth noting that ArMs can also be synthesized by replacing the natural metal ion[93] with other catalytically active metals.[94,95] Artificial metalloenzymes (ArMs),[92,96,97] represent one of the most efficient and promising classes of bio-hybrid systems able to promote carbene transfer reactions in high yields, regio- and enantioselectivities.

Very recently, F. Arnold and co-authors introduced the concept of the direct evolution strategy[98] to engineer the sequence of heme proteins in order to modulate and/or modify their natural activity. The outstanding results, achieved by using these novel ArMs both in carbene and nitrene[99] transfer reactions, encouraged numerous research groups to join this research field. The present review aims to discuss the complete substitution of the prosthetic group with a synthetic iron-porphyrinoid[100] (Scheme 30, pathway b) as well as the conjugation of the synthetic species to a natural bio-scaffold (Scheme 30, pathways c and d). In both cases the activity of the resulting ArMs can benefit from having an active and selective synthetic iron catalyst embedded into a biological environment.

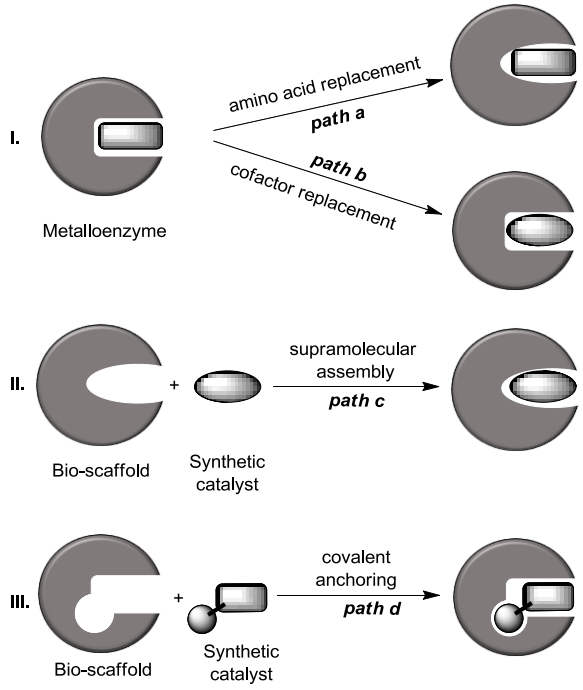

Scheme 30. General approaches for obtaining artificial metalloenzymes (ArMs)

The aminoacidic replacement strategy (Scheme 30, pathway a), in which protein structure rearrangements and changes in the active site shape are responsible for non-natural activities, has been extensively studied[101-107] and reviewed[99,108-111] and it will be not discussed herein. This review only discusses the catalytic activity of artificial biomolecules, which were obtained by inserting a synthetic catalyst into a bio-scaffold.

The strategy to install a synthetic catalyst into a natural scaffold was investigated by Hayashi and co-authors,[112] who compared the catalytic activity of natural heme in native myoglobin (**nMb**) to that of myoglobin reconstituted (**rMb**), which was obtained by inserting iron porphycene (**FePc**) (Fig. 8) in the biological frame. The obtained **rMb**, in the presence of sodium dithionite ($Na_2S_2O_4$) as the reductant species, efficiently promoted the styrene cyclopropanation by EDA forming **3d** in 99% yield, with a complete *trans*-diastereoselectivity and with a TOF value 35 times higher than that of the native myoglobin (**nMb**).

The different kinetics of the cyclopropanation promoted by the natural and non-natural iron catalysts was rationalized by the analysis of the Michaelis-Menten parameters, which were determined at various styrene and EDA concentrations. The superior catalytic efficiency of **rMb** was ascribed to the different reactivity of the two catalysts with respect to the diazo reagent. In particular, the reaction of **rMb** with EDA was investigated by DFT calculations and by using the stopped flow technique. The latter allowed to spectroscopically detect the formation of a new species upon addition of EDA to the starting ferrous **rMb** catalyst. The new species was supposed to be the iron carbene intermediate and the DFT study revealed that the carbene formation was favored by the presence of porphycene. The strong ligand field of porphycene stabilized the triplet state of the iron(II) **rMb** species and reduced the number of intersystem crossing steps, which are necessary to form the active iron carbene intermediate. In addition, the smaller energy barrier observed for **rMb** with respect to that of the native myoglobin **nMb** to reach the singlet carbene species may explains the outstanding TOF values achieved in **rMb**-catalyzed styrene cyclopropanations.

Using the so-called orthogonal enzyme/cofactor pair strategy,[113] which combines the heme substitution with aminoacidic mutations in order to maximize the affinity of the protein heme-binding pocket towards the non-natural cofactor, E. Brustad and co-authors replaced heme with the iron deuteroporphyrin IX (**Fe-DPIX**) in a model bacterial cytochrome P450 ($P450_{BM3}$).[114] Binding studies and structural investigations identified the WIVS-FM variant as the most selective scaffold for embedding **Fe-DPIX** due to the presence of two mutations (L272W and G265F).

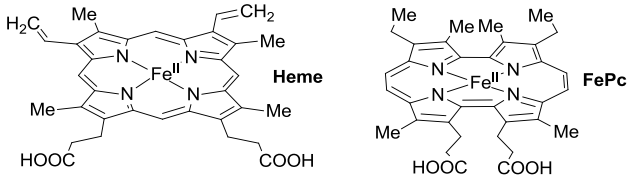

Fig. 8. Heme and iron porphycene (**FePc**)

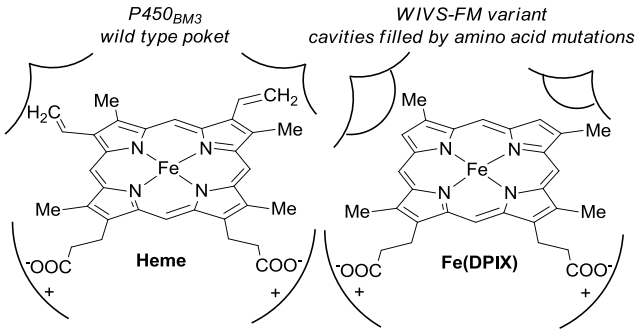

Fig. 9. Natural bacterial cytochrome **P450** and its **WIVS-FM** variant

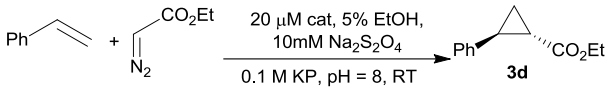

cat.	conditions	yield	*trans*/*cis*	ee_{cis}	ee_{trans}
heme	anaerobic	7%	84:16	0%	-11%
Fe(DPIX):	anaerobic	5%	87:13	3%	-11%
BM3hT268A/heme	anaerobic	57%	99:1	-6%	-97%
BM3hT268A/heme	aerobic	2%	90:10	-15%	-42%
WIVS-FMT268A/Fe(DPIX)	anaerobic	44%	88:12	-51%	-46%
WIVS-FMT268A/Fe(DPIX)	aerobic	12%	88:12	-33%	-37%

Scheme 31. Cyclopropanation of styrene catalyzed by $P450_{BM3}$ ArMs

These two mutations were able to fill the cavities generated in the binding pocket by the lack of vinyl groups onto the deuteroporphyrin ligand (Fig. 9). The two mutations, together with the cofactor replacement, induced conformational rearrangements in the protein scaffold which were responsible for unusual reactivities. In fact, the obtained artificial metalloenzyme showed the loss of the monooxygenase activity and this feature encouraged the authors to test the metalloenzyme as a catalyst of cyclopropanation reactions under aerobic conditions, which are generally prohibitive for P450-mediated carbene transfer reactions.

After the additional mutation T268A, which notably increased the carbene transferase activity,[82] **WIVS-FM T268A/Fe(DPIX)** species was initially tested in the model reaction between styrene and EDA under anaerobic conditions

As expected, **WIVS-FM T268A/Fe(DPIX)** afforded the desired cyclopropane **3d** in a yield and TTN (TTN = total turnover number) comparable with that observed by using the parent heme-containing enzyme **BM3hT268A/heme** (Scheme 31). Even if a lower selectivity was observed, probably as a consequence of a different conformational rearrangement of **WIVS-FM T268A/Fe(DPIX)**, the artificial metalloenzyme maintained part of its reactivity and selectivity in presence of molecular oxygen suggesting the availability of the orthogonal strategy as a general tool to tune the reactivity of ArMs.

In the context of cyclopropanation reactions catalyzed by ArMs under aerobic conditions, R. Fasan and co-authors investigated the oxygen susceptibility and the catalytic activity of myoglobin when iron-chlorin e6 **[Fe(Ce6)]**[115] was embedded in its biologic structure. Considering the possibility of reducing the oxygen affinity of heme by introducing electron-withdrawing substituents on the porphyrin scaffold,[116] the electron-deficient chlorin e6 (**Ce6**) was

incorporated in the well-known carbene transfer catalyst **Mb(H64V,V68A)** variant,[117] to increase the electrophilicity and reactivity of the metal-carbenoid intermediate.

The influence of the non-native cofactor in modifying the structure of the biological environment was examined by performing circular dichroism experiments that showed the absence of perturbations in the secondary structure of **Mb(H64V,V68A)** after the replacement of heme with **[Fe(Ce6)]**.

The **Mb(H64V,V68A)[Fe(Ce6)]** catalyst promoted the styrene cyclopropanation under anaerobic conditions in a quantitative yield and with an excellent diastero- and enantioselectivity (99.6% de, 98.5% ee), showing a reactivity comparable to that of its **Mb(H64V,V68A)** precursor. Thus, the catalytic performance of **Mb(H64V,V68A)[Fe(Ce6)]** was evaluated under aerobic conditions where the artificial enzyme showed higher activity than that observed by using the heme-containing precursor. The desired cyclopropane **3d** was formed in a quantitative yield, diastero- and enantioselectivity (Scheme 32). In contrast, the cyclopropanation activity of **Mb(H64V,V68A)[Fe(Ce6)]** was drastically reduced by the substitution of the proximal His93 with residues such as phenylalanine (Phe) or alanine (Ala) confirming the pivotal role of the iron axial ligand in carbene transfer reactions.

The obtained results established the high oxygen-tolerance of **Mb(H64V,V68A)[Fe(Ce6)]**, which promoted the cyclopropanation of various styrenes in excellent yields (up to 99%) and diastero- and enantioselectivities (de up to 99% and ee up to 98%) (Scheme 32).

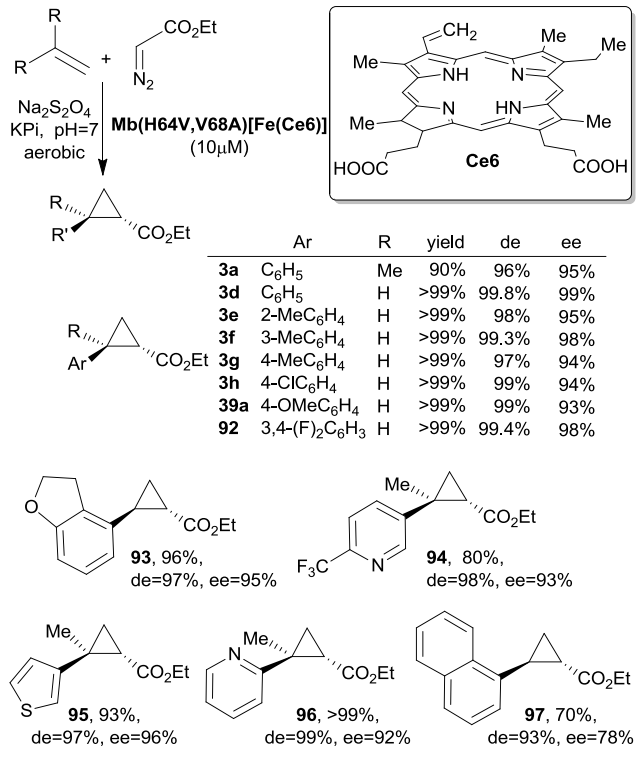

	Ar	R	yield	de	ee
3a	C_6H_5	Me	90%	96%	95%
3d	C_6H_5	H	>99%	99.8%	99%
3e	2-MeC_6H_4	H	>99%	98%	95%
3f	3-MeC_6H_4	H	>99%	99.3%	98%
3g	4-MeC_6H_4	H	>99%	97%	94%
3h	4-ClC_6H_4	H	>99%	99%	94%
39a	4-$OMeC_6H_4$	H	>99%	99%	93%
92	3,4-$(F)_2C_6H_3$	H	>99%	99.4%	98%

93, 96%, de=97%, ee=95%

94, 80%, de=98%, ee=93%

95, 93%, de=97%, ee=96%

96, >99%, de=99%, ee=92%

97, 70%, de=93%, ee=78%

Scheme 32. Alkene cyclopropanation catalyzed by **Mb(H64V,V68A)[Fe(Ce6)]**.

Bearing in mind the role of the protein axial ligand,[118,119] Fasan's group also examined the synergic effect of cofactor and His93 substitutions replacing both the heme, with the electron-deficient analogue iron-2,4-diacetyl deuteroporphyrin IX **[Fe(DADP)],** and mutating the His93 to the non-natural amino acid *N*-methyl-histidine (NMH). The cofactor replacement, together with the axial ligand mutation, didn't modify the protein structure but was responsible for its increasing redox potential. The carbene transferase activity of the artificial **Mb(H64V,V68A,H93NMH)[Fe(DADP)]** was evaluated under different catalytic conditions in the model reaction between styrene and EDA (Scheme 33).[120] The obtained biocatalyst showed a high reactivity affording the product **3d** in an excellent yield and selectivity both under anaerobic/reducing and anaerobic/non-reducing conditions (>99% yield, 99% de, 99% ee). A good catalytic activity was maintained under aerobic/reducing conditions (85% yield, 99% de, 98% ee).

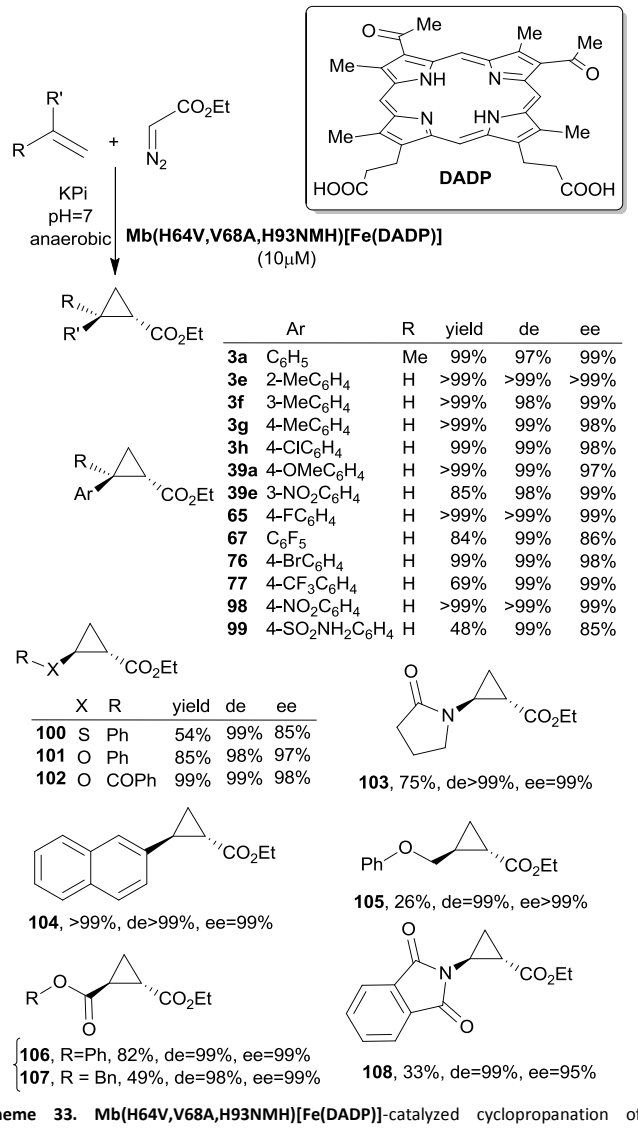

	Ar	R	yield	de	ee
3a	C_6H_5	Me	99%	97%	99%
3e	2-MeC_6H_4	H	>99%	>99%	>99%
3f	3-MeC_6H_4	H	>99%	98%	99%
3g	4-MeC_6H_4	H	>99%	99%	98%
3h	4-ClC_6H_4	H	99%	99%	98%
39a	4-$OMeC_6H_4$	H	>99%	99%	97%
39e	3-$NO_2C_6H_4$	H	85%	98%	99%
65	4-FC_6H_4	H	>99%	>99%	99%
67	C_6F_5	H	84%	99%	86%
76	4-BrC_6H_4	H	99%	99%	98%
77	4-$CF_3C_6H_4$	H	69%	99%	99%
98	4-$NO_2C_6H_4$	H	>99%	>99%	99%
99	4-$SO_2NH_2C_6H_4$	H	48%	99%	85%

	X	R	yield	de	ee
100	S	Ph	54%	99%	85%
101	O	Ph	85%	98%	97%
102	O	COPh	99%	99%	98%

103, 75%, de>99%, ee=99%

104, >99%, de>99%, ee=99%

105, 26%, de=99%, ee>99%

106, R=Ph, 82%, de=99%, ee=99%
107, R = Bn, 49%, de=98%, ee=99%

108, 33%, de=99%, ee=95%

Scheme 33. Mb(H64V,V68A,H93NMH)[Fe(DADP)]-catalyzed cyclopropanation of alkenes.

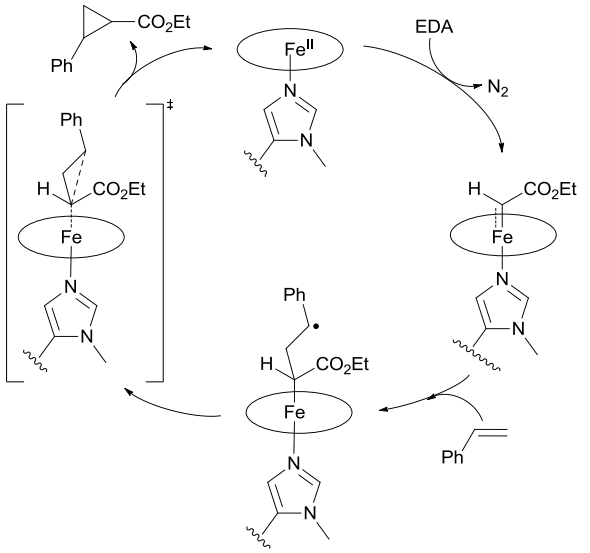

Scheme 34. Proposed mechanism for cyclopropanations catalyzed by **Mb(H64V,V68A,H93NMH)[Fe(DADP)]**

The study of the substrate scope displayed the ability of **Mb(H64V,V68A,H93NMH)[Fe(DADP)]** in efficiently promoting, under anaerobic/non-reducing conditions, the cyclopropanation of both electron-rich and electron-poor alkenes. Very good results were also attained by reacting more challenging substrates, such as acrylate esters and trifluoromethyl-, nitro- and pentafluoro styrenes (Scheme 33).[120] Hammett analyses and radical rearrangement/trapping experiments were undertook to explain the catalytic superiority of **Mb(H64V,V68A,H93NMH)[Fe(DADP)]** with respect to the heme/histidine-containing precursor. Based on the obtained data, the authors proposed a stepwise mechanism in which the formation of a radical-type iron-carbene intermediate was responsible for the expanded reaction scope (Scheme 34). In addition, the cofactor/axial ligand substitution was considered responsible for the high activity under non-reducing conditions. These structural modifications may increase the protein redox potential favoring the reduction -by EDA- of the starting Fe(III) species to the Fe(II) intermediate, which was then involved in the proposed radical mechanism.

The above-mentioned ArMs were all obtained by using a heme protein as the biological scaffold for taking advantage of the presence of a well-defined cofactor binding site and a large hydrophobic binding pocket, which is appropriate for the accommodation of cyclopropanation substrates.

An alternative strategy is the anchorage of either a heme group or an iron porphyrinoid onto a bio-scaffold, using the synthetic approaches illustrated in Scheme 30 (pathways c and d). With this idea in mind, G. Roelfes and co-authors investigated the carbene transfer activity of the heme group assembled to different variants of the lactococcal multidrug resistance regulator (LmrR),[121] a homodimeric protein with a large and hydrophobic binding pocket at the dimer interface, which is well suitable for hosting the hydrophobic reaction components.

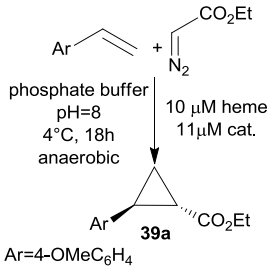

cat.	yield	*trans*/*cis*	ee
heme	5%	>85:15	nd
LmrR/heme	25%	>85:15	17%
LmrR_F93A/heme	23%	>85:15	11%
LmrR_D100A/heme	38%	>85:15	24%
LmrR_W96A/heme	28%	>85:15	>5%
LmrR_V15A/heme	1.5%	>85:15	17%
LmrR_M8A/heme	36%	>85:15	44%

Scheme 35. Synthesis of cyclopropane **39a** catalyzed by LmrR-based catalysts

Some artificial metalloenzymes were obtained by the *in situ* self-assembly of the iron(III) chloroprotoporphyrin IX (hemin) and six different protein scaffolds. The reduction of the so-obtained iron(III) species with sodium dithionate afforded the corresponding iron(II) biomolecules where the hemin group was reduced to the active heme moiety. All the catalysts depicted in Scheme 35 were tested as the promoter of the model cyclopropanation of 4-methoxystyrene by EDA yielding the corresponding cyclopropane **39a** in modest yields and enantioselectivities (Scheme 35).

Except in one case, all the other LmrR-based catalysts worked better than the free hemin cofactor although the heme group in these ArMs should have been inaccessible for the incoming substrates being placed in the protein hydrophobic pocket and sandwiched between two tryptophan residues. The authors proposed, on the basis of molecular dynamic calculations and protein-ligand docking studies, a dynamic behavior of the LmrR-based enzymes, which can rearrange their conformation during the catalytic reaction allowing the substrates access with the consequent formation of the active iron-carbene intermediate.

Roelfes's research group also explored the use of DNA as an alternative bio-scaffold for the synthesis of iron containing artificial biocatalysts.[122] Considering the high affinity of porphyrin ligands towards DNA, several cationic *meso*-tetrakis(*N*-alkylpyridyl)porphyrins (**109**-**113**, Scheme 36) were tested in the self-assembly with salmon testes DNA (st-DNA) and the corresponding iron(III) complexes were examined as catalysts for the cyclopropanation of 2-methoxystyrene. The length and position of *N*-alkyl moieties onto the porphyrin ring influenced the binding with DNA and consequently affected the catalytic effectiveness (Scheme 36).

Comparing the activity of DNA-based catalysts with that of the sole iron porphyrins **109**-**113**, an acceleration effect was observed in presence of DNA and the best compromise, in terms of yield (14%) and enantioselectivity (ee_{trans} = 42%), was achieved by using the hybrid catalyst formed from the conjugation of *ortho*-*N*-methylpyridinium porphyrin **111** with DNA. To explain the obtained positive results, the authors proposed the formation of a catalytically active hydrophobic pocket during the binding of **111** along the DNA chain.

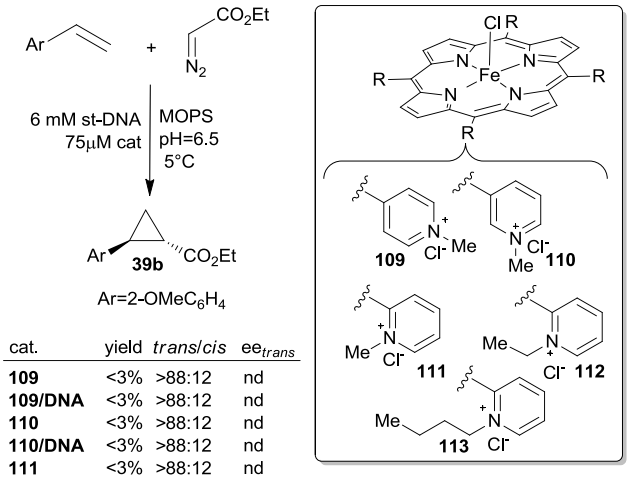

cat.	yield	*trans*/*cis*	ee_{trans}
109	<3%	>88:12	nd
109/DNA	<3%	>88:12	nd
110	<3%	>88:12	nd
110/DNA	<3%	>88:12	nd
111	<3%	>88:12	nd
111/DNA	<14%	>88:12	42%
112	<33%	>88:12	nd
112/DNA	<15%	>88:12	23%
113	26%	>88:12	nd
113/DNA	<11%	>88:12	5%

Scheme 36. Synthesis of cyclopropane **39b** catalyzed by DNA-based catalysts

The authors proposed that i) DNA induced the reaction enantiocontrol and ii) the formation of the hydrophobic pocket permitted a high concentration of the reaction substrates (EDA and styrene derivatives). The local increasing of the molarity of the reaction components can be responsible for the rate acceleration, which was observed when DNA-based catalysts were employed.

The DNA-acceleration effect was also observed by D. Sen and co-authors who studied the catalytic activity of heme in presence of different folds of DNA (single-stranded, double-stranded and G-quadruplex).[123] In the model cyclopropanation of styrene by EDA, only the GQs (GQ = G-quadruplex) derivatives efficiently activated the heme towards the carbene transfer reaction. The formation of the *trans* isomer of **3d** occurred in good yields and high rates but no reaction enantiocontrol was observed. Among all the so-called DNAzymes (Scheme 37), only the artificial metalloenzyme formed by using the DNA variant $\mathbf{(dA_4G_5A_4)_4}$ was active in promoting the formation of **3d** with a poor enantioselectivity (ee=3% at 21°C and 10% at 0°C). The complete absence of the enantiocontrol, which was observed by using the other DNAzymes, was ascribed to their lower structural complexity with respect to $\mathbf{(dA_4G_5A_4)_4}$. In fact, it is well-known that, in view of the end-staking binding mode of heme on GQs, the enantioselectivity can only be obtained in the presence of structurally complex GQs. In these cases the numerous pendant nucleotides form a definite tridimensional chiral cage around the heme where the enantiodiscrimination should occur, as in the case of $\mathbf{(dA_4G_5A_4)_4}$.

2.1.5 Mechanistic investigations. It is widely recognized that the iron porphyrin-promoted cyclopropanation of alkenes by diazo compounds occurs through the formation of a carbene active intermediate. The general reaction mechanism is illustrated in Scheme 38.

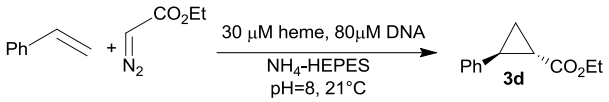

cat.	yield	*trans*/*cis*	ee_{trans}
heme	3%	90:10	nd
dsDNA/heme	3%	90:10	nd
scrambled G4/heme	11%	91:9	nd
G4-AAA/heme	77%	92:8	nd
G4-TTT/heme	80%	92:8	nd
$(dA_4G_5A_4)_4$/heme	51%	85:15	3%

Scheme 37. Synthesis of **3d** catalyzed by DNAzymes

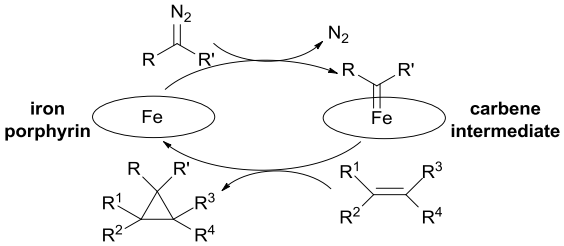

Scheme 38. General proposed mechanism for the iron porphyrin-mediated cyclopropanation of alkenes by diazo compounds

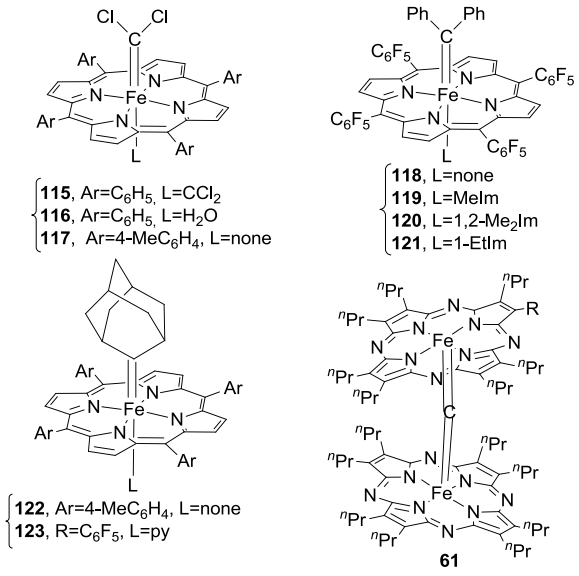

Fig. 10. Iron Carbene complexes whose molecular structure was solved by X-ray analysis

The first iron porphyrin carbene complex was isolated in 1977 by D. Mansuy and co-authors; the reaction of Fe(TPP) (**114**) with CCl_4 yielded the complex $Fe(TPP)CCl_2$ (**115**) (Fig. 10), displaying an iron(II) metal center coordinated to a neutral $:CCl_2$ carbene ligand.[124] Since then, some other porphyrin carbene derivatives have been stable enough to be isolated and structurally characterized. These iron carbene porphyrins were obtained either from diazo compounds, having a reasonable lifetime to be handled in a laboratory, or from alternative carbene sources.

Porphyrin carbene complexes whose molecular structure was solved by X-ray analysis, namely $Fe(TPP)(CCl_2)(H_2O)$ (**116**),[125,126]

Fe(TTP)(CCl_2) (**117**),[126] Fe(TPFPP)(CPh_2) (**118**),[43,126] Fe(TPFPP)(CPh_2)(MeIm) (**119**),[43] Fe(TPFPP)(CPh_2)(1,2-Me_2Im) (1,2-Me_2Im = 1,2-dimethylimidazole) (**120**),[127] Fe(TFPP)(CPh_2)(1-EtIm) (1-EtIm = 1-ethylimidazole) (**121**),[127] Fe(TTP)(Ad)(py) (Ad = 2-adamantylidene) (**122**),[44] Fe(TPFPP)(Ad)(py) (**123**),[44] $(LFe)_2C$ (L = dianion of octapropylporphyrazine) (**61**),[128] are listed in Fig. 10.

It should be noted that, albeit alkyl-substituted carbenes are less stable than homologous halo- or aryl carbenes, complexes **122** and **123** were isolated and characterized thanks to the diamondoid structure of the Ad ligand, which conferred stability to the corresponding carbene complex. Whilst the dimer μ-carbido diiron octapropylporphyrazine **61** shows an unambiguous iron(IV) metal center, all the other complexes were described as iron(II) complexes in a singlet state (*S*=0). Even if the formation of iron(IV) carbene porphyrin intermediates[108] was first proposed, also on the basis of a isomer shifts in Mössbauer spectra,[43] additional experimental (UV-vis, NMR, X-ray, XANES spectroscopies) and theoretical investigations provided a more correct description of complexes reported in Fig. 10. They were represented as iron(II) derivatives, with a terminal, neutral carbene ligand coordinated to the metal center.[129] It was proposed that the iron-carbene bond forms thanks to the sigma donation of the carbon lone-pair to the metal atom, which is followed by a moderate π-back-donation from the metal to the carbene ligand. This electronic picture is in agreement with the electrophilic nature of the carbene moiety and explains the stability of carbene complexes showing EWGs on the porphyrin skeleton.[43,126,127] The positive effect of electron-poor porphyrin ligands in enhancing the chemical stability of corresponding carbenes were also supported by DFT calculations, which elucidated the role of an axial ligand *trans* to the carbene functionality in determining the formation of the iron-carbene bond.[130]

While the electronic structure of stable porphyrin carbene complexes reported in Fig. 10 has been elucidated in detail, the electronic nature of iron carbene species, whose chemical instability prevented their full experimental characterization, has been mainly proposed by using a theoretical approach. In particular, great attention has been devoted to the study of the electronic features of those iron carbenes that have always been proposed as active catalytic intermediates, such as carbenes deriving from the reaction of iron porphyrins with EDA. As previously discussed, both iron(III) and iron(II) derivatives have been used as catalysts. However, it is commonly proposed that the starting iron(III) complex is reduced *in situ*, either by the added reductant ($CoCp_2$, $Na_2S_2O_4$) or by the diazo reagent, to an iron(II) intermediate that is effectual for reacting with EDA. The iron(II) complex first interacts with the diazo compound yielding an iron-diazo adduct, which is transformed into the desired iron-carbene intermediate by extruding molecular nitrogen (Scheme 39a).[110]

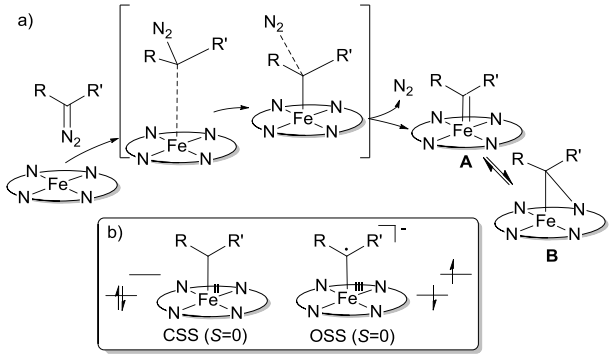

Scheme 39. General scheme of the iron carbene complex formation

The structure of the putative *mono*-substituted Fe(porp)($CHCO_2$Et) (porp = generic porphyrin) carbene intermediate, formed during the alkene cyclopropanation by EDA, was proposed on the basis of *in situ* recorded ^{1}H NMR spectrum,[131] by the mass spectrometry analysis of the gas-phase reaction[132] and DFT calculations.[130,133] The electronic nature of Fe(porp)($CHCO_2$Et) is still under debate because two different structures were proposed, which consist either in a closed-shell singlet (CSS) iron(II) complex reported by Y. Zhang and co-authors[130] or in a diradicaloid antiferromagnetically coupled open-shell singlet (OSS) iron(III) compound, as proposed by S. Shaik and co-authors (Scheme 39b).[133]

To shed some light on this discrepancy, M. Sodupe, X. Solans-Monfort and co-authors modeled complexes with different axial ligands and carbene substituents. Achieved computational results suggested that the electronic and steric characteristic of the environment, in which the iron metal is placed, can be responsible for the reported differences of the carbene electronic structures.[134] For instance, the quantum mechanics (QM) and QM/molecular mechanics (MM) calculations of the styrene cyclopropanation by EDA promoted by iron porphine (the parent compound of porphyrin having hydrogen atoms on the four *meso*-positions), bearing either a methyl thiolate or a methoxide as the axial ligand, revealed the formation of the OSS state as the most stable carbene intermediate. In this specific case the CCS state was 5 kcal/mol higher than both the OSS and the triplet states.[104]

However, independently from the electronic nature of the carbene, it is generally assumed that the active terminal carbene (structure **A** in Scheme 39) is in equilibrium with a bridged carbene (where the carbene carbon atom is contemporarily linked to a pyrrolic nitrogen atom and the iron(III) metal center, structure **B** in Scheme 39). The bridged iron species is usually thermodynamically more stable than the terminal one and does not represent the active intermediate in the reaction with the alkene.[80] This statement was recently corroborated by the X-ray characterization of a bridged carbene complex, which was obtained by reacting EDA with an engineered myoglobin. The DFT study revealed that the cyclopropanation of styrene can occur only upon its equilibration with the catalytically active terminal carbene.[135]

Considering the possible formation of either CSS or OSS iron carbene intermediate, two possible pathways were envisaged

for the further reaction of the carbene species with the alkene. Y. Zhang and co-authors modelled both the iron(II)-based concerted pathway and the iron(III)-based stepwise mechanisms of the reaction between styrene and $(CO_2Et)(Ph)CN_2$ catalyzed by the myoglobin variant **Mb(H64V,V68A)** (Scheme 40). The DFT study, employed by using porphine as the simplified model of **Mb(H64V,V68A)**, indicated that the concerted mechanism was favored with respect to the radical stepwise pathway, as also supported by the irrelevant effect registered after the addition of the radical trap 5,5-dimethyl-1-pyrroline N-oxide (DMPO) to the mixture.

In accordance to the high dependence of the reaction mechanism on the chemical environment surrounding the active iron, the replacement of the catalyst **Mb(H64V,V68A)** by **Mb(H64V,V68A,H93NMH)-[Fe(DADP)]**, in the styrene cyclopropanation by EDA, provoked a drastic change of the catalytic mechanism. As reported by R. Fasan and D. Carminati,[120] when the cyclopropanation was performed in the presence of the radical trap DMPO or 4-hydroxy-2,2,6,6-tetramethylpiperidin-1-oxyl (TEMPOL), a decrease of both the reaction productivity and rate was registered. The obtained experimental results pointed out a stepwise catalytic mechanism in which an OSS carbene species was formed as the active intermediate. The different reaction outcomes observed by using the two engineered iron-catalysts underlined the strong influence of the nature of porphyrin and axial ligands in determining the catalytic pathway.

A similar result was obtained by Y. Liu and co-authors, whose theoretical investigation supported that, in the presence of an axial ligand with a strong "push effect" (such as -SMe or -OMe) the styrene cyclopropanation occurred by a radical mechanism.[104] In addition, a detailed DFT study by R. Fasan and Y. Zhang, indicated a strong dependence of the activation barriers of iron porphyrin-mediated cyclopropanations on the nature of carbene and porphyrin substituents as well as axial ligands coordinated to the iron metal center.[118]

In order to better clarify that, independently from the oxidation state of the starting iron catalyst, an iron(II) derivative is always the active species, M. Torrent-Sucarrat, F. P. Cossío and co-authors investigated the mechanism of Fe(III)(porphine)Cl (**124**)-catalyzed reaction of ethylene with diazomethane by using DFT calculations.

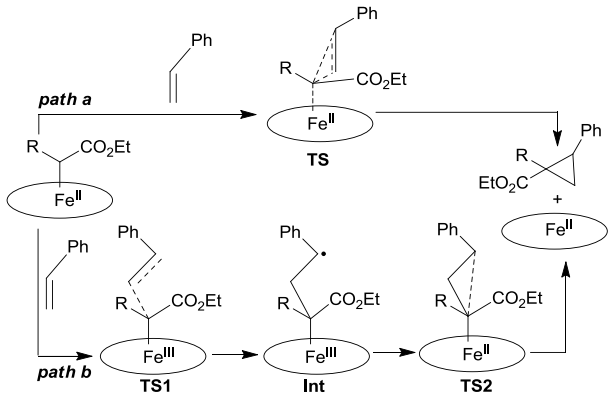

Scheme 40. Concerted (*path a*) and stepwise (*path b*) proposed mechanism of the reaction between the iron carbene and styrene

The computational analysis revealed that the reaction of **124** with CH_2N_2 afforded a very stable bridged complex (Fe-CH_2-N(Pyrrole)), whose transformation into a catalytically active terminal carbene was unfavorable and consequently it must be considered as a dead-end catalytic species.[136]

Conversely, when an iron(II) porphyrin complex was analyzed, the catalytic cycle involved a stepwise multistate (singlet, triplet, and quintet spin states) mechanism. Theoretical data evidenced the formation of both terminal and bridged carbene derivatives, which were interconnected in order to maintain the suitable amount of active terminal carbene in the reaction medium. This bridged-terminal equilibrium allows the catalytic cycle to proceed.[136]

In view of the influence of the molecular architecture in determining the catalytic mechanism of the cyclopropanation, L. Toma, B. Boitrel, E. Gallo and co-authors studied the effect of the tridimensional arrangement of the porphyrin skeleton on the stereocontrol of the reaction.[80] As previously discussed, the C_2 symmetrical porphyrin Fe(**79**)OMe was responsible for very efficient diastereo- and enantio-discriminations. Thus, In order to better understand the role of the entire skeleton of this chiral porphyrin, a very detailed DFT investigation was undertaken. A considerable effort was devoted to modelling the whole molecule in order to evaluate the real influence of the environment surrounding the metal atom in driving the reaction outcome. Fe(**79**)OMe was stable in the sextet state (S=5/2), as also revealed by magnetic measurements,[79] and the DFT analysis disclosed two different conformations as the most stable. The computational analysis of the reaction of Fe(**79**)OMe with EDA indicated the possible formation of both the bridged and terminal carbenes, in the respectively preferred quartet and doublet state. The former bridged carbene was more stable by about 20 kcal/mol than the terminal one, which resulted being the active catalytic species in the alkene cyclopropanation. Next, the DFT analysis of the α-methylstyrene reaction with the terminal carbene permitted the optimization of four TSs, namely two *trans*-TSs, which are responsible for the formation of the two enantiomers of the *trans*-cyclopropanes and two *cis*-TSs that evolve into the other two enantiomers in *cis*-configuration. Calculations indicated that the two *trans*-TSs were considerably more stable than the two *cis*-TSs because in the *cis*-approach the styrene phenyl group pointed towards the most crowded region of the molecule (Fig. 11). Thus, theoretical calculations furnished a geometrical explanation for the excellent diastereoselectivities achieved in the Fe(**79**)OMe-catalyzed cyclopropanations. On the other hand, there was only a small energy difference between the two *trans*-TSs, which justifies the incomplete differentiation between the enantiomeric reaction paths of the cyclopropanation of some alkene substrates.

Successive computational investigations took into account the possible reduction of Fe(**79**)OMe by EDA to give an *in situ* reduced form of the catalyst and evidenced that the reduced species performs much better than the oxidized one due to the higher stability of the OS singlet terminal carbene intermediate and the lower energy barrier of the TS leading to it.

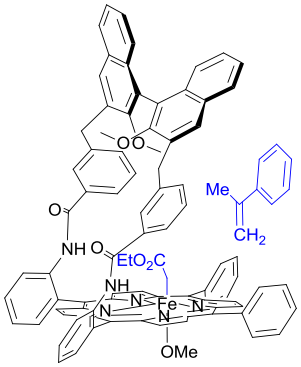

Fig. 11. Schematic *trans*-approach of α-methylstyrene to the modelled carbene intermediate deriving from Fe(**79**)OMe (only one strap was considered) and EDA

Moreover, the computational data disclosed the very significant effect of the organic portion on the reaction energy profile.[130,137]

As previously reported, the replacement of chiral binaphthyl units of porphyrin **79** with amino acid residues yielded chiral porphyrins **89** and **90**, which did not furnish a substantial reaction enantiocontrol. DFT studies, carried out by L. Toma and co-authors,[81] suggested that even if chiral pickets of complexes **89** and **90** are close enough to the active catalytic iron metal, they are too mobile for a discrimination of enantiomeric pathways.

In line with experimental results, the *trans*-TSs of the reaction between the EDA-deriving iron carbene and *α*-methylstyrene were preferred over the *cis*-TSs. As in the case of the Fe(**79**)OMe-catalyzed cyclopropanations, the good diastereoselectivity observed was due to the C_2-symmetrical pickets present in the porphyrin.

2.2 Non-heme iron complexes

Even if porphyrinoids-base iron complexes represent the most studied class of iron catalysts for carbene transfer reactions of diazo compounds, many other nitrogen-ligand iron complexes have been tested.

Iron *bis*-oxazoline derivatives have demonstrated to be efficient catalysts in many asymmetric organic transformations,[138,139] including cyclopropanations. In particular, the ligands depicted in Fig. 12 were employed in combination with $Fe(ClO_4)_2{\cdot}4H_2O$ and $NaBAr_F$ ($NaBAr_F$ = sodium tetrakis-[3,5-*bis*(trifluoromethyl)phenyl]borate) to promote the asymmetric intramolecular cyclopropanation of different unsaturated substrates.

The catalytic **(*R*$_a$,*S*,*S*)-125**/$Fe(ClO_4)_2{\cdot}4H_2O$/$NaBAr_F$ system (cat A in Scheme 41) was active in mediating the cyclopropanation of diazoesters forming the corresponding [3.1.0]bicycloalkane lactones **127a**-**127t**.[140] The study of the reaction scope underlined, except in few cases, good catalytic productivities (yields up to 96%). The enantioselectivity was related to both the electronic the steric characteristics of α-diazoesters. Substrates having internal double bonds formed corresponding cyclopropanes with a low ee (**127s**, **127t**) as well as α-diazoesters showing EDG substituents on the ortho position of the phenyl ring (**127d**).

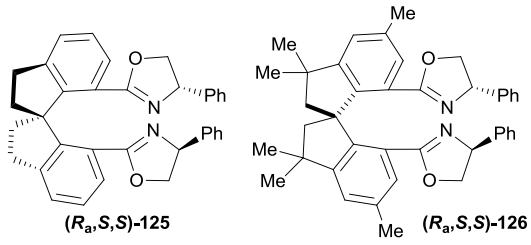

Fig. 12. Structure of chiral spiro-*bis*-oxazoline ligands used in combination with an iron salt to promote intramolecular cyclopropanations

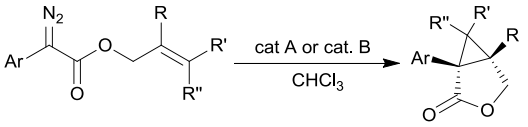

cat A: **(*R*$_a$,*S*,*S*)-125** (12 mol%)/$Fe(ClO_4)_2{\cdot}4H_2O$(10 mol%)/$NaBAr_F$ (12 mol%)
cat B: **(*R*$_a$,*S*,*S*)-126** (12 mol%)/$FeCl_2{\cdot}4H_2O$ (10 mol%)/$NaBAr_F$ (12 mol%)

		cat A		cat B	
	Ar	yield	ee	yield	ee
127a	C_6H_5	94%	92%	92%	91%
127b	2-FC_6H_4	93%	93%	-	-
127c	2-ClC_6H_4	96%	94%	96%	95%
127d	2-MeC_6H_4	88%	4%	-	-
127e	3-$CF_3C_6H_4$	89%	96%	84%	91%
127f	3-ClC_6H_4	90%	94%	93%	96%
127g	3-MeC_6H_4	86%	90%	-	-
127h	3-$OMeC_6H_4$	90%	93%	85%	91%
127i	4-FC_6H_4	94%	91%	92%	91%
127j	4-ClC_6H_4	91%	90%	93%	92%
127k	4-MeC_6H_4	90%	85%	-	-
127l	4-$OMeC_6H_4$	93%	44%	-	-
127m	3,4-$Cl_2C_6H_3$%	94%	94%	-	-
127n	2-naphthyl	92%	93%	-	-
130a	3-FC_6H_4	-	-	94%	94%
130b	4-BrC_6H_4	-	-	91%	91%
130c	3-BrC_6H_4	-	-	90%	80%
130d	2-BrC_6H_4	-	-	90%	91%
130e	4-$CF_3C_6H_4$	-	-	90%	90%
130f	4-$NO_2C_6H_4$	-	-	80%	85%
130g	3-$NO_2C_6H_4$	-	-	76%	92%

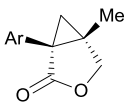

	Ar	R	yield	ee	cat
127o	C_6H_5	Ph	87%	97%	A
127p	C_6H_5	Et	82%	81%	A
127q	C_6H_5	^{i}Pr	76%	71%	A
127r	C_6H_5	H	52%	6%	A
130h	4-ClC_6H_4	^{i}Pr	73%	74%	B
130i	4-ClC_6H_4	Ph	82%	63%	B

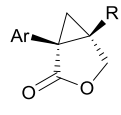

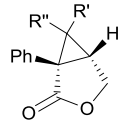

127s, R'=Me, R"=Me, 85%, ee=33%, cat. A
127t, R'=H, R"=C_6H_5, 55%, ee=5%, cat. A

Scheme 41. Synthesis of [3.1.0]bicycloalkane lactones **127a**-**127t** and **130a**-**130i** catalyzed by the **(*R*$_a$,*S*,*S*)-125**/$Fe(ClO_4)_2{\cdot}4H_2O$/$NaBAr_F$ (cat A) or **(*R*$_a$,*S*,*S*)-126**/$FeCl_2{\cdot}4H_2O$/$NaBAr_F$ (cat B) systems.

A slight structural modification of spiro-*bis*-oxazoline **125** yielded **126**, which was used also by X. Lin and co-authors for the intramolecular asymmetric cylopropanation of α-diazoesters.[141] As reported in Scheme 41 (cat B), reaction yields and enantioselectivities of compounds were comparable to those achieved by using **(*R*$_a$,*S*,*S*)-125**/$Fe(ClO_4)_2{\cdot}4H_2O$/$NaBAr_F$ system as the reaction promoter. In addition to compounds already obtained by using cat A, **(*R*$_a$,*S*,*S*)-126**/$FeCl_2{\cdot}4H_2O$/$NaBAr_F$ (cat B) was active in promoting the synthesis of **130a**-**130i** compounds (scheme 41).

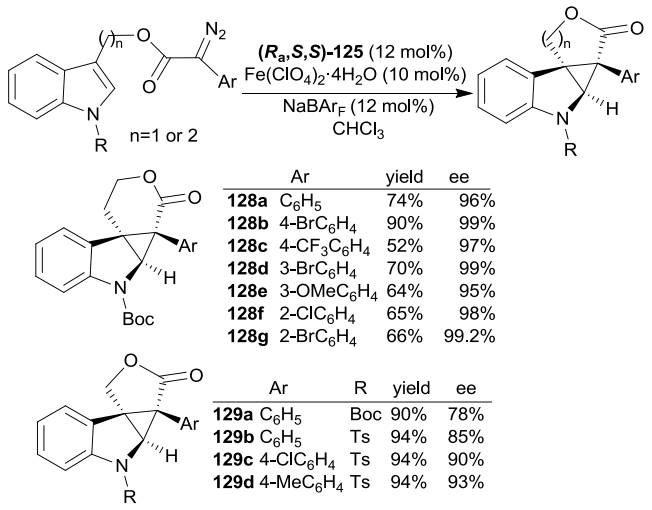

	Ar	yield	ee
128a	C_6H_5	74%	96%
128b	4-BrC_6H_4	90%	99%
128c	4-$CF_3C_6H_4$	52%	97%
128d	3-BrC_6H_4	70%	99%
128e	3-$OMeC_6H_4$	64%	95%
128f	2-ClC_6H_4	65%	98%
128g	2-BrC_6H_4	66%	99.2%

	Ar	R	yield	ee
129a	C_6H_5	Boc	90%	78%
129b	C_6H_5	Ts	94%	85%
129c	4-ClC_6H_4	Ts	94%	90%
129d	4-MeC_6H_4	Ts	94%	93%

Scheme 42. Intramolecular cyclopropanation of indoles **128a**-**128g** and **129a**-**129d** mediated by **(*R*a,*S*,*S*)-125**/$Fe(ClO_4)_2{\cdot}4H_2O$/$NaBAr_F$

Both electron-poor and electron-rich substrates reacted well with both systems yielding the desired compounds in good yields and enantioselectivities. In addition, the synthesis of **127j** was promoted by **(*R*a,*S*,*S*)-126**/$FeCl_2{\cdot}4H_2O$/$NaBAr_F$ (cat B) in a large scale underlining the practical application of the methodology. It worth noting that although both systems also worked by using an iron(III) source, lower performances were observed.

The **(*R*a,*S*,*S*)-125**/$Fe(ClO_4)_2{\cdot}4H_2O$/$NaBAr_F$ catalytic combination was also employed for the intramolecular cyclopropanation of indoles.[142]Desired [3.1.0]bicyclic rings were achieved in excellent yields (up to 94%) and enantioselectivities (up to 99.2% ee) (Scheme 42). Experimental results indicated that the tosyl protecting group was more efficient in determining the reaction enantiocontrol. The so-obtained bicyclic molecules were reactive enough to be transformed into more-complex polycyclic species by stereospecific reactions.[142]

Besides the nitrogen ligands used to synthesize iron derivatives active in promoting cyclopropanation reactions, *bis*(imino)pyridine compounds have recently been applied in carbene transfer reactions to alkenes.

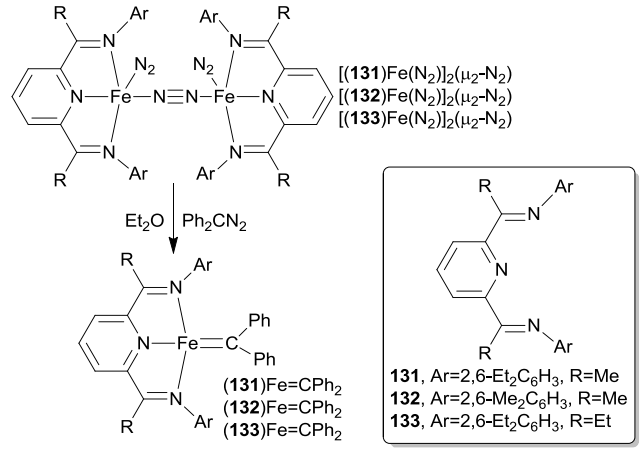

Scheme 43. Synthesis of Fe(**L**)CPh_2 (**L** = **131**-**133**)

Ligands **131-133** were originally used by P. J. Chirik and co-authors for synthesizing the iron complexes $[(\mathbf{L})Fe(N_2)]_2(\mu_2\text{-}N_2)$, (**L** = **131**-**133**) which reacted with Ph_2CN_2 yielding the high-spin iron(II) carbene derivatives Fe(**L**)CPh_2 with the metal center involved in an antiferromagnetic coupling with the *bis*(imino)pyridine and carbene radicals (Scheme 43).[143]

Complexes Fe(**L**)CPh_2 (L = **131**-**133**) did not mediate the transfer of the carbene moiety to unsaturated ligands, in line with the well-known stability of iron complexes containing the :CPh_2 carbene functionality.[144]

On the other hand, *bis*(imino)pyridine **134** was more recently employed for synthesizing the corresponding $[(\mathbf{134})Fe(II)(MeCN)_2](SbF_6)_2$ complex, which promoted the activation of donor-acceptor aryldiazoacetate reagents towards several reactions, including cyclopropanations.[145]

Several unsaturated compounds were cyclopropanated by $(CO_2Et)(Ar)CN_2$ in the presence of $[(\mathbf{134})Fe(II)(MeCN)_2](SbF_6)_2$, as shown in Scheme 44.

The authors attributed the good observed reactivity to the marked iron electrophilicity due to the presence of hexafluoroantimonate (SbF_6^-) counterion. Although the reaction was less effective when using sterically hindered diazo compounds, disubstituted styrenes were also successfully transformed into corresponding cyclopropanes.

Remarkably, a good enantiocontrol was achieved by using a chiral version of this catalyst. The ligand **140** was used *in situ* in the presence of $FeCl_2$ and $AgSbF_6$ yielding cyclopropane **135i** in a good yield and 67% ee (Scheme 45).[145]

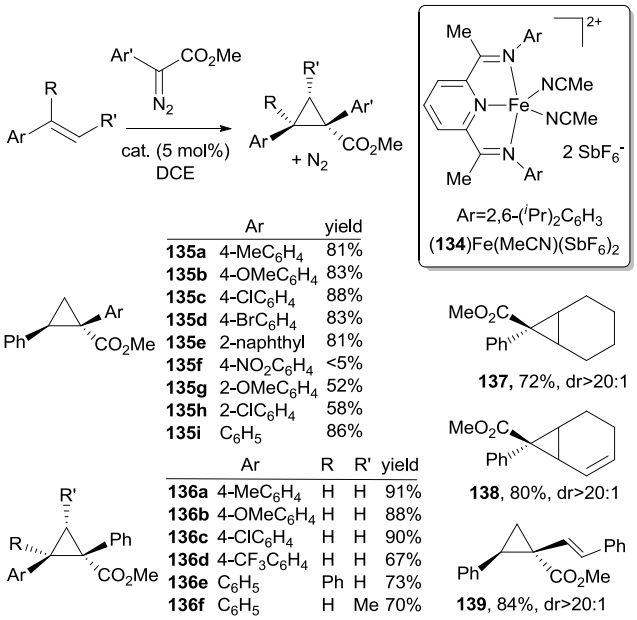

	Ar	yield
135a	4-MeC_6H_4	81%
135b	4-$OMeC_6H_4$	83%
135c	4-ClC_6H_4	88%
135d	4-BrC_6H_4	83%
135e	2-naphthyl	81%
135f	4-$NO_2C_6H_4$	<5%
135g	2-$OMeC_6H_4$	52%
135h	2-ClC_6H_4	58%
135i	C_6H_5	86%

	Ar	R	R'	yield
136a	4-MeC_6H_4	H	H	91%
136b	4-$OMeC_6H_4$	H	H	88%
136c	4-ClC_6H_4	H	H	90%
136d	4-$CF_3C_6H_4$	H	H	67%
136e	C_6H_5	Ph	H	73%
136f	C_6H_5	H	Me	70%

137, 72%, dr>20:1

138, 80%, dr>20:1

139, 84%, dr>20:1

Scheme 44. Cyclopropanation mediated by $[(\mathbf{134})Fe(II)(MeCN)_2](SbF_6)_2$ catalyst

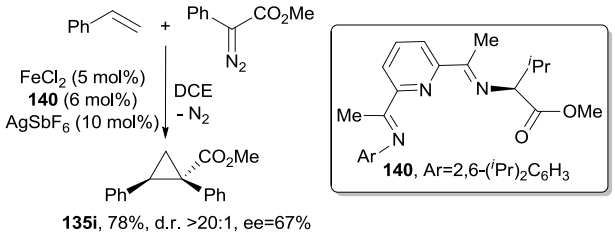

Scheme 45. Cyclopropanation mediated by $FeCl_2$/**140**/$AgSbF_6$ catalytic system

Chiral C_2-symmetric **141**-**144** and C_1-symmetric terpyridine ligands **145**-**146** (Fig. 13) were reacted with $FeCl_2$ forming corresponding iron(II) complexes of the general formula Fe(**L**)Cl_2. In addition, the less sterically hindered **145**-**146** ligands were also employed to synthesize iron(III) Fe(**L**)Cl_3 derivatives by the reaction of **L** with $FeCl_3$.

All the obtained iron complexes were used to promote the cyclopropanation of styrene by EDA by using silver triflate (AgOTf) to generate an unsaturated iron species reactive towards the diazo reagent.[146] While the most sterically encumbered iron(II) Fe(II)(**143**)Cl_2 complex promoted the synthesis of **3d** with the highest values of enantioselectivities, the best diastereoselectivity was observed when using Fe(II)(**141**)Cl_2 as the reaction catalyst. C_1-symmetrical Fe(II)(**145**)Cl_2 and Fe(II)(**146**)Cl_2 complexes showed a poor catalytic efficiency as their iron(III) equivalents did (Scheme 46).

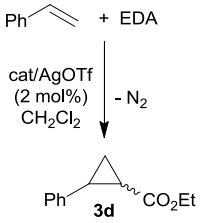

cat	yield	*trans*/*cis*	ee_{trans}	ee_{cis}
Fe^{II}(**141**)Cl_2	78%	76:24	36%	33%
Fe^{II}(**142**)Cl_2	71%	68:32	54%	54%
Fe^{II}(**143**)Cl_2	65%	65:35	65%	67%
Fe^{II}(**144**)Cl_2	41%	72:28	4%	5%
Fe^{II}(**145**)Cl_2	48%	58:42	44%	7%
Fe^{II}(**146**)Cl_2	60%	66:34	2%	5%
Fe^{III}(**145**)Cl_3	39%	59:41	5%	5%
Fe^{III}(**146**)Cl_3	55%	65:35	4%	6%

Scheme 46. Synthesis of **3d** mediated by iron complexes of terpyridine ligands

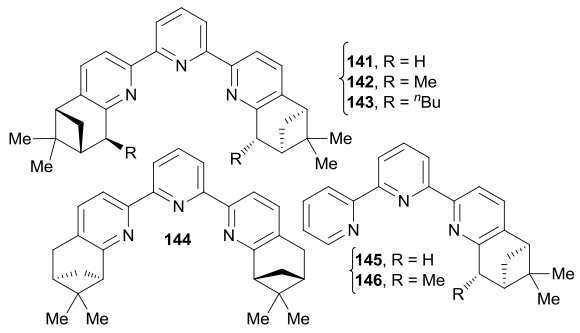

Fig. 13. Structure of ligands **141**-**146**

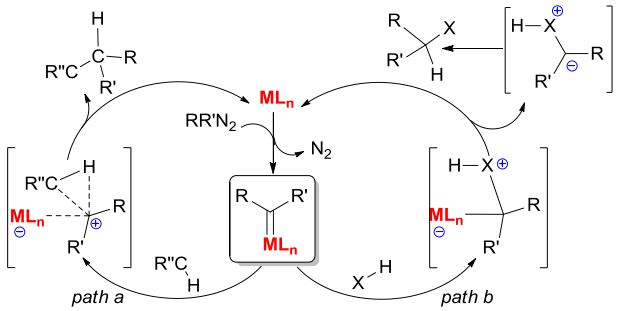

Scheme 47. Two of the most usually proposed mechanisms for the metal-catalyzed carbene insertion into C-H and X-H bonds

3. Carbene Insertion into C-H and X-H Bonds

Alongside the carbene transfer reaction to C=C bonds forming cyclopropanes, diazo compounds and their precursors have been largely used to form new C-C and C-X bonds (X = N, O, S, Si, etc.) by the metal-catalyzed carbene insertion into C-H and X-H functionalities, respectively.

Since the first example of the copper-catalyzed O-H insertion by diazoketones reported in the 1950s,[147] the diazo-based carbene transfer into C-H and X-H bonds has been widely investigated and reviewed[3,5,6,148-154] highlighting dirhodium(II) complexes as the most efficient catalysts, particularly for promoting C-H activations.

In view of the importance of applying non-noble metals in more sustainable processes, extensive efforts have been made to replace the rhodium-based catalysts with iron-containing systems, which are now widely recognized as very active catalysts in mediating carbene insertions.[11,13,155-157]

In this section, the most recent published data on the iron-mediated C-H and X-H functionalization are discussed by taking into account the influence of the catalyst environment and the electronic/steric nature of the employed diazo reagent on the reaction mechanism. The analysis of the high number of reported studies has allowed the identification of some general mechanisms and among them, two pathways were proposed passing through the formation of a carbene intermediate (Scheme 47). The C-H functionalization was suggested occurring through either a concerted mechanism (*path a*), with the direct insertion of the carbene species into the hydrocarbon moiety, or a stepwise mechanism (see below). On the other hand, a stepwise mechanism (*path b*) was usually proposed for the X-H carbene insertion during which the generation of an ylide intermediate occurred (Scheme 47).

3.1 Iron porphyrin and other porphyrinoid catalysts

Iron porphyrin and porphyrinoid complexes, in addition to being excellent cyclopropanation catalysts as extensively discussed in section 2.1, they are also very active in driving the insertion of carbenes into C-H and X-H bonds. Considering the very good efficiency of iron porphyrin complexes in catalyzing C-H functionalizations,[158] the scientific community is currently devoting great effort in developing sustainable porphyrin-

based procedures for the activation of less reactive hydrocarbons and for the formation of C-heteroatom bonds.

In this context, the catalytic application of artificial metalloenzymes (ArMs) is assuming a particular importance in view of the efficiency of ArMs in mediating carbene insertion reactions into both C-H[159-161] and X-H[162-168] bonds (X = N, S, Si, B). However, all the ArMs applied in carbene insertion reactions have been synthesized by replacing aminoacidic residues in heme proteins (*pathway a* of Scheme 30) rather than embedding a synthetic molecule into the biological framework. Thus, as stated for ArMs-based cyclopropanations, the analysis of their catalytic activity will not be covered in this review.

3.1.1 C-H carbene insertion. The chemoselectivity of the carbene C-H bond insertion is an important issue due to the frequent coexistence in the same molecule of CH-containing functional groups that display a similar reactivity towards diazo reagents. Thus, in order to opportunely drive the reaction into the desired C-H bond, the choice of both the catalyst and the diazo compound is crucial.

The activity of iron porphyrins in catalyzing the intermolecular C-H alkylation was first reported by K. Woo and co-authors who investigated the catalytic efficiency of Fe(TPP)Cl (**1**) by using dimethyl diazomalonate $(MeCO_2)_2CN_2$ and methyl 2-aryl diazoacetates $(MeCO_2)(Ar)CN_2$ as acceptor-acceptor and donor-acceptor diazo reagents, respectively.[169] When substituted aromatic hydrocarbons were tested as substrates, a poor chemoselectivity was observed due to the presence of both C(sp^3)-H and C(sp^2)-H bonds in the molecule (Scheme 48).

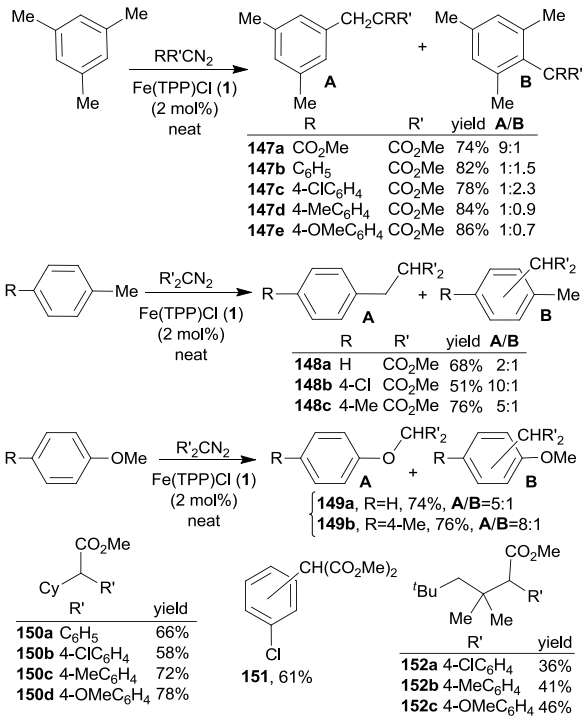

Scheme 48. Intermolecular C-H insertion catalyzed by Fe(TPP)Cl (**1**)

A mixture of compounds deriving from the insertion of the carbene functionality into the two types of C-H bonds were observed using both $(MeCO_2)_2CN_2$ and $(MeCO_2)(Ar)CN_2$ as the carbene source. A slight predominance of the C(sp^3)-H insertion was achieved by employing the more hindered $(MeCO_2)_2CN_2$ diazo reagent (compare products **147a** and **147b** of Scheme 48). The electronic nature of the diazo compound influenced the **A**/**B** ratio; an EDG on the arylic moiety of $(MeCO_2)(Ar)CN_2$ favored the insertion into a mesitylene C(sp^3)-H bond over the C(sp^2)-H ones. Experimental results and a Hammett study of the cyclohexane functionalization, yielding **151a**-**151d** compounds, suggested the formation of an electrophilic carbene intermediate.

As discussed in section 2.1, an iron-carbene was also proposed as the key-intermediate of the reaction of allylic phosphorous ylides with diazo derivatives forming alkylated compounds rather than cyclopropanes (Scheme 6).[40] This peculiar reactivity of ylides had previously been investigated by Y. Tang and co-authors who discovered that the poor reactive C(sp^2)-H bonds of α,β-unsaturated esters can be activated towards the carbene insertion by introducing a phosphorous ylide in the allylic position which is able to increase the electron density of the double bond.[41] The reaction between allylic phosphorous ylides and MDA was efficiently catalyzed by Fe(TCP)Cl (**7**); the mechanistic study revealed the occurrence of a tandem reaction in which first the double bond was cyclopropanated and then a ring-opening reaction was responsible for the formation of the product of the C-H insertion. The reaction, executed by using a phosphonium salt, LiHMDS (lithium hexamethyldisilazide) as a base, MDA and different aldehydes, yielded 1,1,4-trisubstituted 1,3-butadienes with high stereoselectivities (Scheme 49).

The same strategy was applied to transfer the carbene functionality to trisubstituted allylic phosphonium salts by using ^{t}BuOK as the base and different aldehydes. Tetrasubstituted dienes listed in Scheme 50a were obtained with an excellent stereocontrol.[170]

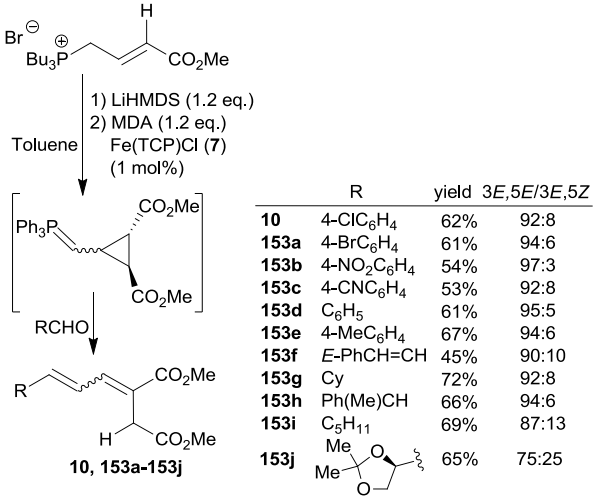

Scheme 49. Synthesis of 1,1,4-trisubstituted 1,3-butadienes catalyzed by Fe(TCP)Cl (**7**)

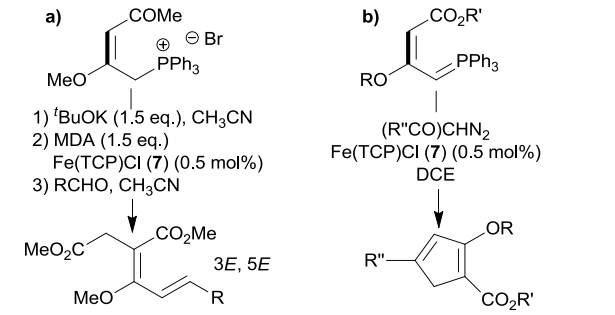

	R	yield
154a	4-ClC_6H_4	89%
154b	4-BrC_6H_4	86%
154c	2-$NO_2C_6H_4$	78%
154d	3-$NO_2C_6H_4$	83%
154e	4-$NO_2C_6H_4$	90%
154f	C_6H_5	90%
154g	2-MeC_6H_4	71%
154h	3-MeC_6H_4	77%
154i	4-MeC_6H_4	77%
154j	4-$OMeC_6H_4$	55%
154k	2,4-$Cl_2C_6H_3$	95%
154l	1-naphthyl	86%
154m	*trans*-PhCH=CH	64%
154n	R=PhC_2H_4	72%
154o	*n*-octyl	49%

	R	R'	R"	yield
155a	Me	Me	C_6H_5	65%
155b	Et	Me	C_6H_5	74%
155c	Et	Et	C_6H_5	76%
155d	Et	tBu	C_6H_5	50%
155e	Et	Et	4-$OMeC_6H_4$	45%
155f	Et	Et	4-MeC_6H_4	50%
155g	Et	Et	4-FC_6H_4	57%
155h	Et	Et	4-ClC_6H_4	48%
155i	Et	Et	4-BrC_6H_4	48%
155j	Et	Et	3-BrC_6H_4	70%
155k	Et	Et	*E*-PhCH=CH	46%
155l	Et	Et	*2*-furyl	76%

Scheme 50. Synthesis of tetrasubstituted dienes (a) and cyclopentadiene (b) derivatives catalyzed by Fe(TCP)Cl (**7**)

When aryl diazoketones (R''CO)CHN_2 were used in place of MDA, cyclopentadiene derivatives were obtained in good yields (Scheme 50b). In both cases, the authors proposed the formation of an unstable cyclopropane intermediate which evolved into the desired compounds by ring-opening reactions.[170]

In order to functionalize poor reactive C(sp^3)-H bonds, the choice of the opportune diazo compounds, which is able to form a very electrophilic iron-carbene intermediate, is fundamental. To reach this goal, C. White and co-authors screened the reactivity of various acceptor-acceptor electrophilic diazo compounds and π-acceptor iron catalysts. The catalytic combination of Fe(Pc)Cl (**56**) and $NaBAr_F$, to convert **56** into the more electrophilic [Fe(Pc)](BAr_F) catalyst *in situ,* was efficient in mediating the intramolecular C(sp^3)-H alkylation of sulfonate diazoaesters leading to the compounds illustrated in Scheme 51. The allylic-diazoesters simultaneously acted as the substrate and carbene source.[171]

Catalyst **56** efficiently promoted the reaction of several allylic and benzylic C-H bonds and the biologically relevant compound **165**, precursor of the antioxidant δ-tocopherol, was isolated in a good yield (Scheme 51). Mechanistic studies supported the involvement of an iron-carbene intermediate as well as the occurrence of the homolytic cleavage of the C-H bond followed by the formation of the C-C bond *via* a radical rebound mechanism. The carbene transfer methodology can be applied for functionalizing pharmaceutically relevant heterocycles, such as indoles.[172,173]

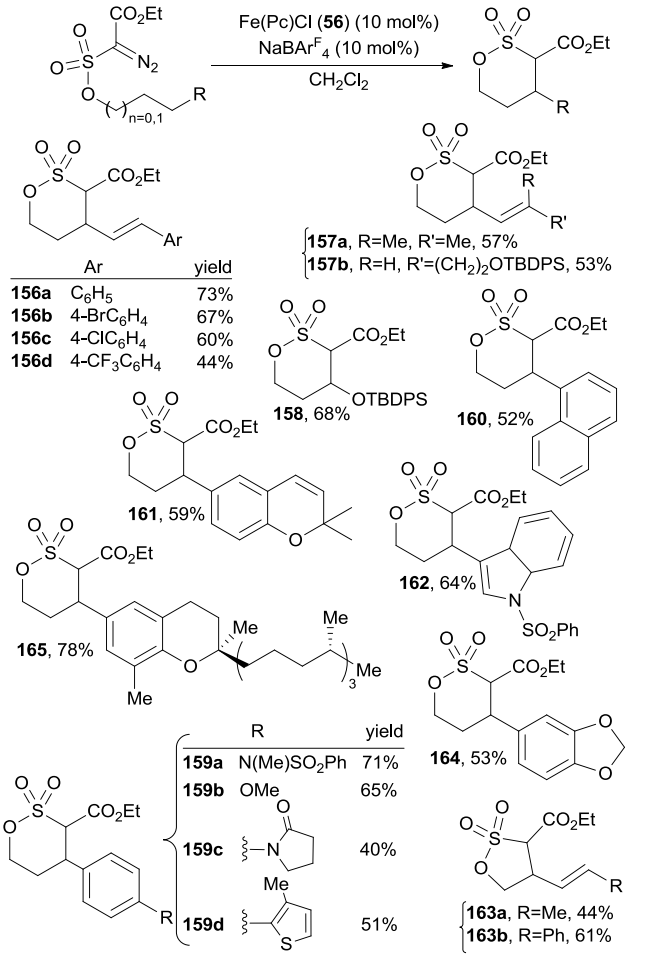

	Ar	yield
156a	C_6H_5	73%
156b	4-BrC_6H_4	67%
156c	4-ClC_6H_4	60%
156d	4-$CF_3C_6H_4$	44%

	R	yield
159a	$N(Me)SO_2Ph$	71%
159b	OMe	65%
159c		40%
159d		51%

Scheme 51. Fe(Pc)Cl (**56**)-catalyzed carbene intramolecular insertion into C-H bonds of sulfonate diazoaesters

The catalytic activity of iron porphyrins in driving the indole C-H functionalization, was recently explored by R. M. Koenigs and co-authors who used diazoacetonitrile ((CN)CHN_2) as the diazo reagent. In view of the instability and hazardous nature of (CN)CHN_2, the diazo compound was generated in continuous flow.[174] Among the iron complexes tested in the model reaction between *N*-methylindole and (CN)CHN_2, Fe(TPP)Cl (**1**) showed the best catalytic activity, affording the desired compound **166a** (Scheme 52) in 92% yield. A very low catalytic loading was required and **166a** was obtained in 97% and 92% yield using 1% mol and 0.1% mol of **1**, respectively also in the gram-scale. The procedure was effective for the regioselective functionalization of both *N*-protected (yields up to 99%) and unprotected indoles (yields up to 75%), despite the presence of the free N-H bond, which would have been suitable for reacting with the carbene species (Scheme 52). Considering that the reaction was completely inhibited by the addition of TEMPO and on the basis of a preliminary mechanistic study, the authors proposed the formation of a radical key-intermediate, whose formation remained unclear.

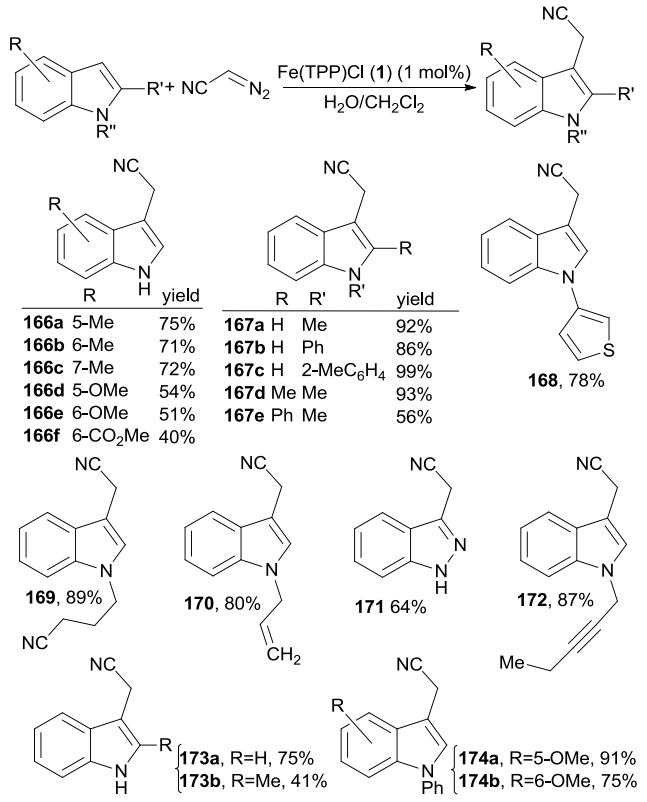

Scheme 52. Fe(TPP)Cl (**1**)-catalyzed C-H functionalization of indoles by $(CN)CHN_2$

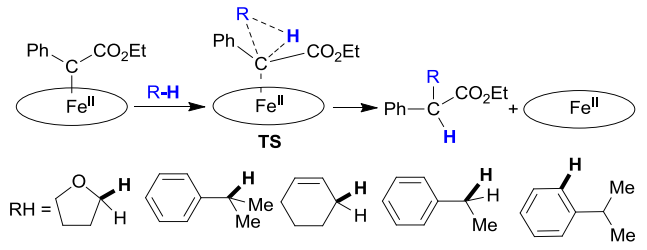

Scheme 53. Suggested mechanism of the carbene C-H insertion

A more detailed study of the mechanism of the carbene C-H insertion was theoretically carried out by Y. Zhang and R. L. Khade.[175] DFT calculations indicated a concerted mechanism for the reaction of the putative iron(II) carbene CSS species, already proposed by the same authors as intermediate of cyclopropanations,[130] and five different acceptor substrates, tetrahydrofurane (THF), cumene C(sp^3)-H bond, ethylbenzene, cyclohexene and aromatic C(sp^2)-H bond of cumene (Scheme 53).

The theoretical investigation suggested that the reaction occurred by a triplet Fe(II)-based hydride transfer mechanism. It was proposed that the transformation of reactants into products involved changes of spin-states with the formation of the iron-carbene intermediate as the rate-limiting step of the reaction.

3.1.2 X-H carbene insertion. The catalytic activity of iron-porphyrinoids in the carbene transfer into N-H bonds was reported by Z. Gross and I. Aviv in 2006,[176] who employed EDA to synthesize differently substituted α-amino esters. Iron corroles Fe(TPFC)Cl (**175**) and Fe(TPFC)$(OEt_2)_2$ (**176**) (TPFC = 5,10,15-*tris*(pentafluorophenyl)corrole) as well as iron porphyrins Fe(TPFPP)Cl (**177**) and Fe(TPP)Cl (**1**) mediated the synthesis of compounds shown in Scheme 54 in good yields. Even if corrole catalysts were very selective towards the single insertion of the carbene fragment into a primary RNH_2 bond, the product of the second insertion was obtained by treating **178a** with an EDA excess. Also secondary amines showed a good reactivity in the presence of iron corroles as demonstrated by the functionalization of morpholine that produced **179** in a good yield.

An interesting approach for the synthesis of non-protected amino acids was reported by Z. Gross and co-authors by using Fe(TPP)Cl (**1**) as catalysts for the carbene transfer from diazoacetates to ammonia.[177] The reported data showed that the selectivity of the **1**-catalyzed N-H insertion can be modulated by changing the NH_3/EDA ratio as well as the reaction solvent. The use of ammonia as the nitrogen source may produce three different products depending if one, two or three carbene moieties have been inserted into the N-H bond (Scheme 55). The desired glycine ester **180a** was obtained with a 100% selectivity either by treating EDA at room temperature with a saturated solution of NH_3 in THF or by performing the reaction under a NH_3 flow. On the other hand, the triple alkylated product **180c** was achieved by replacing NH_3 with ammonium acetate as the nitrogen source. The di-alkylated compound **180b** was never obtained. Catalyst **1** was also active in promoting the synthesis of alanine ester **181a**, which was formed with a very good selectivity under the same experimental conditions reported for the synthesis of **180a**.

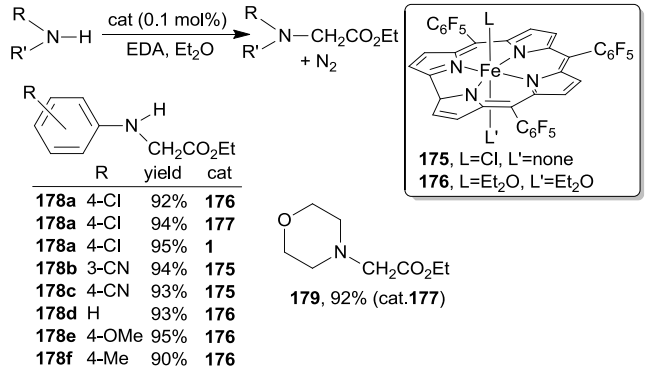

Scheme 54. Synthesis of differently functionalized α-amino esters by amines and EDA

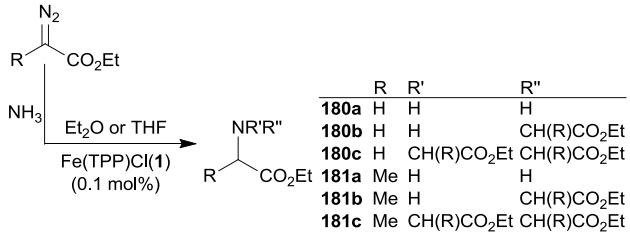

Scheme 55. Fe(TPP)Cl (**1**)-catalyzed synthesis of compounds **180a**, **180c**, **181a** and **181b**

In this latter case, a higher temperature (65°C) was applied due to the lower reactivity of diazopropionate with respect to that of EDA. Although the di-alkylated compound **181b** was achieved by treating **181a** with diazopropionate, the formation of the fully alkylated compound **181c** was never observed.

Z. Gross and I. Aviv compared the activity of iron-porphyrinoids in mediating the N-H alkylation to that of other metal complexes, which efficiently catalyzed carbene transfer reactions, such as cyclopropanations.[178] The observed superiority of iron-porphyrinoids was ascribed to the poor coordination affinity of amines towards the iron center. This prevents a catalyst's deactivation, which conversely occurs in a larger extent when other catalysts are treated with amines. The N-H alkylation worked well also using ethyl 2-diazopropanoate ($(CO_2Et)(Me)CN_2$) (EDP) as the carbene source both in organic solvents, using iron-porphyrinoid catalysts, and in aqueous solution, where either myoglobin (**Mb**) or the non-covalent conjugate between iron corrole **182** and BSA (bovine serum albumin) or HAS (human serum albumin) (Scheme 56) were used as promoters. Unfortunately, no chiral induction was observed in the presence of myoglobin or a serum albumin. Catalysts **175**-**177** and **1** were also active in alkylating S-H bonds of thiols by using both EDA and EDP as the carbene precursors (Scheme 57).[178]

The N-H functionalization was also investigated by G. Simonneaux and co-authors using aniline as the model acceptor substrate and diazoacetophenone $(COPh)CHN_2$ and α-methyl diazoacetophenone $(COPh)(Me)CN_2$ as the carbene sources.[72] Iron porphyrins Fe(TPP)Cl (**1**) and $Fe(TPP)(CF_3SO_3)$ (**186**) catalyzed the mono-alkylation of the aniline N-H bond at room temperature and, in the presence of **1**, compounds **187a** and **187b** were obtained in 90% and 66% yield, respectively.

No enantiocontrol was observed when aniline was reacted with $(COPh)(Me)CN_2$ in the presence of the chiral catalyst Fe(Halt*)Cl (**72**). The alkylated **187b** product was formed in 51% yield as a racemic mixture (Scheme 58a).

The reactivity of diazoketones towards X-H bonds was also investigated by employing the N- and O-protected 6-diazo-5-oxo-L-norleucine (DON) as the diazo reagent in the presence of iron porphyrin Fe(TPP)Cl (**1**) as the catalyst.[38] Products deriving from the DON insertion into N-H and S-H bonds were obtained in moderate yields and a long reaction time (Scheme 58b).

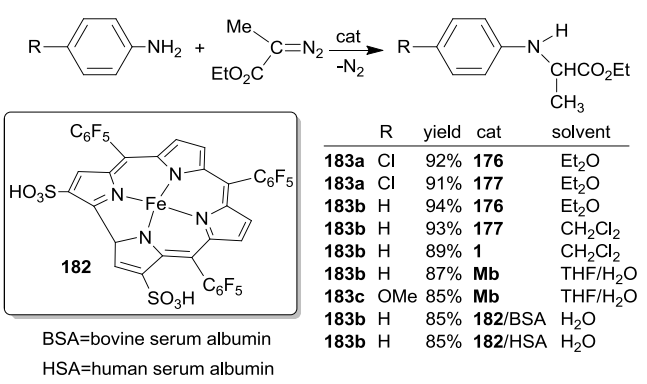

	R	yield	cat	solvent
183a	Cl	92%	**176**	Et_2O
183a	Cl	91%	**177**	Et_2O
183b	H	94%	**176**	Et_2O
183b	H	93%	**177**	CH_2Cl_2
183b	H	89%	**1**	CH_2Cl_2
183b	H	87%	**Mb**	THF/H_2O
183c	OMe	85%	**Mb**	THF/H_2O
183b	H	85%	**182**/BSA	H_2O
183b	H	85%	**182**/HSA	H_2O

Scheme 56. Synthesis of differently fuctionalized α-amino esters by amines and $((CO_2Et)(Me)CN_2)$ in organic solvents and in a water medium

The authors ascribed the unfavorable reaction rate to the high steric hindrance of DON, whose substituents may interfere with the porphyrin ring during the carbene formation with a consequent decrease of the reaction efficiency.

K. Woo and co-authors explored the catalytic activity of different iron porphyrins in the reaction between EDA and amines in order to underline the ligand effect on the catalytic performances.[179] Differently substituted porphyrin catalysts were tested in the model reaction between EDA and piperidine, forming **192** (Fig. 14). Achieved data indicated a positive catalytic effect of EDGs on the porphyrin periphery. Electron-rich catalysts, such as Fe(TMOP)Cl (**193**) (TMOP = dianion of tetra(*p*-methoxyphenyl)porphyrin) complexes, were more efficient than the electron-poor Fe(TPFPP)Cl (**177**) complex in promoting the synthesis of compound **192**. This experimental observation was in contrast to what was observed for the C-H alkylation, where better catalytic activities were obtained by using electron deficient catalysts.[171]

The presence of sterically-hindered ligands lowered the reaction rate, as occurred when Fe(TMP)Cl (**194**) (TMP = dianion of tetramesitylporphyrin) was the catalyst (80% in 1 hour) (Fig. 14). The study of the reaction scope disclosed the capability of Fe(TPP)Cl (**1**) in driving the carbene insertion in N-H bonds of primary and secondary alkyl amines, aryl amines and *N*-heterocyclic compounds yielding the products shown in Fig. 14. In addition, Fe(TPP)Cl (**1**) also promoted the double N-H alkylation of primary amines when an excess of EDA was used (products **196a**-**196g**, Fig. 14).[179]

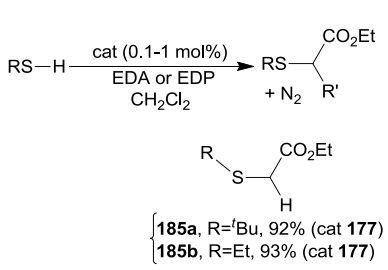

	R	R'	yield	cat
184a	H	H	95%	**175**
184a	H	H	95%	**176**
184a	H	H	98%	**177**
184a	H	H	97%	**1**
184b	4-Me	H	96%	**177**
184c	4-Me	Me	89%	**177**
184c	4-Me	Me	90%	**175**

Scheme 57. Carbene insertion into S-H bonds catalyzed by catalysts **175**-**177** and **1**

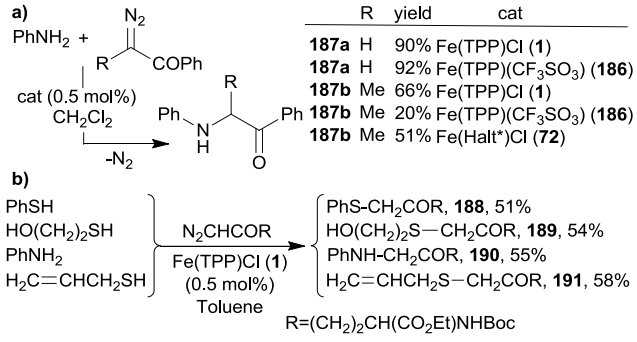

	R	yield	cat
187a	H	90%	Fe(TPP)Cl (**1**)
187a	H	92%	$Fe(TPP)(CF_3SO_3)$ (**186**)
187b	Me	66%	Fe(TPP)Cl (**1**)
187b	Me	20%	$Fe(TPP)(CF_3SO_3)$ (**186**)
187b	Me	51%	Fe(Halt*)Cl (**72**)

Scheme 58. Synthesis of compounds **187-191** catalyzed by iron (III) porphyrins

The EDA/substrate ratio also influenced the product distribution when 1,2-diamines and 1,2-alcoholamines were the chosen reactants. When bifunctional substrates were reacted with EDA in presence of Fe(TPP)Cl (**1**), a tandem N-H insertion/cyclization reaction occurred with the consequent formation of corresponding piperazinones, morpholinones and related analogous as the major products (Scheme 59).[180] The reaction did not afford cyclic compounds as the sole products and in order to increase the reaction selectivity, an EDA excess was employed. While compound **199** was isolated in 40% yield when one EDA equivalent was used, the addition of two EDA equivalents, followed by a thermic treatment, allowed the isolation of compound **200** in 60% yield.

When both O-H and N-H bonds were present in the molecule, the alkylation of the latter was always preferred.

More challenging carbenes deriving from donor-donor diazo reagents were investigated by C. M. Che and co-authors, who described the iron porphyrin-mediated insertion in X-H bonds using Ph_2CN_2 as the carbene source.[44] The insertions of the :CPh_2 carbene moiety into C-H, N-H, O-H and S-H bonds was efficiently attained in the presence of Fe(TPFPP)Ad (**14**) catalyst (Scheme 60). As previously explained in the cyclopropanation section, the Ad ligand of **14** played a fundamental role both in activating the carbene group in the *trans*-position as well as in stabilizing the active Fe(II) state, allowing the catalyst recovery after most of the mentioned catalytic reactions.

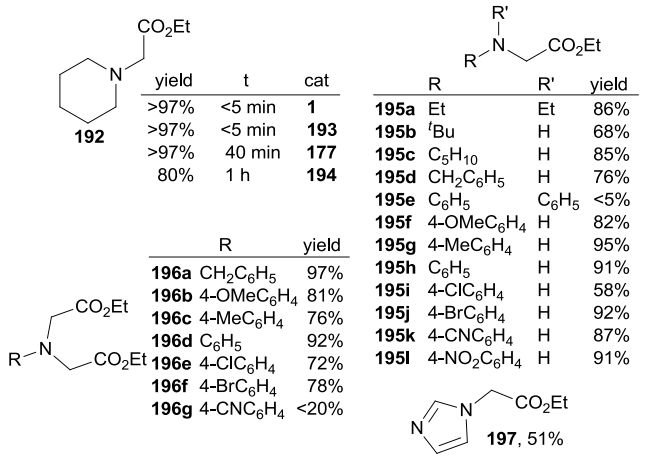

Fig. 14. *N*-alkylation by EDA catalyzed by Fe(TPP)Cl (**1**)

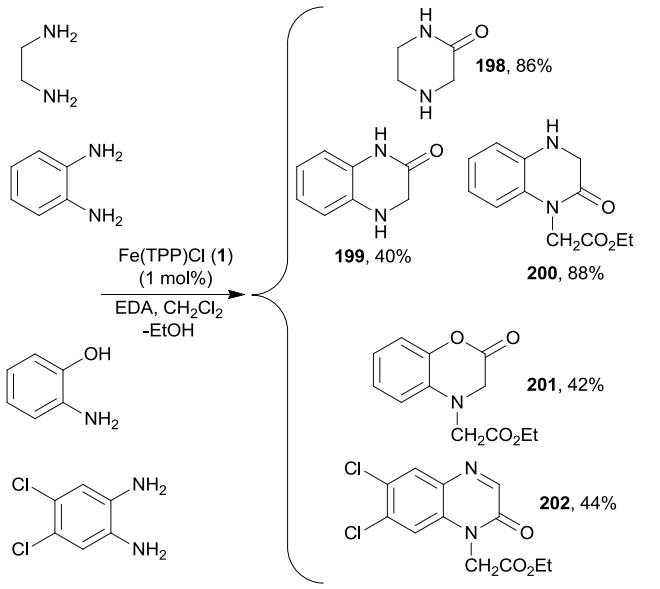

Scheme 59. Synthesis of compounds **198**-**202** catalyzed by Fe(TPP)Cl (**1**)

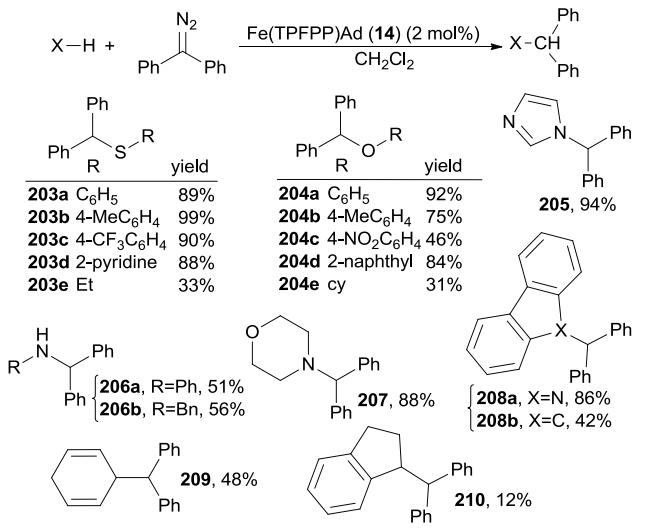

Scheme 60. Carbene insertion into X-H bonds catalyzed by Fe(TPFPP)Ad (**14**)

Analogous to that previously discussed for cyclopropanations, when diazo compounds are too reactive to be safely handled, the carbene transfer reaction is performed by using a more stable precursor, which forms the carbene functionality *in situ*. As already described in the section dedicated to cyclopropanations, X. Bi and co-authors generated $(CF_3)CHN_2$ diazo compound from $(CF_3)CH{=}NNHTfs$ under basic conditions. This reagent was also employed for functionalizing a variety of C-H and X-H-containing molecules.[63] Surprisingly, rather than promoting the expected insertion of the :CCF_3 group in S-H bonds, the tested iron porphyrins mediated the S-H difluoroalkenylation, during which the RS-CH=CF_2 functionality was formed. In the presence of the very robust iron(III) porphyrin **211**, the reaction worked well with several substituted thiols yielding compounds of Scheme 61.

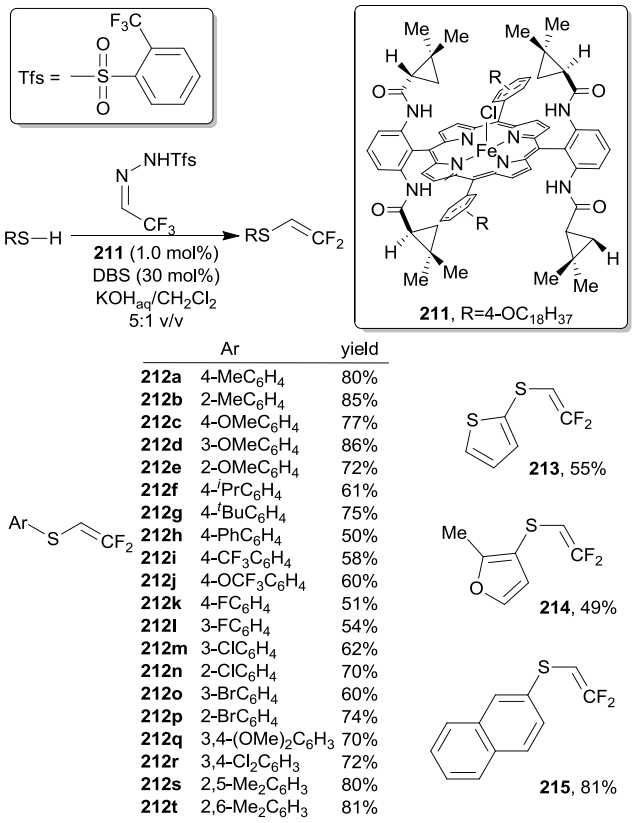

Scheme 61. Difluoroalkenylation of S-H bonds catalyzed by **211** catalyst

Considering the time-consuming procedure for synthesizing **211**, the commercially available Fe(TPP)Cl (**1**) was employed as alternative catalyst for the gram-scale synthesis of **212i**, which was isolated in a yield comparable to that observed in the presence of the iron complex **211**.

The difluoroalkenylation occurred only under basic conditions and when the reaction was run in neutral water, the classic S-H alkylation was observed. Based on experimental results, the authors proposed a general reaction mechanism in which the ylide, formed by the reaction of the substrate with the metal carbene intermediate, underwent a β-fluoride elimination under basic conditions affording the *gem*-difluoroalkenylation product together with the metal catalyst (Scheme 62).

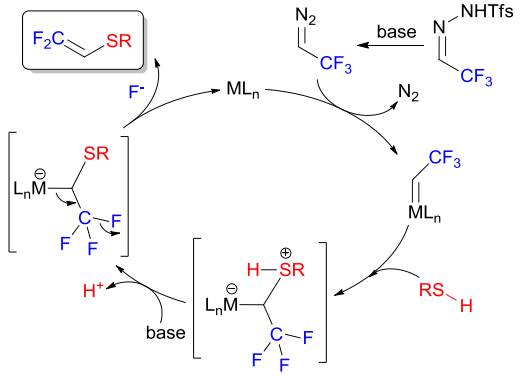

Scheme 62. Proposed mechanism for the difluoroalkenylation of S-H bonds.

Complex Fe(TPP)Cl (**1**) was also very active in transferring the carbene :CCF_3 functionality of $(CF_3)CH$=NNHTfs in the Doyle-Kirmse reaction[181] of either allylic or propargyl thioethers.[63] Considering that this review deals with carbene transfer reaction to C=C, C-H and X-H bonds, papers published since 2006 on the Doyle-Kirmse reaction, catalyzed by iron complex of nitrogen ligands, will not be discussed herein.[99,145,182-184]

N-tosylhydrazone precursors were also used by C. M. Che and co-authors under basic conditions to perform the iron porphyrin-catalyzed carbene insertion into Si-H, Sn-H and Ge-H bonds.[185] Among the different iron porphyrins tested in the synthesis of **216a** from triethylsilane (Et_3SiH), Fe(TPP)Cl (**1**) showed the best performance affording the desired compound in a 92% yield. The reaction scope showed the catalytic ability of **1** in promoting the carbene insertion in several primary and secondary Si-H bonds (yield up to 90%) by using differently substituted *N*-tosylhydrazones. Additionally, the utility of the Fe(TPP)Cl (**1**)-based procedure was demonstrated by the gram-scale synthesis of **221c**, which was isolated in 64% yield. Fe(TPP)Cl (**1**) complex also catalyzed the carbene insertion into several Sn-H and Ge-H-containing compounds in very high yields (up to 99%) (Scheme 63).

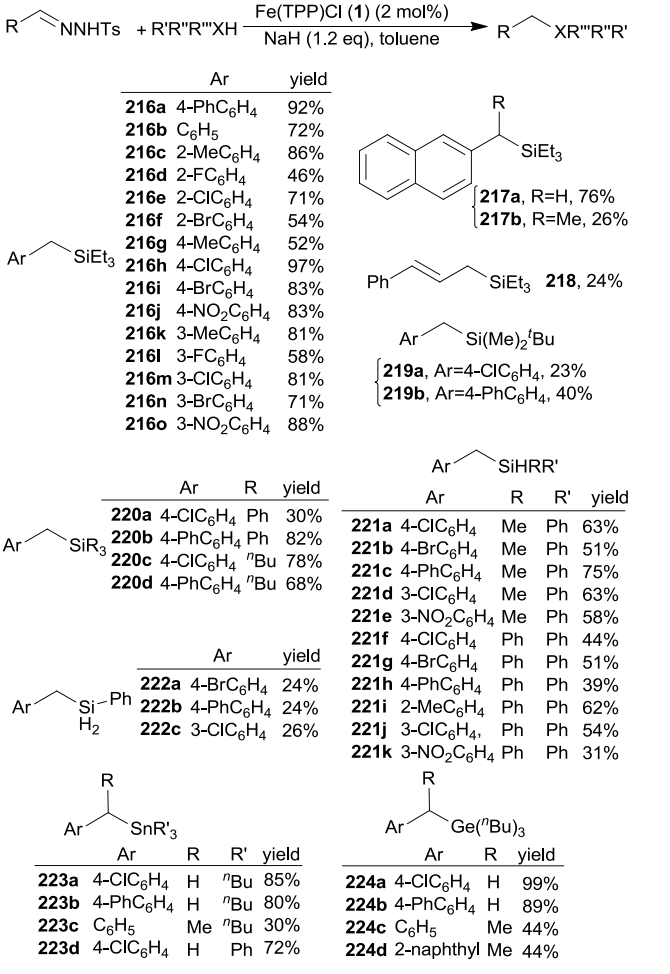

Scheme 63. Fe(TPP)Cl (**1**)-catalyzed carbene insertion into Si-H, Sn-H and Ge-H bonds

3.1.3 Mechanistic investigations of the carbene insertion into N-H bonds. Mechanistic investigations disclosed that the iron(III) porphyrin-mediated carbene insertion into an N-H bond does not follow the same pathway already described for the C-H alkylation. In this latter case, the first step should be the reduction of the iron(III) center to the corresponding iron(II) complex by EDA and then the so-formed iron(II) intermediate should react with the diazo compound generating the iron carbene reactive towards the amine (Scheme 64, *path a*). In order to support or exclude this mechanistic proposal, L. H. Woo and co-authors explored the reactivity of both iron(III) and iron(II) porphyrins towards EDA in the presence of pyridine, which does not react with the alkylating agent. While the EDA decomposition, which forms products of the carbene dimerization (diethyl fumarate and diethyl maleate), proceeded well in the presence of iron(III) derivatives and pyridine, it was suppressed when iron(II) complex was treated with pyridine. This was probably due to the formation of a coordinatively saturated Fe(II)(porphyrin)$(Py)_2$ complex, which does not have free coordinative positions for activating EDA. This experiment suggested that the initial reduction of iron(III) to iron(II) did not take place and consequently, *path b* of Scheme 64 was proposed as the more probable catalytic mechanism.

In addition, the ability of Fe(TPP)Cl (**1**) to promote the N-H carbene insertion in open air supported the involvement on an air-stable iron(III) intermediate rather than an air-sensitive iron(II) carbene species. The Hammet study suggested the formation of a positively charged intermediate state.

The proposed mechanism indicated the key-role of the amine substrate in stabilizing the five-coordinated amine complex **A** that rapidly evolves into the iron(III) carbene intermediate **B**, active for transferring the carbene moiety to the substrate (Scheme 64, *path b*).[179]

Some years later, I. Aviv and Z. Gross proposed an alternative mechanism in which, rather than an iron carbene, a nitrogen ylide was formed as the active intermediate.[178] The experimental study indicated the two possible *path c* and *path d* for the N-H alkylation by EDA.

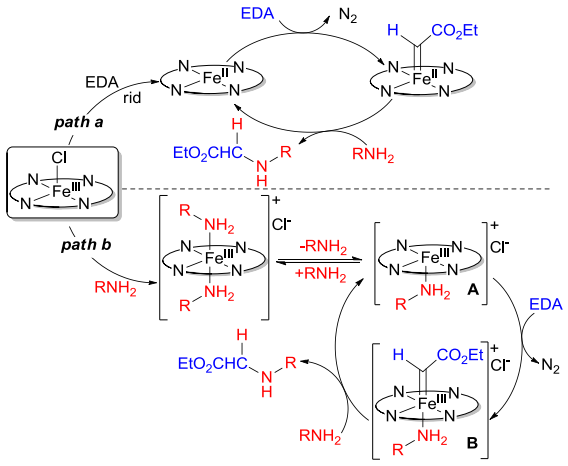

Scheme 64. Proposed mechanisms for the carbene N-H insertion catalyzed by Fe(TPP)Cl (**1**)

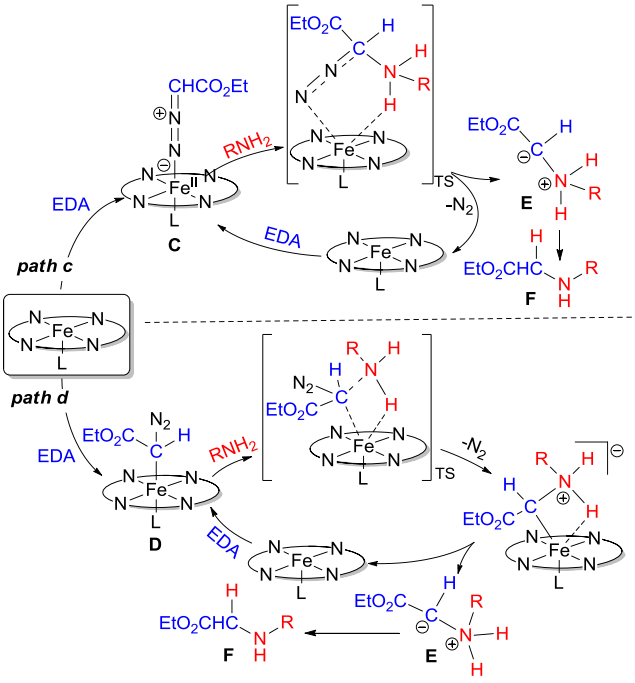

Scheme 65. Carbene N-H insertion through formation of a nitrogen ylide

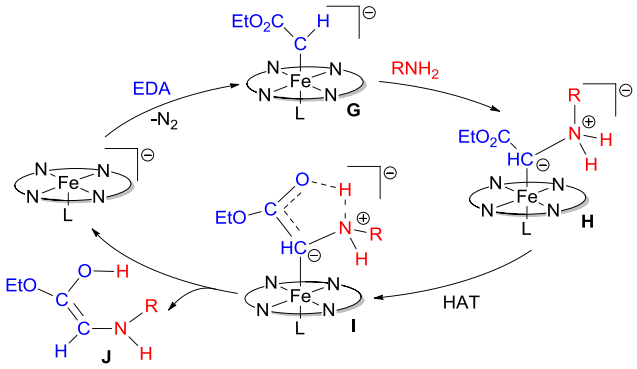

Scheme 66. Mechanism suggested on the basis of DFT study of the iron(II) porphyrin-mediated carbene N-H insertion

The formation of a carbene was discharged by Gross and co-authors in view of the lack of reactivity of Fe(TPP)Cl (**1**) towards EDA in the absence of an amine. Conversely, they proposed the coordination of amine to an adduct Fe(porphyrin)L/EDA, in which either the γ-nitrogen (adduct **C**, Scheme 65) or the carbon (adduct **D**, Scheme 65) atom coordinates the metal center, and N_2 is still present. Next, the release of molecular nitrogen was responsible for the formation of either a non-coordinated (*path c*) or coordinated (*path d*) nitrogen ylide **E** and finally, a hydride transfer reaction yielded the desired alkylated amine **F**. The authors proposed that the last step plays an important role in the mechanism in view of the similar reactivity of amines displaying a different nucleophilicity but a similar hydride donor capacity.

The mechanism of the reaction was also theoretically investigated by S. Shaik and co-authors, who highlighted that different mechanisms takes place when the starting catalyst is an iron(III) or iron(II) species. The N-H functionalization

mediated by iron(II) derivatives was studied in order to shed some light on the catalytic activity of engineered iron(II)-containing enzymes.[133] The authors proposed that when an iron(II) porphyrin is the starting complex, the active intermediate is an OSS iron-carbene (adduct **G**, Scheme 66). DFT calculations supported that the nucleophilic attack of amine to the electrophilic carbene intermediate forms the ylide **H** (Scheme 66), which rearranges to the final product **J** by a hydrogen atom transfer (HAT) process. The energy profile of the reaction showed that the HAT process had an energy barrier as high as that of the nucleophilic attack of amine to the carbene species and that both energetic barriers had values compatible to the experimental conditions employed for the catalytic reactions.

3.2 Non-heme iron complexes

Alongside porphyrinoids, many other nitrogen ligands have been used to synthesize metal complexes for promoting the insertion of a carbene functionality into C-H and X-H bonds.[5,186] A plethora of structurally different non-heme complexes have been synthesized and consequently, the selective activation of a specific bond has been feasible by using the suitable catalyst. Generally speaking, for activating very stable C-H and X-H bonds it is necessary to enhance the electrophilicity of the catalyst, in order to render it more reactive towards non-activated bonds.

3.2.1 C-H and Si-H carbene insertion. Considering the importance in developing catalysts showing a remarkable electrophilicity, A. Hernán-Gómez, M. Costas and co-authors reported the synthesis and the catalytic efficiency of an iron(II) complex coordinated to the very electron-poor *N*,*N*'-*bis*(pentafluorophenyl)-*o*-phenylenediamide (^{F}pda) ligand. The complex [Fe(^{F}pda)(THF)]$_2$ (**225**) was used in combination with LiAl(OR^{F})$_4$ (OR^{F}=(OC(CF$_3$)$_3$) to alkylate strong alkyl C(sp^3)-H bonds.[187] The catalytic binary system was efficient in catalyzing intramolecular C-H functionalization yielding products depicted in Scheme 67.

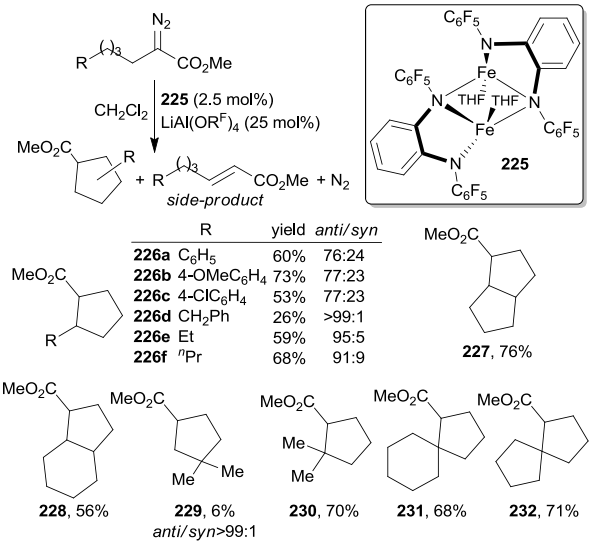

Scheme 67. Intramolecular alkylation of C(sp^3)-H bonds catalyzed by the [Fe(^{F}pda)(THF)]$_2$ (**225**)/LiAl(OR^{F})$_4$ system

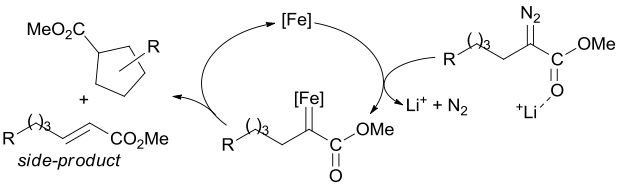

Scheme 68. Suggested mechanism of the reaction catalyzed by the [Fe(^{F}pda)(THF)]$_2$ (**225**)/LiAl(OR^{F})$_4$ system

Electron-rich substrates reacted better than electron-deficient ones in accordance to the electrophilic nature of the suggested carbene intermediate. The Lewis acid LiAl(OR^{F})$_4$ was necessary for rendering the reaction possible by activating the diazo molecule. Experimental results indicated that the coordination of lithium to the oxygen atom of the diazo carbonyl group avoids the deactivation of the iron(II) catalyst, which seems due to the interaction of C=O with the metal center. Finally, either a β-hydride migration process or two consecutive hydrogen atom abstraction reactions were considered responsible for the formation of the α,β-unsaturated ester side-product (Scheme 67). A preliminary mechanistic study indicated the concerted mechanism illustrated in Scheme 68.

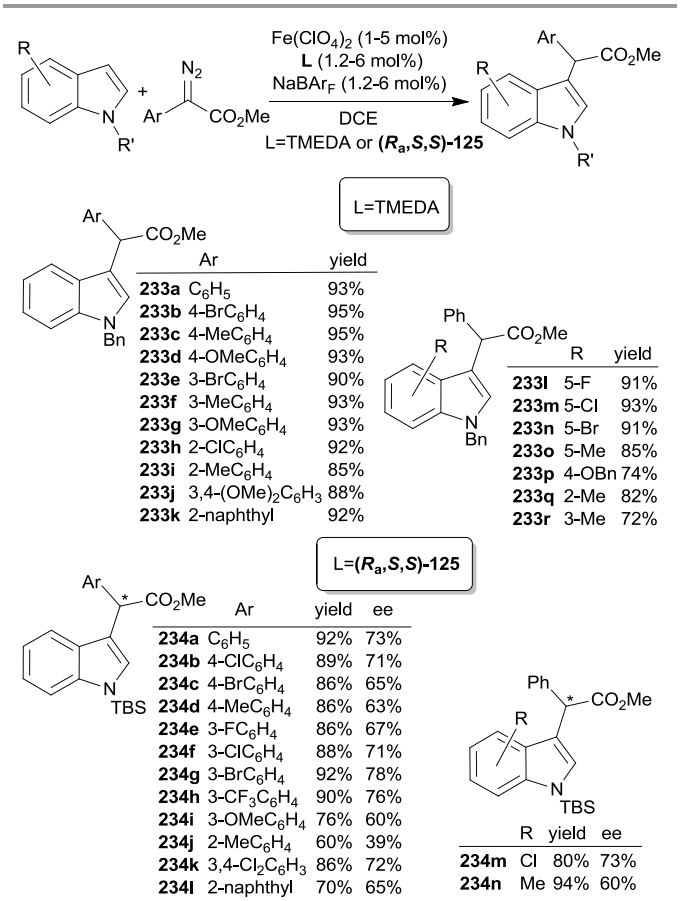

Scheme 69. Synthesis of C-3 substituted indoles mediated by Fe(ClO$_4$)$_2$ and either TMEDA or (***R*$_a$,*S*,*S*)-125** ligands

The C-H alkylation can be a valuable procedure for the functionalization of biologically relevant scaffolds, such as indoles. Q.-L. Zhou and co-authors reported both the achiral and the chiral version of the synthesis of substituted indoles by using α-aryl-α-diazoesters as the alkylating reagents and $Fe(ClO_4)_2$ as the iron source. The ligands TMEDA (TMEDA = *N*,*N*,*N*′,*N*′-tetramethylethylenediamine) and the spiro-*bis*-oxazoline **(R_a,*S*,*S*)-125** (Fig. 12) were employed for the achiral and enantioselective reaction, respectively (Scheme 69).[188] The catalytic $Fe(ClO_4)_2$/TMEDA combination was efficient for the alkylation of differently substituted 1-benzylindoles in the C-3 position. When the C-3 position of indole was substituted, as in the case of the reaction of 3-methyl-1-benzylindole with methyl phenyl diazoacetate ($(CO_2Me)(Ph)CN_2$), the alkylation took place at the C-2 indole position in a good yield (72%). The asymmetric functionalization occurred with enantioselectivities from moderate to good (39%-78% ee).

In order to envisage a catalytic mechanism, the kinetic isotope effect (KIE=k_H/k_D) was investigated by reacting the diazo reagent with an indole/C-3 deuterium-labeled indole mixture. The obtained KIE value of 5.06 indicated that the C-H cleavage should be the rate-determining step of the cycle. The authors proposed that the C-3 functionalization occurred through the formation of the metal-associated zwitterionic intermediate **A** and then the HAT reaction is responsible for the formation of the final compound (Scheme 70).

Chiral spiro-bis-oxazolines were also employed as ligands in the iron-mediated alkylation of Si-H bonds.[189]

[6] The catalytic **(R_a,*S*,*S*)-126**/$Fe(OTf)_2$/$NaBAr_F$ combination was very active in promoting the synthesis of α-silyl esters depicted in Scheme 71 (see Fig. 12 for the structure of **(R_a,*S*,*S*)-126**). The presence of $NaBAr_F$ was probably necessary to provide the coordinatively unsaturated [Fe(OTf)(**(R_a,*S*,*S*)-126**)](BAr_F) active catalyst, displaying the non-coordinated BAr_F anion. The synthetic protocol furnished desired compounds in yields up to 99% and ee up to 96%. The study of the kinetic isotope effect indicated that the Si–H bond cleavage was not the rate-determining step of the reaction, which probably consisted in the concerted oxidative addition of the Si–H bond which was followed by the hydride insertion. DFT calculations revealed the occurrence of a quintet transition state of an iron(II) species and also suggested that the steric repulsion between the phenyl moiety and the ester group in the transition state determined the very good enantioselectivity achieved.

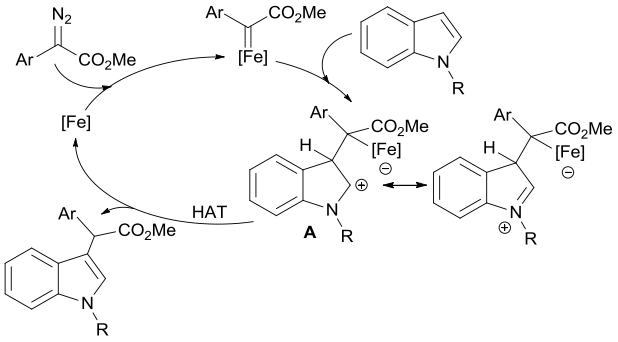

Scheme 70. Proposed mechanism for the C-3 alkylation of indoles

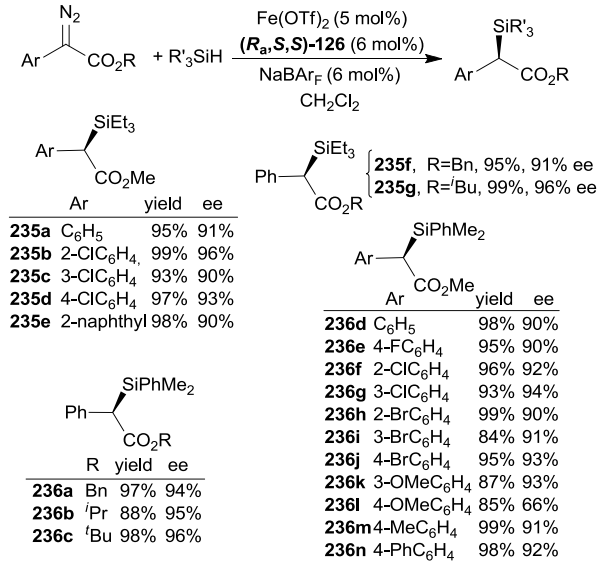

	Ar	yield	ee
235a	C_6H_5	95%	91%
235b	2-ClC_6H_4,	99%	96%
235c	3-ClC_6H_4	93%	90%
235d	4-ClC_6H_4	97%	93%
235e	2-naphthyl	98%	90%

	R	yield	ee
236a	Bn	97%	94%
236b	^{i}Pr	88%	95%
236c	^{t}Bu	98%	96%

	Ar	yield	ee
236d	C_6H_5	98%	90%
236e	4-FC_6H_4	95%	90%
236f	2-ClC_6H_4	96%	92%
236g	3-ClC_6H_4	93%	94%
236h	2-BrC_6H_4	99%	90%
236i	3-BrC_6H_4	84%	91%
236j	4-BrC_6H_4	95%	93%
236k	3-$OMeC_6H_4$	87%	93%
236l	4-$OMeC_6H_4$	85%	66%
236m	4-MeC_6H_4	99%	91%
236n	4-PhC_6H_4	98%	92%

Scheme 71. Asymmetric synthesis of α-silyl esters catalyzed by (R_a,*S*,*S*)-126/$Fe(OTf)_2$/$NaBAr_F$ system

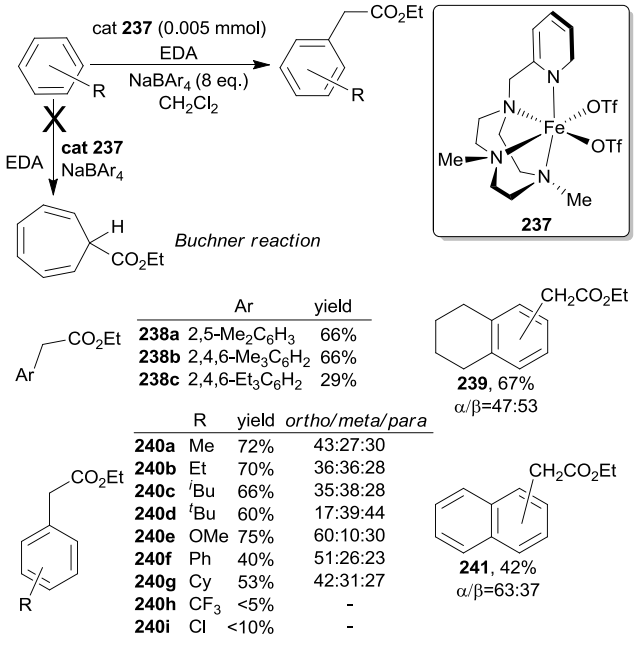

	Ar	yield
238a	2,5-$Me_2C_6H_3$	66%
238b	2,4,6-$Me_3C_6H_2$	66%
238c	2,4,6-$Et_3C_6H_2$	29%

	R	yield	*ortho/meta/para*
240a	Me	72%	43:27:30
240b	Et	70%	36:36:28
240c	^{i}Bu	66%	35:38:28
240d	^{t}Bu	60%	17:39:44
240e	OMe	75%	60:10:30
240f	Ph	40%	51:26:23
240g	Cy	53%	42:31:27
240h	CF_3	<5%	-
240i	Cl	<10%	-

Scheme 72. Functionalization of aromatic C-H bonds mediated by iron(II) complex **237**

The choice of the opportune catalyst allowed the alkylation of more challenging C-H bonds, such as non-activated aryl $C(sp^2)$-H bonds of benzene. The under-developing of efficient synthetic methodologies for inserting a carbene moiety into aromatic C-H bonds is due to the existence of side-reactions such as the Buchner reaction[190] and the carbene coupling process.

M. M. Díaz-Requejo, M. Costas, P. J. Pérez and co-authors reported a very chemoselective functionalization of benzene by using the iron(II) complex **237** of the polydentate amino-based ligands showed in Scheme 72.[191] Complex **237** was used in the presence of the additive $NaBAr_F$, which, as already discussed above, renders the iron metal coordinatively

unsaturated and in turn more reactive. The catalytic **237**/$NaBAr_F$ combination was effective in forming all the derivatives reported in Scheme 72 by using EDA as the carbene source. The product of the Buchner reaction, formed by the carbene addition to the aromatic C=C bond, was never obtained. In addition, the procedure was selective towards C(sp^2)-H aromatic bonds in the presence of C(sp^3)-H bonds of aromatic substituents which were never alkylated.

A preliminary mechanistic investigation indicated the formation of an electrophilic metal-carbene intermediate that was involved in an aromatic electrophilic substitution. The formation of long-lived radicals was excluded.

The alkylation of aromatic C-H bonds was also studied by Y. Deng and co-authors,[145] who reported the C–H insertion in the para-position of *N*,*N*-dimethylaniline by using $(CO_2Me)(Ph)CN_2$, as the carbene source and [(**134**)Fe(II)$(MeCN)_2$]$(SbF_6)_2$ *bis*(imino)pyridine complex as the catalyst (ligand structure in Scheme 44). The alkylated compound **247** (Fig. 15) was obtained with 71% yield.

3.2.2 Mechanistic investigation of the carbene C-H insertion.

A deeper investigation of the alkylation of non-activated aromatic C(sp^2)-H bonds was undertaken by using both experimental and theoretical approaches.[192] The catalytic procedure reported above[191] for the functionalization of aromatic C-H bonds required two equivalents of $NaBAr_F$, with respect to complex **237**, to allow the reaction to proceed. This indicated that two available coordination sites on the metal center are necessary for accomplishing the carbene insertion. The computational analysis of the reaction between **237** and EDA revealed that the first step of the reaction is the formation of an adduct, in which the iron metal is coordinated to the oxygen atom of the diazo carbonyl group. The coordination of either the carbon atom of the C=O functionality or the EDA nitrogen atom was less energetically favored. The adduct can be transformed into the carbene intermediate by passing an energy barrier of 29.5 kcal/mol and extruding molecular nitrogen. DFT data indicated the formation of a carbene with an iron(III) metal coupled with a radical alkyl substituent (see Scheme 39b for the general structure of a diradicaloid iron(III) compound). The electronic structure of the proposed iron(III) carbene resembles that described in the iron(II) porphyrin-mediated N-H alkylations as an open-shell singlet (OSS) iron(III) species.[133] Analogously to what was calculated by S. Shaik and co-authors, the DFT study indicated a stepwise mechanism of the carbene insertion into the aromatic C-H bond. It was proposed that both the desired product of the C(sp^2)-H insertion and the side-compound cycloeptatriene should originate from the same precursor, namely **A** in Scheme 73. Besides the three different pathways calculated for the decomposition of **A,** the carbonyl-assisted insertion (*path b*) was the less energetically demanding. The higher calculated energetic barrier associated to pathway c, explained the lack of the formation of cycloheptatriene in the **237**-catalyzed alkylation of aromatic C(sp^2)-H bonds.

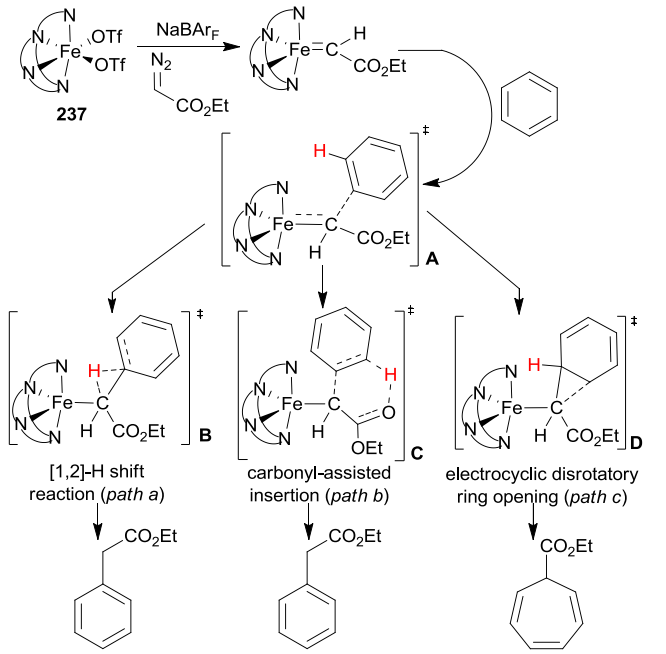

Scheme 73. Mechanistic proposal for the alkylation of aromatic C-H bonds mediated by iron(II) complex **237**

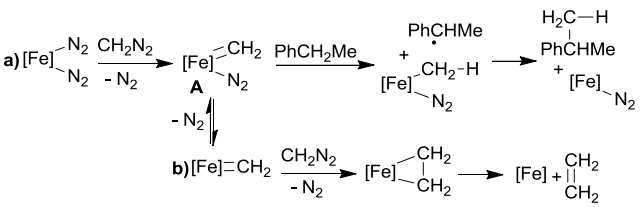

Scheme 74. a) (PDI)Fe(II)$(N_2)_2$-mediated reaction of CH_2N_2 with ethylbenzene; b) homocoupling reaction of carbene functionalities

The catalytic activity of iron(II) *bis*(imino)pyridine complexes (PDI)Fe(II)L_2, in mediating the alkylation of benzylic C(sp^3)-H bond of ethylbenzene ($PhCH_2Me$), was investigated from a theoretical point of view by using either diazomethane (CH_2N_2) or the donor-acceptor diazo derivative $(CHO)(Ph)CN_2$ as the carbene source.[193]

The DFT study of the (PDI)Fe(II)$(N_2)_2$-mediated reaction of CH_2N_2 with $PhCH_2Me$ revealed that the first formation of the carbenoid (PDI)Fe(II)$(CH_2)(N_2)$ species was an exergonic process (ΔG = -15.3 kcal/mol) with a barrier of 7.6 kcal/mol. The subsequent alkylation of the benzylic C–H bond follows a stepwise pathway where an H-atom first abstraction occurs and then the so-formed benzylic radical reacts with the iron intermediate yielding the alkylated compound (Scheme 74a). The last coupling process is the rate-determining step of the cycle. Even if the benzylic alkylation may be feasible, the homocoupling reaction of carbene functionalities (Scheme 74b) resulted in being more energetically favored (16.8 kcal/mol smaller) and consequently, (PDI)Fe(II)$(N_2)_2$ complex is not the ideal catalyst for performing the insertion of a :CH_2 carbene moiety into a C(sp^3)-H benzylic bond.

The same trend was observed by calculating the reaction of $PhCH_2Me$ with $(CHO)(Ph)CN_2$ in the presence of

(PDI)Fe(II)$(N_2)_2$. Conversely, the homocoupling reaction was partially inhibited by introducing a strongly bonded Cl ligand onto the metal center in order to provide only one coordinative site accessible during the catalysis. By using the catalyst (PDI)Fe(II)Cl(OMe), only one carbene functionality can be activated and, even if the homocoupling reaction is still energetically favored, the benzylic functionalization by CH_2N_2 becomes more accessible. When (CHO)(Ph)CN_2 was the involved carbene source, the homocoupling reaction was further depressed. Even if the barrier to achieve the carbene intermediate from (CHO)(Ph)CN_2 was higher, the energy required for the reaction of the corresponding iron carbene intermediate with the C-H benzyl bond was less than that necessary for the homocoupling process.

3.2.3 X-H carbene insertion. Considering papers which have been published from 2006 to now, the catalytic activity of non-heme iron-complexes in the insertion of carbene functionalities into N-H and O-H bonds has been well established. Recently, the axially chiral 2,2'-biimidazole ligand **242** was employed in combination with $Fe(OTf)_2$ and $NaBAr_F$ for the enantioselective insertion of α-aryl-α-diazoacetates into the N–H bonds of carbazoles (Scheme 75).[194] The reaction furnished desired compounds in good yields (up to 84%) and very good enantioselectivities (ee up to 94%) with the best values achieved when benzyl esters of diazo derivatives were employed**.**

The carbene insertion into the N-H bond of aniline was also executed by using [(**134**)Fe(II)$(MeCN)_2$]$(SbF_6)_2$[145] (ligand structure in Scheme 44), which was already used to promote both cyclopropanations and carbene C-H insertions.

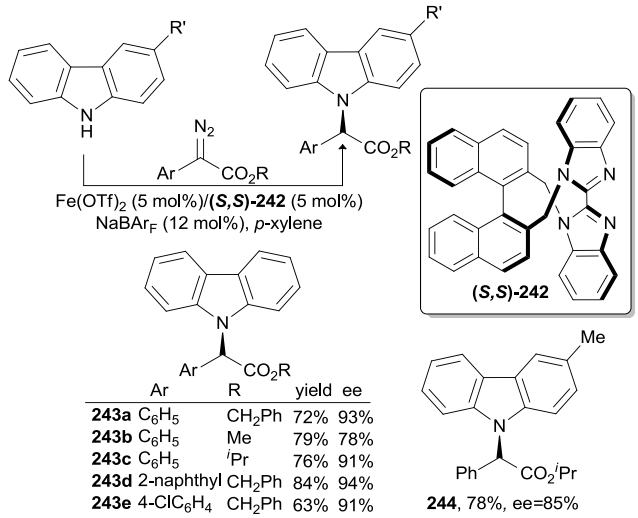

	Ar	R	yield	ee
243a	C_6H_5	CH_2Ph	72%	93%
243b	C_6H_5	Me	79%	78%
243c	C_6H_5	^{i}Pr	76%	91%
243d	2-naphthyl	CH_2Ph	84%	94%
243e	4-ClC_6H_4	CH_2Ph	63%	91%

244, 78%, ee=85%

Scheme 75. Enantioselective insertion of α-aryl-α-diazoacetates into the N-H bonds of carbazoles catalyzed by $Fe(OTf)_2$/(***S,S***)-**242**/$NaBAr_F$ system

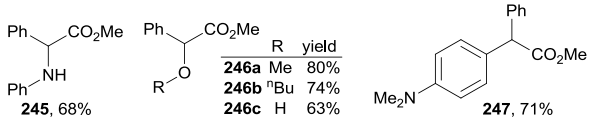

	R	yield
246a	Me	80%
246b	^{n}Bu	74%
246c	H	63%

245, 68%

247, 71%

Fig. 15. Enantioselective insertion in N-H and O-H bonds catalyzed by [(**134**)Fe(II)$(MeCN)_2$]$(SbF_6)_2$ by using (Ph)$(CO_2Me)CN_2$ as the carbene source

The reaction of $PhNH_2$ with (Ph)$(CO_2Me)CN_2$ afforded ((Ph)(CO_2Me)CH)N(Ph)H (**245**) in 68% yield. The same catalyst also promoted the alkylation of O-H bonds of alcohols by (Ph)$(CO_2Me)CN_2$ yielding compounds **246a-246c** (Fig. 15).[145]

The insertion of a carbene moiety into an O-H bond was also carried out in the presence of chiral iron(II) spiro-bis-oxazoline that occurred with an outstanding enantiocontrol by using mild experimental reaction conditions. The chiral ***(Sa,S,S)*-248** and ***(Sa,S,S)*-249** ligands (Fig. 16) in combination with $FeCl_2{\cdot}4H_2O$ and $NaBAr_F$ mediated the asymmetric carbene transfer reaction into O-H bonds of alcohols (Scheme 76) and water (Scheme 77), respectively.[195]

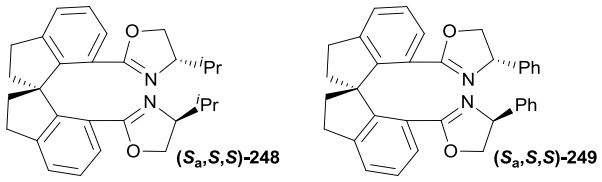

Fig. 16. Structure of chiral spiro-*bis*-oxazoline ***(Sa,S,S)*-248** and ***(Sa,S,S)*-249** ligands

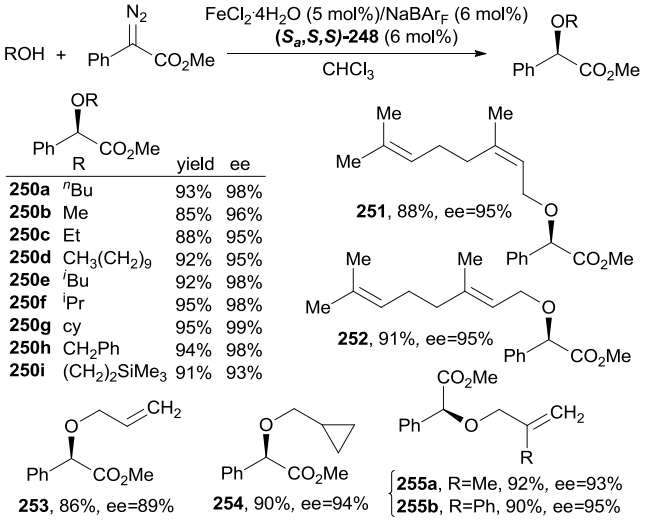

	R	yield	ee
250a	^{n}Bu	93%	98%
250b	Me	85%	96%
250c	Et	88%	95%
250d	$CH_3(CH_2)_9$	92%	95%
250e	^{i}Bu	92%	98%
250f	^{i}Pr	95%	98%
250g	cy	95%	99%
250h	CH_2Ph	94%	98%
250i	$(CH_2)_2SiMe_3$	91%	93%

251, 88%, ee=95%

252, 91%, ee=95%

253, 86%, ee=89%

254, 90%, ee=94%

255a, R=Me, 92%, ee=93%
255b, R=Ph, 90%, ee=95%

Scheme 76. Selective asymmetric insertion of carbene into O-H bonds of alcohols catalyzed by $FeCl_2{\cdot}4H_2O$/(***Sa,S,S*)-248**/$NaBAr_F$ system

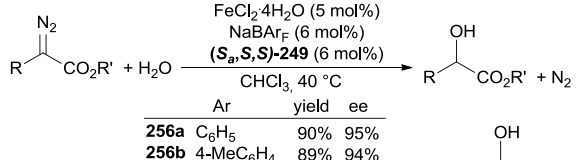

	Ar	yield	ee
256a	C_6H_5	90%	95%
256b	4-MeC_6H_4	89%	94%
256c	4-ClC_6H_4	90%	94%
256d	4-BrC_6H_4	93%	92%
256e	3-MeC_6H_4	93%	92%
256f	3-$OMeC_6H_4$	92%	94%
256g	3-ClC_6H_4	92%	91%
256h	3-BrC_6H_4	93%	90%
256i	2-MeC_6H_4	87%	94%
256j	2-$OMeC_6H_4$	72%	92%
256k	2-FC_6H_4	91%	90%
256l	2-ClC_6H_4	92%	95%
256m	2-BrC_6H_5	94%	94%
256n	2,4-$Cl_2C_6H_3$	93%	88%
256o	2-naphthyl	90%	91%

257, 66%, ee=92%

258, 80%, ee=76%

Scheme 77. Selective asymmetric insertion of carbene into O-H bonds of water catalyzed by $FeCl_2{\cdot}4H_2O$/(***Sa,S,S*)-249**/$NaBAr_F$ system

The reported system was competent in inserting the carbene functionality into the O-H bond of several alcohols also in the presence of functional groups which would be potentially reactive towards diazo reagents, such as C=C double bonds. In fact, O-H bonds of allylic alcohols selectively reacted with $(CO_2Me)(Ph)CN_2$ and no cyclopropanation of the C=C bond was observed. The achieved high chemoselectivity confers a practical importance to the methodology because collected molecules can be used as starting materials of other synthetic protocols in which the carbon-carbon double bond is the target functionality to transform. Very interestingly, the $FeCl_2 \cdot 4H_2O$/**(*Sa,S,S*)-249**/$NaBAr_F$ catalytic system permitted the use of water as the acceptor substrate of the carbene transfer process. Several diazo reagents were active in the reaction with H_2O forming chiral alcohols which are valuable reagents in many organic transformations.

4. Conclusions

In this review we furnished the state of art of the catalytic activity of iron complexes with nitrogen ligands (porphyrinoids and non-heme ligands) in transferring the carbene functionality from a diazo reagent (or its precursor) to C=C, C-H and X-H bonds.

As depicted in Chart 1, great effort has been devoted to developing porphyrin-based cyclopropanation catalysts for conferring enhanced diastereo- and/or enantioselectivity to the reaction. The analysis of literature data revealed that the commercially available Fe(TPP)Cl (**1**) was an excellent catalyst under different experimental conditions. It activated diazo reagents both in the presence and in the absence of a reducing agent and showed a remarkable chemical stability, which permitted performing catalytic reactions both in organic and water medium as well as under basic or acid conditions. Thus, the use of porphyrin catalysts, whose synthesis requires time consuming and expensive experimental procedures, has to be justified by additional benefits, such as the stereoselective synthesis of cyclopropanes. With this goal, chiral iron porphyrins were synthesized. An increasing attention has been focused on the catalytic ability of engineered iron enzymes, in which the activity of the iron tetrapyrrolic core is coupled to the chiral arrangement of the biological pockets.

While synthetic iron porphyrins usually show the metal in the oxidation state +3, artificial biocatalysts display an iron(II) in the pyrrolic cavity. It was assumed that in both cases the active species is an iron (II) carbene intermediate, whose electronic structure is currently a topic of scientific discussions.

Iron complexes of non-heme nitrogen ligands (Chart 1) were usually synthesized *in situ* by mixing an iron(II) salt with the desired neutral ligand. A co-catalyst, showing a non-coordinating anion, is usually added to render the metal center coordinatively unsaturated and in turn more reactive. Also in these catalytic reactions, the formation of an iron carbene intermediate was proposed as the key-step of the catalytic mechanism. Even if iron(III) porphyrins were also extensively employed in carbene insertion in C-H and X-H bonds, the enantioselective version of these reactions was widely developed by using achiral and chiral non-heme ligands (Chart 2). Non-heme iron complexes were active in alkylating poor reactive aromatic $C(sp^2)$-H bonds and interesting results were achieved in the synthesis of amino acids by reacting diazo compounds with amines. Alcohols and even water were suitable substrates for carbene transfer reactions. The formation of active ylide intermediates was suggested for the alkylation of X-H bonds.

Regarding the diazo reagents, it should be noted that new procedures (flow chemistry) and the use of stable diazo-precursors have permitted the introduction of chemically different carbene fragments into organic frameworks by applying safe procedures (Chart 3).

The analysis of published data revealed that carbene transfer reactions are becoming a useful and practical synthetic procedure for creating new C-C and C-X bonds. Reported data pave the way for a rapid future development of this strategy as much as and beyond other coupling reactions, which have received more attention in the last decades. In addition, the use of iron as the active metal represents an additional benefit in view of its low-cost and high eco-tolerability.

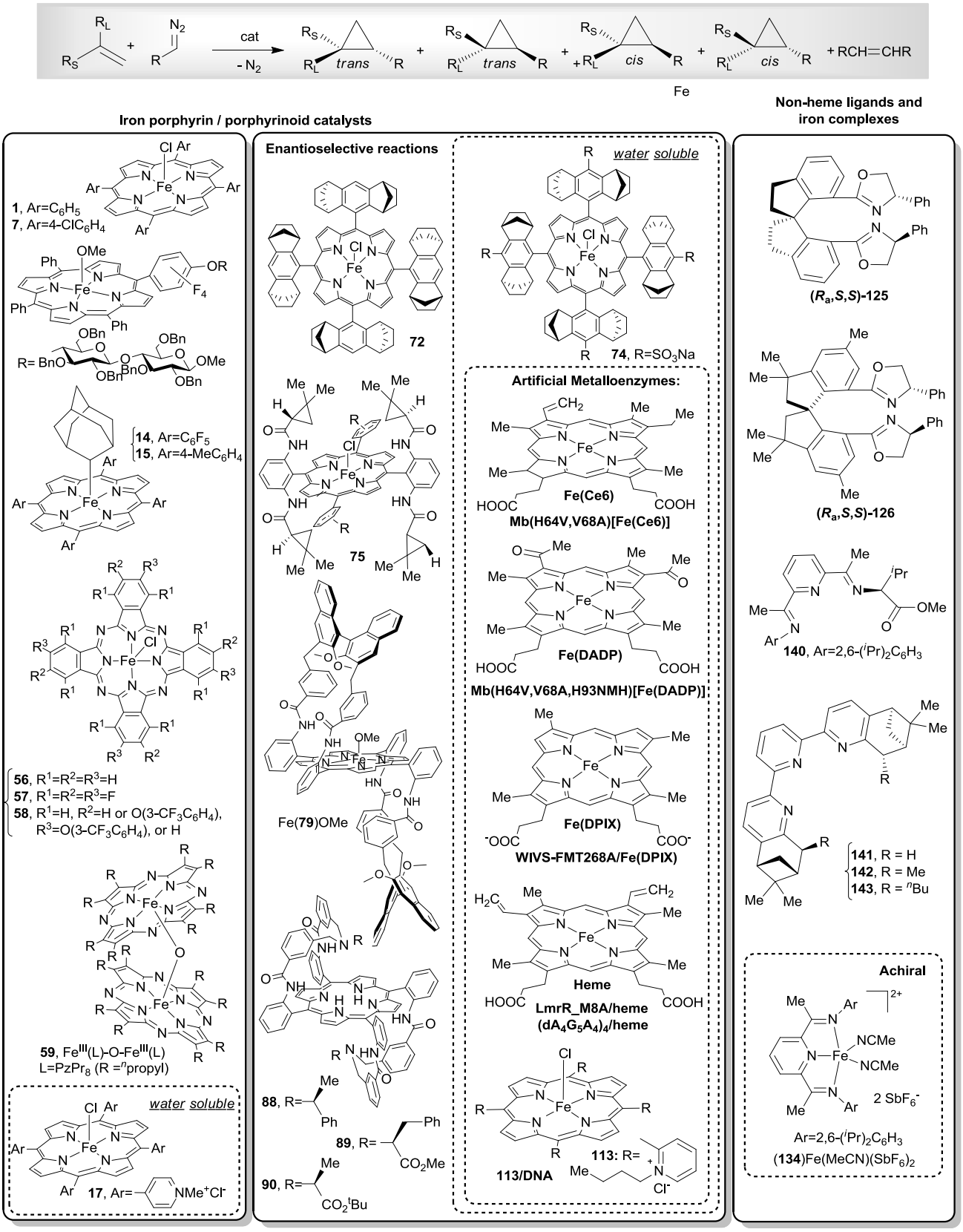

Chart 1. Selection of the most used catalysts for promoting cyclopropanation reactions since 2006

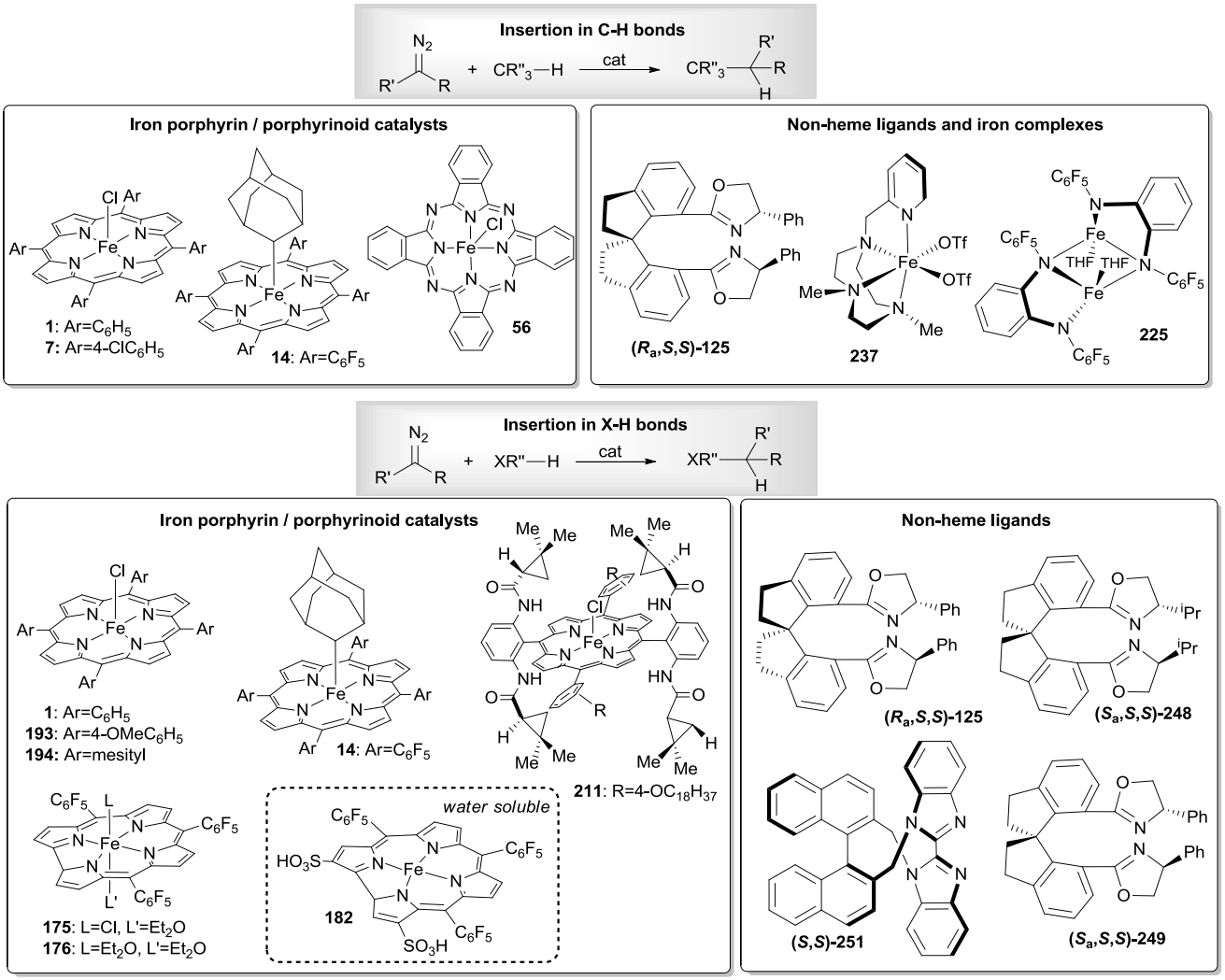

Chart 2. Selection of the most used catalysts in C-H and X-H carbene insertions since 2006

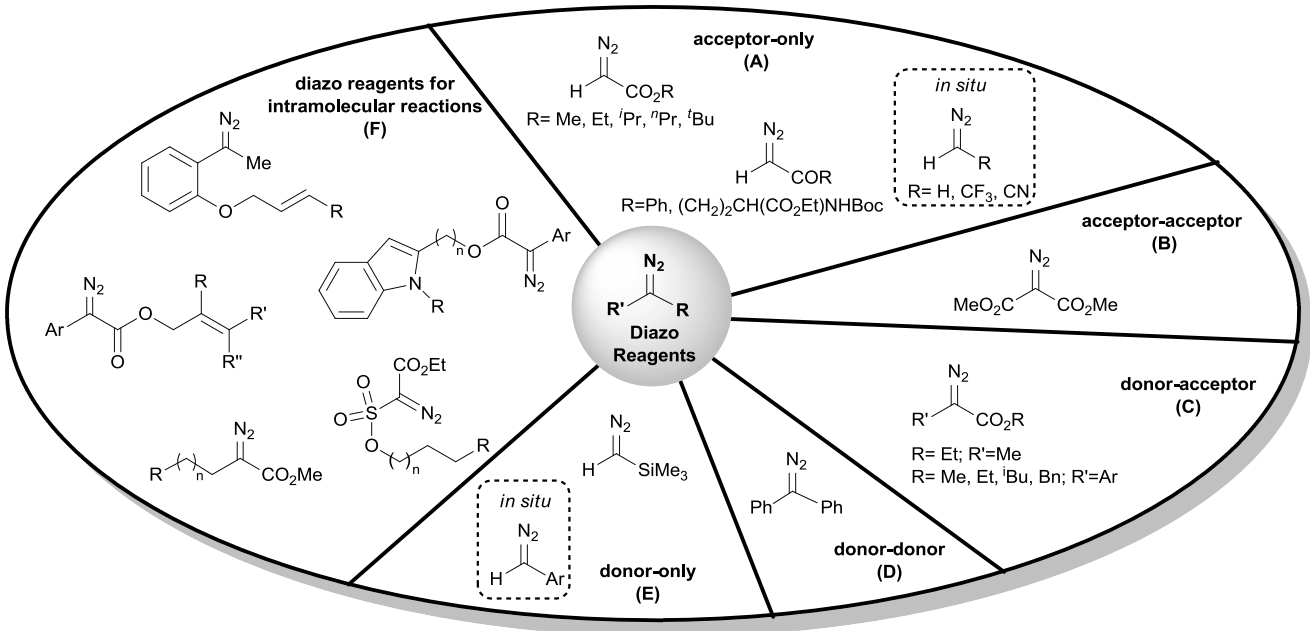

Chart 3. Diazo-reagents discussed in the present review

Conflicts of interest

There are no conflicts to declare.

Notes and references

1 H. M. L. Davies and R. E. J. Beckwith, *Chem. Rev.*, 2003, **103**, 2861-2904.
2 D. Zhu, L. Chen, H. Fan, Q. Yao and S. Zhu, *Chem. Soc. Rev.*, 2020, **49**, 908-950.
3 A. Ford, H. Miel, A. Ring, C. N. Slattery, A. R. Maguire and M. A. McKervey, *Chem. Rev.*, 2015, **115**, 9981-10080.
4 Z. Chen, M.-Y. Rong, J. Nie, X.-F. Zhu, B.-F. Shi and J.-A. Ma, *Chem. Soc. Rev.*, 2019, **48**, 4921-4942.
5 Y.-Y. Ren, S.-F. Zhu and Q.-L. Zhou, *Org. Biomol. Chem.*, 2018, **16**, 3087-3094.
6 A. Caballero, M. M. Díaz-Requejo, M. R. Fructos, A. Olmos, J. Urbano and P. J. Pérez, *Dalton Trans.*, 2015, **44**, 20295-20307.
7 L. Mertens and R. M. Koenigs, *Org. Biomol. Chem.*, 2016, **14**, 10547-10556.
8 K. J. Hock and R. M. Koenigs, *Chem. Eur. J.*, 2018, **24**, 10571-10583.
9 D. Qiu, F. Mo, Y. Zhang and J. Wang, in *Adv. Organomet. Chem.*, Ed. P. J. Pérez, Academic Press, 2017, vol. 67, pp. 151-219.
10 K. S. Egorova and V. P. Ananikov, *Angew. Chem. Int. Ed.*, 2016, **55**, 12150-12162.
11 I. Bauer and H.-J. Knölker, *Chem. Rev.*, 2015, **115**, 3170-3387.
12 K. Gopalaiah, *Chem. Rev.*, 2013, **113**, 3248-3296.
13 S.-F. Zhu and Q.-L. Zhou, *Natl. Sci. Rev.*, 2014, **1**, 580-603.
14 C. Empel and R. M. Koenigs, *Synlett*, 2019, **30**, 1929-1934.
15 D. Arunprasath, B. D. Bala and G. Sekar, *Adv. Synth. Catal.*, 2019, **361**, 1172-1207.
16 T. T. Talele, *J. Med. Chem.*, 2016, **59**, 8712-8756.
17 D. Y.-K. Chen, R. H. Pouwer and J.-A. Richard, *Chem. Soc. Rev.*, 2012, **41**, 4631-4642.
18 W. A. Donaldson, *Tetrahedron*, 2001, **57**, 8589-8627.
19 C. Ebner and E. M. Carreira, *Chem. Rev.*, 2017, **117**, 11651-11679.
20 R. D. Taylor, M. MacCoss and A. D. G. Lawson, *J. Med. Chem.*, 2014, **57**, 5845-5859.
21 V. Ganesh and S. Chandrasekaran, *Synthesis*, 2016, **48**, 4347-4380.
22 A. Pons, T. Poisson, X. Pannecoucke, A. B. Charette and P. Jubault, *Synthesis*, 2016, **48**, 4060-4071.
23 V. A. Rassadin and Y. Six, *Tetrahedron*, 2016, **72**, 4701-4757.
24 K. R. Babu, X. He and S. Xu, *Synlett*, 2020, **31**, 117-124.
25 G. Purushothaman and C. Srinivasan, *Curr. Org. Chem.*, 2019, **23**, 276-312.
26 Y. Liu, Q.-L. Wang, Z. Chen, C.-S. Zhou, B.-Q. Xiong, P.-L. Zhang, C.-A. Yang and Q. Zhou, *Beilstein J. Org. Chem.*, 2019, **15**, 256-278.
27 E. M. D. Allouche and A. B. Charette, *Synthesis*, 2019, **51**, 3947-3963.
28 D. Intrieri, D. M. Carminati and E. Gallo, *Dalton Trans.*, 2016, **45**, 15746-15761.
29 M. M. Q. Simões, D. T. G. Gonzaga, M. F. C. Cardoso, L. D. S. M. Forezi, A. T. P. C. Gomes, F. D. C. da Silva, V. F. Ferreira, M. G. P. M. S. Neves and J. A. S. Cavaleiro, *Molecules*, 2018, **23**, 792.
30 D. Intrieri, D. M. Carminati and E. Gallo, 'Recent Advances in Metal Porphyrinoid-Catalyzed Nitrene and Carbene Transfer Reactions' in *Handbook of Porphyrin Science*, Edited by K. M. Kadish, and R. Guilard, World Scientific Publishing Co. Pte. Ltd., 2016, vol. 38, pp. 1-99.
31 D. Intrieri, A. Caselli and E. Gallo, *Eur. J. Inorg. Chem.*, 2011, 5071-5081.
32 J. R. Wolf, C. G. Hamaker, J.-P. Djukic, T. Kodadek and L. K. Woo, *J. Am. Chem. Soc.*, 1995, **117**, 9194-9199.
33 L. A. Wessjohann, W. Brandt and T. Thiemann, *Chem. Rev.*, 2003, **103**, 1625-1648.
34 C. J. Thibodeaux, W.-c. Chang and H.-w. Liu, *Chem. Rev.*, 2012, **112**, 1681-1709.
35 R. G. Salomon and J. K. Kochi, *J. Am. Chem. Soc.*, 1973, **95**, 3300-3310.
36 T.-S. Lai, F.-Y. Chan, P.-K. So, D.-L. Ma, K.-Y. Wong and C.-M. Che, *Dalton Trans.*, 2006, 4845-4851.
37 P. Tagliatesta and A. Pastorini, *J. Mol. Catal. A: Chem.*, 2003, **198**, 57-61.
38 P. Le Maux, I. Nicolas, S. Chevance and G. Simonneaux, *Tetrahedron*, 2010, **66**, 4462-4468.
39 C. Damiano, S. Gadolini, D. Intrieri, L. Lay, C. Colombo and E. Gallo, *Eur. J. Inorg. Chem.*, 2019, 4412-4420.
40 P. Wang, L. Ling, S.-H. Liao, J.-B. Zhu, S. R. Wang, Y.-X. Li and Y. Tang, *Chem. Eur. J.*, 2013, **19**, 6766-6773.
41 S. R. Wang, C.-Y. Zhu, X.-L. Sun and Y. Tang, *J. Am. Chem. Soc.*, 2009, **131**, 4192-4193.
42 X.-L. Sun, J.-C. Zheng and Y. Tang, *Pure Appl. Chem.*, 2010, **82**, 625-634.
43 Y. Li, J.-S. Huang, Z.-Y. Zhou, C.-M. Che and X.-Z. You, *J. Am. Chem. Soc.*, 2002, **124**, 13185-13193.
44 H. Wang, Q. Wan, K.-H. Low, C. Zhou, J.-S. Huang, J.-L. Zhang and C.-M. Che, *Chem. Sci.*, 2020, **11**, 2243-2259.
45 R. V. Maaskant, E. A. Polanco, R. C. W. van Lier and G. Roelfes, *Org. Biomol. Chem.*, 2020, **18**, 638-641.
46 S. P. Green, K. M. Wheelhouse, A. D. Payne, J. P. Hallett, P. W. Miller and J. A. Bull, *Org. Process. Res. Dev.*, 2020, **24**, 67-84.
47 V. K. Aggarwal, J. de Vicente and R. V. Bonnert, *Org. Lett.*, 2001, **3**, 2785-2788.
48 W. R. Bamford and T. S. Stevens, *J. Chem. Soc.* 1952, 4735-4740.
49 B. Morandi and E. M. Carreira, *Science*, 2012, **335**, 1471-1474.
50 J. Kaschel, T. F. Schneider and D. B. Werz, *Angew. Chem. Int. Ed.*, 2012, **51**, 7085-7086.
51 S. M. Grayson and J. M. J. Fréchet, *Chem. Rev.*, 2001, **101**, 3819-3867.
52 P. Vinš, A. de Cózar, I. Rivilla, K. Nováková, R. Zangi, J. Cvačka, I. Arrastia, A. Arrieta, P. Drašar, J. I. Miranda and F. P. Cossío, *Tetrahedron*, 2016, **72**, 1120-1131.
53 R. L. Svec and P. J. Hergenrother, *Angew. Chem. Int. Ed.*, 2020, **59**, 1857-1862.
54 S. Purser, P. R. Moore, S. Swallow and V. Gouverneur, *Chem. Soc. Rev.*, 2008, **37**, 320-330.
55 B. Morandi and E. M. Carreira, *Angew. Chem., Int. Ed.*, 2010, **49**, 938-941.
56 B. Morandi, J. Cheang and E. M. Carreira, *Org. Lett.*, 2011, **13**, 3080-3081.
57 K. J. Hock, R. Spitzner and R. M. Koenigs, *Green Chem.*, 2017, **19**, 2118-2122.
58 B. Morandi, A. Dolva and E. M. Carreira, *Org. Lett.*, 2012, **14**, 2162-2163.
59 K. Bartels, B. Schinor and G. Haufe, *J. Fluorine Chem.*, 2017, **203**, 200-205.
60 Q. Xiao, Y. Zhang and J. Wang, *Acc. Chem. Res.*, 2013, **46**, 236-247.
61 E. M. D. Allouche, A. Al-Saleh and A. B. Charette, *Chem. Commun.*, 2018, **54**, 13256-13259.
62 Y. Xia and J. Wang, *Chem. Soc. Rev.*, 2017, **46**, 2306-2362.

63 X. Zhang, Z. Liu, X. Yang, Y. Dong, M. Virelli, G. Zanoni, E. A. Anderson and X. Bi, *Nat. Commun.*, 2019, **10**, 284.
64 V. Sharma, S. L. Jain and B. Sain, *Catal. Lett.*, 2004, **94**, 57-59.
65 D. L. Ventura and R. W. Kubiak, *Tetrahedron Lett.*, 2014, **55**, 2715-2717.
66 V. B. Sharma, S. L. Jain and B. Sain, *Catal. Commun.*, 2006, **7**, 454-456.
67 H.-H. Liu, Y. Wang, Y.-J. Shu, X.-G. Zhou, J. Wu and S.-Y. Yan, *J. Mol. Catal. A: Chem.*, 2006, **246**, 49-52.
68 L. P. Cailler, M. Clémancey, J. Barilone, P. Maldivi, J.-M. Latour and A. B. Sorokin, *Inorg. Chem.*, 2020, **59**, 1104-1116.
69 R. L. Halterman and S.-T. Jan, *J. Org. Chem.*, 1991, **56**, 5253-5254.
70 M. Frauenkron and A. Berkessel, *Tetrahedron Lett.*, 1997, **38**, 7175-7176.
71 W.-C. Lo, C.-M. Che, K.-F. Cheng and T. C. W. Mak, *Chem. Commun.*, 1997, 1205-1206.
72 I. Nicolas, T. Roisnel, P. Le Maux and G. Simonneaux, *Tetrahedron Lett.*, 2009, **50**, 5149-5151.
73 P. Le Maux, S. Juillard and G. Simonneaux, *Synthesis*, 2006, 1701-1704.
74 I. Nicolas, P. Le Maux and G. Simonneaux, *Tetrahedron Lett.*, 2008, **49**, 5793-5795.
75 X. Cui and X. P. Zhang, *Wiley Ser. React. Intermed. Chem. Biol.*, 2014, **7**, 491-525.
76 Y. Chen and X. P. Zhang, *J. Org. Chem.* 2007, **72**, 5931-5934.
77 S. Fantauzzi, E. Gallo, E. Rose, N. Raoul, A. Caselli, S. Issa, F. Ragaini and S. Cenini, *Organometallics*, 2008, **27**, 6143-6151.
78 E. Gallo, E. Rose, B. Boitrel, L. Legnani and L. Toma, *Organometallics*, 2014, **33**, 6081-6088.
79 D. Intrieri, S. Le Gac, A. Caselli, E. Rose, B. Boitrel and E. Gallo, *Chem. Commun.*, 2014, **50**, 1811-1813.
80 D. M. Carminati, D. Intrieri, A. Caselli, S. Le Gac, B. Boitrel, L. Toma, L. Legnani and E. Gallo, *Chem. Eur. J.*, 2016, **22**, 13599-13612.
81 D. M. Carminati, D. Intrieri, S. Le Gac, T. Roisnel, B. Boitrel, L. Toma, L. Legnani and E. Gallo, *New J. Chem.*, 2017, **41**, 5950-5959.
82 S. C. Hammer, A. M. Knight and F. H. Arnold, *Curr. Opin. Green Sustain. Chem*, 2017, **7**, 23-30.
83 P. S. Coelho, E. M. Brustad, A. Kannan and F. H. Arnold, *Science*, 2013, **339**, 307-310.
84 O. F. Brandenberg, K. Chen and F. H. Arnold, *J. Am. Chem. Soc.*, 2019, **141**, 8989-8995.
85 A. L. Chandgude, X. Ren and R. Fasan, *J. Am. Chem. Soc.*, 2019, **141**, 9145-9150.
86 C. K. Prier and F. H. Arnold, *J. Am. Chem. Soc.*, 2015, **137**, 13992-14006.
87 G. Sreenilayam, E. J. Moore, V. Steck and R. Fasan, *Adv. Synth. Catal.*, 2017, **359**, 2076-2089.
88 P. Dydio, H. M. Key, A. Nazarenko, J. Y.-E. Rha, V. Seyedkazemi, D. S. Clark and J. F. Hartwig, *Science*, 2016, **354**, 102-106.
89 E. N. Mirts, A. Bhagi-Damodaran and Y. Lu, *Acc. Chem. Res.*, 2019, **52**, 935-944.
90 M. W. Wolf, D. A. Vargas and N. Lehnert, *Inorg. Chem.*, 2017, **56**, 5623-5635.
91 M. Hoarau, C. Hureau, E. Gras and P. Faller, *Coord. Chem. Rev.*, 2016, **308**, 445-459.
92 H. J. Davis and T. R. Ward, *ACS Cent. Sci.*, 2019, **5**, 1120-1136.
93 T. Hayashi, Y. Sano and A. Onoda, *Isr. J. Chem.*, 2015, **55**, 76-84.
94 H. M. Key, P. Dydio, D. S. Clark and J. F. Hartwig, *Nature*, 2016, **534**, 534-537.
95 S. N. Natoli and J. F. Hartwig, *Acc. Chem. Res.*, 2019, **52**, 326-335.
96 F. Rosati and G. Roelfes, *ChemCatChem*, 2010, **2**, 916-927.
97 T. K. Hyster and T. R. Ward, *Angew. Chem. Int. Ed.*, 2016, **55**, 7344-7357.
98 F. H. Arnold, *Angew. Chem. Int. Ed.*, 2018, **57**, 4143-4148.
99 O. F. Brandenberg, R. Fasan and F. H. Arnold, *Curr. Opin. Biotechnol.*, 2017, **47**, 102-111.
100 K. Oohora, A. Onoda and T. Hayashi, *Acc. Chem. Res*., 2019, **52**, 945-954.
101 N. Taxak, B. Patel and P. V. Bharatam, *Inorg. Chem*., 2013, **52**, 5097-5109.
102 J. G. Gober, S. V. Ghodge, J. W. Bogart, W. J. Wever, R. R. Watkins, E. M. Brustad and A. A. Bowers, *ACS Chem. Biol.*, 2017, **12**, 1726-1731.
103 A. M. Knight, S. B. J. Kan, R. D. Lewis, O. F. Brandenberg, K. Chen and F. H. Arnold, *ACS Cent. Sci.*, 2018, **4**, 372-377.
104 H. Su, G. Ma and Y. Liu, *Inorg. Chem.*, 2018, **57**, 11738-11745.
105 A. Tinoco, Y. Wei, J.-P. Bacik, D. M. Carminati, E. J. Moore, N. Ando, Y. Zhang and R. Fasan, *ACS Catal.*, 2019, **9**, 1514-1524.
106 D. A. Vargas, R. L. Khade, Y. Zhang and R. Fasan, *Angew. Chem. Int. Ed.*, 2019, **58**, 10148-10152.
107 T. Kim, A. M. Kassim, A. Botejue, C. Zhang, J. Forte, D. Rozzell, M. A. Huffman, P. N. Devine and J. A. McIntosh, *ChemBioChem*, 2019, **20**, 1129-1132.
108 G.-D. Roiban and M. T. Reetz, *Angew. Chem. Int. Ed.*, 2013, **52**, 5439-5440.
109 T. K. Hyster and F. H. Arnold, *Isr. J. Chem.*, 2015, **55**, 14-20.
110 Y. Zhang, *Chem. Eur. J.*, 2019, **25**, 13231-13247.
111 M. J. Weissenborn and R. M. Koenigs, *ChemCatChem*, 2020, **12**, 2171-2179.
112 K. Oohora, H. Meichin, L. Zhao, M. W. Wolf, A. Nakayama, J.-y. Hasegawa, N. Lehnert and T. Hayashi, *J. Am. Chem. Soc.*, 2017, **139**, 17265-17268.
113 E. W. Reynolds, T. D. Schwochert, M. W. McHenry, J. W. Watters and E. M. Brustad, *ChemBioChem*, 2017, **18**, 2380-2384.
114 E. W. Reynolds, M. W. McHenry, F. Cannac, J. G. Gober, C. D. Snow and E. M. Brustad, *J. Am. Chem. Soc.*, 2016, **138**, 12451-12458.
115 G. Sreenilayam, E. J. Moore, V. Steck and R. Fasan, *ACS Catal.*, 2017, **7**, 7629-7633.
116 T. Shibata, S. Nagao, M. Fukaya, H. Tai, S. Nagatomo, K. Morihashi, T. Matsuo, S. Hirota, A. Suzuki, K. Imai and Y. Yamamoto, *J. Am. Chem. Soc.*, 2010, **132**, 6091-6098.
117 M. Bordeaux, V. Tyagi and R. Fasan, *Angew. Chem. Int. Ed.*, 2015, **54**, 1744-1748.
118 Y. Wei, A. Tinoco, V. Steck, R. Fasan and Y. Zhang, *J. Am. Chem. Soc.*, 2018, **140**, 1649-1662.
119 E. J. Moore and R. Fasan, *Tetrahedron*, 2019, **75**, 2357-2363.
120 D. M. Carminati and R. Fasan, *ACS Catal.*, 2019, **9**, 9683-9697.
121 L. Villarino, K. E. Splan, E. Reddem, L. Alonso-Cotchico, C. Gutiérrez de Souza, A. Lledós, J.-D. Maréchal, A.-M. W. H. Thunnissen and G. Roelfes, *Angew. Chem. Int. Ed.*, 2018, **57**, 7785-7789.
122 A. Rioz-Martínez, J. Oelerich, N. Ségaud and G. Roelfes, *Angew. Chem. Int. Ed.*, 2016, **55**, 14136-14140.
123 H. Ibrahim, P. Mulyk and D. Sen, *ACS Omega*, 2019, **4**, 15280-15288.
124 D. Mansuy, M. Lange, J.-C. Chottard, P. Guerin, P. Morliere, D. Brault and M. Rougee, *J. Chem. Soc., Chem. Commun.*, 1977, 648-649.
125 D. Mansuy, M. Lange, J. C. Chottard, J. F. Bartoli, B. Chevrier and R. Weiss, *Angew. Chem. Int. Ed.*, 1978, **17**, 781-782.

126 Y. Liu, W. Xu, J. Zhang, W. Fuller, C. E. Schulz and J. Li, *J. Am. Chem. Soc.*, 2017, **139**, 5023-5026.
127 H. Wang, C. E. Schulz, X. Wei and J. Li, *Inorg. Chem.*, 2019, **58**, 143-151.
128 C. Colomban, E. V. Kudrik, D. V. Tyurin, F. Albrieux, S. E. Nefedov, P. Afanasiev and A. B. Sorokin, *Dalton Trans.*, 2015, **44**, 2240-2251.
129 R. L. Khade, W. Fan, Y. Ling, L. Yang, E. Oldfield and Y. Zhang, *Angew. Chem. Int. Ed.*, 2014, **53**, 7574-7578.
130 R. L. Khade and Y. Zhang, *J. Am. Chem. Soc.*, 2015, **137**, 7560-7563.
131 C. G. Hamaker, G. A. Mirafzal and L. K. Woo, *Organometallics*, 2001, **20**, 5171-5176.
132 J. T. Aldajaei and S. Gronert, *Int. J. Mass Spectrom.*, 2012, **316-318**, 68-75.
133 D. A. Sharon, D. Mallick, B. Wang and S. Shaik, *J. Am. Chem. Soc.*, 2016, **138**, 9597-9610.
134 E. de Brito Sá, A. Rimola, L. Rodríguez-Santiago, M. Sodupe and X. Solans-Monfort, *J. Phys. Chem. A*, 2018, **122**, 1702-1712.
135 T. Hayashi, M. Tinzl, T. Mori, U. Krengel, J. Proppe, J. Soetbeer, D. Klose, G. Jeschke, M. Reiher and D. Hilvert, *Nat. Catal.*, 2018, **1**, 578-584.
136 M. Torrent-Sucarrat, I. Arrastia, A. Arrieta and F. P. Cossío, *ACS Catal.*, 2018, **8**, 11140-11153.
137 E. Casali, E. Gallo, and L. Toma manuscript in preparation
138 T. Ollevier, *Catal. Sci. Technol.* 2016, **6**, 41-48.
139 C. A. Schall, M. Seitz, A. Kaiser and O. Reiser, in 'Activating Unreactive Substrates: The Role of Secondary Interactions' Editor(s): Prof. Dr. Carsten Bolm, Prof. Dr. F. Ekkehardt Hahn, Wiley 2009, 339-348.
140 J.-J. Shen, S.-F. Zhu, Y. Cai, H. Xu, X.-L. Xie and Q.-L. Zhou, *Angew. Chem. Int. Ed.*, 2014, **53**, 13188-13191.
141 H. Gu, S. Huang and X. Lin, *Org. Biomol. Chem.*, 2019, **17**, 1154-1162.
142 H. Xu, Y.-P. Li, Y. Cai, G.-P. Wang, S.-F. Zhu and Q.-L. Zhou, *J. Am. Chem. Soc.*, 2017, **139**, 7697-7700.
143 S. K. Russell, J. M. Hoyt, S. C. Bart, C. Milsmann, S. C. E. Stieber, S. P. Semproni, S. DeBeer and P. J. Chirik, *Chem. Sci.*, 2014, **5**, 1168-1174.
144 H. M. L. Davies and J. R. Denton, *Chem. Soc. Rev.*, 2009, **38**, 3061-3071.
145 B. Wang, I. G. Howard, J. W. Pope, E. D. Conte and Y. Deng, *Chem. Sci.*, 2019, **10**, 7958-7963.
146 C.-T. Yeung, K.-C. Sham, W.-S. Lee, W.-T. Wong, W.-Y. Wong and H.-L. Kwong, *Inorg. Chim. Acta*, 2009, **362**, 3267-3273.
147 P. Yates, *J. Am. Chem. Soc.*, 1952, **74**, 5376-5381.
148 H. M. L. Davies and J. R. Manning, *Nature*, 2008, **451**, 417-424.
149 M. P. Doyle, R. Duffy, M. Ratnikov and L. Zhou, *Chem. Rev.*, 2010, **110**, 704-724.
150 S.-F. Zhu and Q.-L. Zhou, *Acc. Chem. Res.*, 2012, **45**, 1365-1377.
151 D. Gillingham and N. Fei, *Chem. Soc. Rev.*, 2013, **42**, 4918-4931.
152 H. Keipour, V. Carreras and T. Ollevier, *Org. Biomol. Chem.*, 2017, **15**, 5441–5456.
153 P. Gandeepan, T. Müller, D. Zell, G. Cera, S. Warratz and L. Ackermann, *Chem. Rev*. 2019, **119**, 2192−2452.
154 H. M. L. Davies, *J. Org. Chem.* 2019, **84**, 12722−12745.
155 C. Bolm, J. Legros, J. Le Paih and L. Zani, *Chem. Rev.*, 2004, **104**, 6217-6254.
156 R. Shang, L. Ilies and E. Nakamura, *Chem. Rev.*, 2017, **117**, 9086-9139.
157 C. Empel, S. Jana and R. M. Koenigs, *Molecules* 2020, **25**, 880.
158 C.-M. Che, V. K.-Y. Lo, C.-Y. Zhou and J.-S. Huang, *Chem. Soc. Rev.*, 2011, **40**, 1950-1975.
159 D. A. Vargas, A. Tinoco, V. Tyagi and R. Fasan, *Angew. Chem. Int. Ed.*, 2018, **57**, 9911-9915.
160 J. Zhang, X. Huang, R. K. Zhang and F. H. Arnold, *J. Am. Chem. Soc.*, 2019, **141**, 9798-9802.
161 R. K. Zhang, K. Chen, X. Huang, L. Wohlschlager, H. Renata and F. H. Arnold, *Nature*, 2019, **565**, 67-72.
162 Z. J. Wang, N. E. Peck, H. Renata and F. H. Arnold, *Chem. Sci.*, 2014, **5**, 598-601.
163 G. Sreenilayam and R. Fasan, *Chem. Commun.*, 2015, **51**, 1532-1534.
164 V. Tyagi, R. B. Bonn and R. Fasan, *Chem. Sci.*, 2015, **6**, 2488-2494.
165 S. B. J. Kan, R. D. Lewis, K. Chen and F. H. Arnold, *Science*, 2016, **354**, 1048-1051.
166 S. B. J. Kan, X. Huang, Y. Gumulya, K. Chen and F. H. Arnold, *Nature*, 2017, **552**, 132-136.
167 X. Huang, M. Garcia-Borràs, K. Miao, S. B. J. Kan, A. Zutshi, K. N. Houk and F. H. Arnold, *ACS Cent. Sci.*, 2019, **5**, 270-276.
168 K. Chen, X. Huang, S.-Q. Zhang, A. Z. Zhou, S. B. J. Kan, X. Hong and F. H. Arnold, *Synlett*, 2019, **30**, 378-382.
169 H. M. Mbuvi and L. K. Woo, *Organometallics*, 2008, **27**, 637-645.
170 P. Wang, S. Liao, S. R. Wang, R.-D. Gao and Y. Tang, *Chem. Commun.*, 2013, **49**, 7436-7438.
171 J. R. Griffin, C. I. Wendell, J. A. Garwin and M. C. White, *J. Am. Chem. Soc.*, 2017, **139**, 13624-13627.
172 D. V. Vorobyeva and S. N. Osipov, *Synthesis*, 2018, **50**, 227-240.
173 R. A. Jagtap and B. Punji, *Asian J. Org. Chem.*, 2020, **9**, 326-342.
174 K. J. Hock, A. Knorrscheidt, R. Hommelsheim, J. Ho, M. J. Weissenborn and R. M. Koenigs, *Angew. Chem. Int. Ed.*, 2019, **58**, 3630-3634.
175 R. L. Khade and Y. Zhang, *Chem. Eur. J.*, 2017, **23**, 17654-17658.
176 I. Aviv and Z. Gross, *Synlett*, 2006, 951-953.
177 I. Aviv and Z. Gross, *Chem. Commun.*, 2006, 4477-4479.
178 I. Aviv and Z. Gross, *Chem. Eur. J.*, 2008, **14**, 3995-4005.
179 L. K. Baumann, H. M. Mbuvi, G. Du and L. K. Woo, *Organometallics*, 2007, **26**, 3995-4002.
180 H. M. Mbuvi, E. R. Klobukowski, G. M. Roberts and L. K. Woo, *J. Porphyrins Phthalocyanines*, 2010, **14**, 284-292.
181 S. Jana and R. M. Koenigs, *Asian J. Org. Chem.*, 2019, **8**, 683-686.
182 K. J. Hock, L. Mertens, R. Hommelsheim, R. Spitzner and R. M. Koenigs, *Chem. Commun*., 2017, *53*, 6577-6580.
183 X. Xu, C. Li, Z. Tao and Y. Pan, *Green Chem*., 2017, **19**, 1245-1249
184 V. Tyagi, G. Sreenilayam, P. Bajaj, A. Tinoco, and R. Fasan, *Angew. Chem. Int. Ed*. 2016, **55**, 13562-13566.
185 E.-H. Wang, Y.-J. Ping, Z.-R. Li, H. Qin, Z.-J. Xu and C.-M. Che, *Org. Lett.*, 2018, **20**, 4641-4644.
186 M. M. Díaz-Requejo and P. J. Pérez, *Eur. J. Inorg. Chem.*, 2020, 879-885.
187 A. Hernán-Gómez, M. Rodríguez, T. Parella and M. Costas, *Angew. Chem. Int. Ed.*, 2019, **58**, 13904-13911.
188 Y. Cai, S.-F. Zhu, G.-P. Wang and Q.-L. Zhou, *Adv. Synth. Catal.*, 2011, **353**, 2939-2944.
189 H. Gu, Z. Han, H. Xie and X. Lin, *Org. Lett.*, 2018, **20**, 6544-6549.
190 E. Buchner and T. Curtius, *Ber. Dtsch. Chem. Ges.* 1885, **18**, 2377–2379
191 A. Conde, G. Sabenya, M. Rodríguez, V. Postils, J. M. Luis, M. M. Díaz-Requejo, M. Costas and P. J. Pérez, *Angew. Chem. Int. Ed.*, 2016, **55**, 6530-6534.

192 V. Postils, M. Rodríguez, G. Sabenya, A. Conde, M. M. Díaz-Requejo, P. J. Pérez, M. Costas, M. Solà and J. M. Luis, *ACS Catal.*, 2018, **8**, 4313-4322.
193 A. Varela-Álvarez and D. G. Musaev, *Chem. Sci.*, 2013, **4**, 3758-3764.
194 H.-Q. Shen, B. Wu, H.-P. Xie and Y.-G. Zhou, *Org. Lett.*, 2019, **21**, 2712-2717.
195 S.-F. Zhu, Y. Cai, H.-X. Mao, J.-H. Xie and Q.-L. Zhou, *Nat. Chem.*, 2010, **2**, 546-551.

Iron Catalysts with N-Ligands for Carbene Transfer of Diazo Reagents

Caterina Damiano,[a] Paolo Sonzini[a] and Emma Gallo[a]*

This review provides an overview of the catalytic activity of iron complexes with nitrogen ligands in driving carbene transfer reactions towards C=C, C-H and X-H bonds. The reactivity of different diazo reagents, or their precursors, is discussed as well as the proposed catalytic mechanisms.

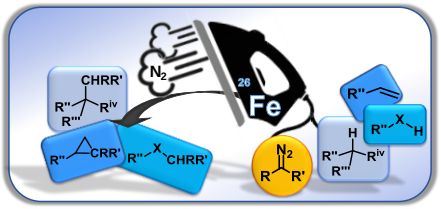

Biography of Authors

Caterina Damiano

Paolo Sonzini

Emma Gallo

Caterina Damiano received her master's degree in Chemical Science (2016) from the University of Naples "Federico II" under the supervision of prof. Angela Lombardi. In 2016, she moved to the University of Milan where she received her PhD (2020) under the supervision of prof. Emma Gallo. She worked on the synthesis and catalytic application of hybrid catalytic systems for carbene and nitrene transfer reactions as well as for carbon dioxide activation. She is currently a post-doctoral researcher at University of Milan in Emma Gallo's group and her current research interest is focused on the development of heterogeneous eco-compatible systems for promoting sustainable and atom efficient catalytic processes.

Paolo Sonzini received his master's degree in Chemical Sciences (2018) from the University of Milan under the supervision of prof. Emma Gallo. The same year he started his PhD at the University of Milan in prof. Emma Gallo's group. His current research interest is focused on the catalytic application of free-base porphyrins and their metal complexes in the synthesis of fine-chemicals by using carbon dioxide as a renewable C1 synthetic building block.

Emma Gallo received her Ph.D degree in Chemistry from the University of Lausanne (Switzerland) under the supervision of Prof. Carlo Floriani. Then, she spent one year in Floriani's Group as "Maître-assistant" before moving to Milan University (Italy) for a post-doctoral training with Prof. Sergio Cenini. She is currently associate professor at Milan University and research interests of her group include the synthesis of homogeneous catalysts for the synthesis of fine chemicals by using sustainable catalytic processes, the heterogenization of homogeneous catalysts and the synthesis of porphyrin-based chemosensors to detect emerging pollutant.